Frequency Domain Tuning Approach for Adaptive Feedforward Controllers

Ramarao Siddha©

A THESIS SUBMITTED IN PARTIAL FULFILMENT OF
THE REQUIREMENTS OF MScEng DEGREE
IN
CONTROL ENGINEERING
FACULTY OF ENGINEERING
LAKEHEAD UNIVERSITY
THUNDER BAY, ONTARIO

March 19, 2003

Your file Votre référence
ISBN: 0-612-83426-3
Our file Notre référence
ISBN: 0-612-83426-3

Contents

List of Figures

List of Tables

ABSTRACT

Feedforward control provides a means for compensating measurable disturbances before the process output is affected. A novel tuning strategy for tuning feedforward controllers in frequency domain is developed in this thesis. The adaptive method consists of continuous identification of process transfer function(G_p) and disturbance transfer function(G_d) by the extended recursive least squares technique and subsequent tuning of a gain with lead-lag compensator(G_{ff}) by minimizing the function $G_{ff} + \frac{G_d}{G_p}$ in frequency domain. The effectiveness of the tuning approach is compared with Shinskey's tuning rule based controllers in frequency domain for the nine possible dynamic combinations. For cases where dead time in the manipulated path is greater than or equal to that of the dead time in disturbance path, the frequency domain tuning of G_{ff} results in as good or better fit to the theoretical frequency response of $\frac{G_d}{G_p}$ required for perfect cancellation, compared to Shinskey's tuning. For cases where the dead time in manipulated path is less than that of the disturbance path, considerable improvement in the fit of frequency response is observed with frequency domain tuning compared to Shinskey's tuning rule based controllers. The validity of these simulations is tested for one dynamic combination by experimental work on a methanol-water distillation column.

Different alternatives of obtaining the $\frac{G_d}{G_p}$ ratio through closed loop identification techniques and subsequent tuning of feedforward controllers have also been studied by simulations.

ACKNOWLEDGEMENTS

I would like to thank my principal supervisor, Dr.A.F.Gilbert for his guidance and financial support. I would like to thank my co-supervisor, Dr.K.Natarajan for his suggestions and guidance. I would also like to thank Dr.S.Siddiqui for his assistance in writing this manuscript in LaTex. Finally, I would like to thank Carol Goodwin, Chemical Engineering technologist for his assistance during the experimental work of this thesis.

Chapter 1

An introduction to feedforward control and its tuning methods

1.1 Introduction

All control loops in a plant are normally subjected to various disturbances. The traditional PI/PID feedback controller rejects these disturbances by applying proper control action on the basis of the error e, computed as $e = r - y$, the difference between the setpoint(r) and the disturbance affected process output(y). Quite often it is possible to measure some of the disturbances entering the control loop. Application of feedforward control provides the means for compensating such measurable disturbances before they effect the process output. The feedback part of the control system is retained in almost all cases to keep the process output under control in the presence of other unmeasurable and random disturbances. Examples of feedforward control in process industries include, compensation for variation in feed flow rate or feed concentration in the composition control of a distillation column and compensation for deviations in flow rates/concentrations of the feed components in the mixture composition control of a blending system.

A typical feedforward control system is shown in Figure 1.1. It is a common practice in process control to characterize most chemical processes in terms of First Order Plus Dead Time(FOPDT) models. For perfect cancellation of the disturbance, the feedforward controller should be of the form shown in Equation 1.1:

$$G_{ff} = -\frac{G_d}{G_p} = -\frac{K_q}{K_m}\frac{(\tau_m s + 1)}{(\tau_q s + 1)} e^{-(\tau_{dq} - \tau_{dm})s} \tag{1.1}$$

Application of feedforward controllers using the above representation is effective only for the cases where $\tau_{dq} - \tau_{dm} >= 0$, i.e. the cases where the dead time in the disturbance path is as much or greater than that of the process path. Further, it is not reasonable to implement the controllers in the cases where the lead time is much greater than lag time($\tau_m >> \tau_q$) as lead dominant controllers are known to amplify noise. Such controllers also result in a rapid change in the manipulated variable making them not practical to implement in process industries. In order to attain the best possible cancellation of the disturbance, accurate identification of process transfer function, G_p and disturbance transfer function,

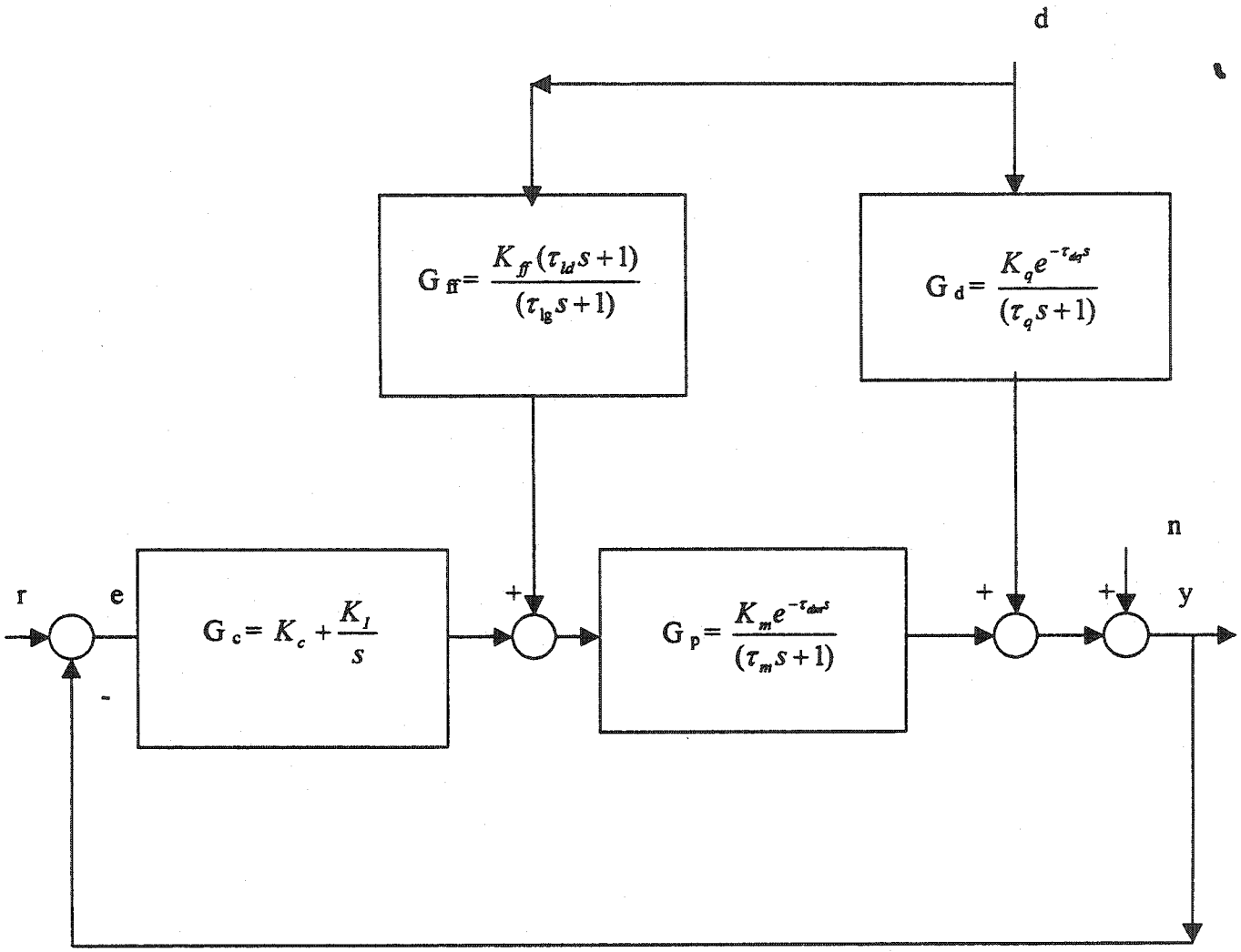

Figure 1.1: Typical structure of a feedforward plus feedback control system

G_d are needed. It has been shown[1] that significant errors in the determination of lead time(τ_{ld}), lag time(τ_{lg}) and feedforward gain(K_{ff}) can still decrease the Integrated Absolute Error(IAE) significantly when compared to the application of feedback control alone.

1.2 System Identification

Conventionally, process models are identified by fitting FOPDT models to step responses. Similar approaches can also be used in identifying the models for feedforward control. Tuning is often based on the judgement of these parameters by the operator or by trial and error. Chemical process dynamics are influenced by various factors and they change with time. Adaptive controllers provide better performance in such cases than using fixed gain controllers[2]. Numerous adaptive control strategies have been developed in the literature for feedback control. But adaptive tuning strategies for feedforward control have gained very little attention. Tuning feedforward controllers manually is an alternative, but it is not always possible to manipulate the disturbances that enter the loop for a tuning trial. Hence to tune for such disturbances the operator has to wait for the disturbances to occur and cause significant transients in the controlled variable. On the other hand, it is rather convenient to evaluate and tune feedback controllers, as the required setpoint variation for such purposes is in the hands of the operator. Application of adaptive control algorithms which continuously monitor and compensate the disturbances are therefore particularly suitable for feedforward control[6,10]. It is a common practice in adaptive control to design the controller on the basis of the estimated model using the certainty equivalence principle[2]. Hence accurate identification of process models is a prerequisite for achieving satisfactory performance through adaptive control techniques.

Application of Recursive Least Squares(RLS) techniques for online process identification is a well explored field[2,6,7,18]. This method is simple and convenient for use in adaptive control techniques. It provides a means for estimating the parameters at time instant k on the basis of the measurement at time k and the estimate at the previous time instant, k-1. This estimation procedure gives unbiased estimates provided the error e is of zero mean, e_k and e_{k-1} are uncorrelated and the elements of the regression vector are uncorrelated. If these conditions are not satisfied, the recursive least squares scheme results in biased estimates. Several alternatives to overcome this problem have been proposed in the literature[2]. The recursive least squares algorithm used in this thesis is summarized in the following set of equations[2]:

$$\hat{\theta}(t) = \hat{\theta}(t-1) + K(t)(y(t) - \varphi^T(t)\hat{\theta}(t-1))$$

$$K(t) = P(t)\varphi(t) = P(t-1)\varphi(t)(\lambda I + \varphi^T(t)P(t-1)\varphi(t))^{-1} \tag{1.2}$$

$$P(t) = (I - K(t)\varphi^T(t))P(t-1)/\lambda$$

where:

$K(t)$ is the gain at discrete time instant, t
λ is the forgetting factor, I is the Identity matrix
$\hat{\theta}(t), \hat{\theta}(t-1)$ are the parameter estimates at time instants t and $t-1$ respectively
$P(t), P(t-1)$ are the co-variance at time instants t and $t-1$ respectively
$\varphi(t), \varphi(t-1)$ are the regressor vectors at time instants t and $t-1$ respectively

It has also been noticed that the estimator results in the true value of the estimate as the data set used for estimation tends to infinity. In practice, the quantity of data used for estimation is determined by the forgetting factor λ. Typical values of λ range from 0.95 to 0.99. A forgetting factor of one implies no forgetting and is suitable when the process conditions do not change. But if the process conditions change, the RLS estimation can adjust to these changes and provide accurate estimation results only when λ is less than one. Several alternatives to overcome the slow convergence of recursive least squares have been proposed in the literature. One such approach is to use variable forgetting factor[7]. In this approach the forgetting factor of the algorithm is decreased to a small value, like 0.4 or so when the process changes such that the most recent data alone is taken into consideration for estimation. Other methods that enhance the speed of the recursive least squares schemes include co-variance resetting in which the co-variance matrix of estimation is reset at regular intervals, which is based on how fast the process changes[2]. All such methods require an indication of change in process conditions such as a limit on the error bound, limit on the co-variance of the estimates, etc.

In this thesis, different approaches are taken in the estimation of the process and disturbance transfer functions. In the first approach, an extended least squares type of estimation is used to continuously estimate both the process and disturbance transfer functions. Such an approach can take changes in both the process and disturbance characteristics into account simultaneously. The second set of approaches utilize recursive least squares in a number of closed loop identification structures. Recursive least squares techniques require the order of the discrete transfer function to be estimated. Accurate knowledge of the order of the system is indicated to be necessary in order to obtain unbiased estimates of the transfer function[12]. The representation of process models by FOPDT sufficiently indicates the order of the denominator polynomial of the discrete time transfer function as one. The order of the numerator polynomial will be a function of the time delay and the sampling period. Hence it is logical to get around the problem of accurate determination of the order of the system by sufficiently overparameterizing the transfer function polynomials. Overparameterizing the numerator polynomial of discrete time transfer functions for systems with unknown dead time has been well explored by Lee and Hang[8]. Such an overparameterized RLS estimation is often quite sensitive to moderate levels of noise and presence of step like disturbances. Alternatives like recursive instrumental variable method, extended least squares method etc. have been suggested by these authors. It has also been shown in their work that the overparameterized transfer function coefficients take fairly large samples to converge in the presence of disturbances when compared to estimation with the true order of the system. The significant advantage of over-parameterization is in the presence of un-

modelled dynamics. Over-parameterization is equivalent to implicit filtering of data, which makes the residuals white thereby resulting in unbiased estimates[9]. The major drawback of over-parameterization method is the computational overhead. Model reduction techniques overcome this problem. Marques da costa *et al.*[9] provided a moments based method for this purpose. These authors also proposed a method based on prefiltering to reduce the order of the overparameterized least squares.

In this thesis the overparameterized models are used to obtain the frequency response of the system. Using this approach, after convergence of the frequency response of the system it is always possible to reparameterize the model based on the obtained frequency response. Especially in process control systems where very fast Distributed Control Systems(DCS) are in use, the approach of obtaining the frequency response of the system is rather useful. The speed of DCS's virtually makes it possible to consider the processes as continuous. Hence the operator has the convenience of obtaining the continuous time parameters from the frequency response and to tune the loop subsequently.

1.3 Feedforward controller tuning techniques in time domain

The rapid progress of adaptive control research resulted in a wide variety of controller tuning strategies. Broadly all such tuning methods can be divided into two categories, time domain and frequency domain. One of the early works in the feedforward control tuning is by Astrom and Wittenmark[5]. Minimum variance control is a well developed tuning strategy. The extension of minimum variance feedback control principle to feedforward control has been indicated in this work. Astrom and Wittenmark[5] also indicate the drawback of this strategy for non-minimum phase systems where it is found to be extremely sensitive to variation of parameters. The authors also suggest several ways to overcome this problem like using sub-optimal strategies. The characterization of process models in this thesis as FOPDT type and subsequent over-parameterization of the numerator polynomial for variable delay could give rise to non-minimum phase systems. In addition, rapid change in the control output as a result of the application of minimum variance control is a major drawback. Several parameter optimizing algorithms for adaptive feedforward control tuning in the absence of feedback have been explored by Schumann and Christ[6]. In their work, the identification of the process and disturbance transfer functions are done using recursive least squares. The tuning methods studied include complete dynamic, static, partial static, minimum variance, extended minimum variance, minimum time and deadbeat feedforward control methods. These controllers are designed on the basis of the certainty equivalence principle. Schumann and Christ[6] indicated that in almost all cases the adaptive controller performs better than the constant gain feedforward controllers. Again this work is based on the knowledge of the system order and time delays. The approach of over-parameterization of system models would result in slow convergence of parameters when compared to the models with known order. Hence the design of controllers on the basis of such parameters would take a large amount of time for convergence in addition to the specific problems of time domain strategies.

It is also a common practice to tune controllers on the basis of various performance criteria

like Integrated Absolute Error(IAE), Integrated Error(IE) etc. Tuning rules for feedforward control on the basis of these criteria were designed by Shinskey[3]. Based on the point where the disturbance enters a loop with respect to the process input, there are 9 possible dynamic combinations of process and disturbance dynamics. Shinskey characterized all such combinations on the basis of the step response in the presence of static feedforward control. Table 1.1 shows the list of possible combinations and the type of controller required for perfect cancellation of the disturbance for different combinations. The simplest of all these combinations is Case I b, where the dead times and time constants in both the paths are equal. Perfect cancellation of disturbance is theoretically possible in this case with a simple gain compensator. Cases III b and II b, in which the dead times are equal but the time constants vary in either direction result in a rounded deviation with a gain compensator. It is possible to achieve perfect compensation in these cases, through the application of dynamic compensation using a gain with lead-lag compensator. Cases II a and II c processes, where the dead time in the disturbance path is greater than that of the manipulated variable path require dead time compensation. In the absence of a dead time compensator, the lead-lag compensator can provide an approximation of dead time through negative lead. The most significant advantage of dynamic compensation is perceptible in Case III processes, where the dead time in the manipulated variable path is greater than that of the disturbance path. Application of dynamic compensation is found to considerably decrease the IAE in the loop for these type of processes[1]. Shinskey[3] derived a set of empirical rules for these cases in order to drive the IE in the loop to zero and to minimize the IAE. Table 1.2 gives a list of Shinskey's tuning rules for the different dynamic combinations. These rules were derived empirically to fit experimental results.

1.4 Feedforward controller tuning in frequency domain

Representation of processes by parametric transfer functions is common and widely used in designing adaptive controllers. Such representations of process models have some significant shortcomings. Design of adaptive controllers on the basis of such transfer functions result in lack of robustness for the adaptive controllers[10]. Such an estimation is often extremely sensitive to unmodelled dynamics. Further it is possible for the parameters of a transfer function to change rapidly without changing the transmission properties of the system. This can particularly happen when poles and zeros of a transfer function are close[10]. One of the drawbacks of over-parameterization approach is the problem of pole-zero cancellation and hence the parameters of such transfer functions may vary rapidly. Tuning controllers on the basis of such rapidly varying parameters would result in rapid change in controller gains.

Representation of systems by frequency response is convinient and accurate. Design of control systems on the basis of frequency response characteristics is becoming widely popular. Earlier methods of using frequency response information are oriented towards obtaining a single point on the frequency response and subsequent design of controllers based upon this information. These methods became popular in industry as it is easy to obtain a single point on frequency response. The relay feedback technique developed by Astrom and Wittenmark[2] is a significant contribution towards this methodology. However design of controllers

Case	Process dead time(τ_{dm}) - Disturbance dead time(τ_{dq})	Process time constant(τ_m) - Disturbance time constant(τ_q)	Nature of controller required
III c	> 0	> 0	Lead + Prediction
I c	$= 0$	> 0	Lead
II c	< 0	> 0	Lead + Dead time
III b	> 0	$= 0$	Prediction
I b	$= 0$	$= 0$	-
II b	< 0	$= 0$	Dead time
III a	> 0	< 0	Lag + Prediction
I a	$= 0$	< 0	Lag
II a	< 0	< 0	Lag + Dead time

Table 1.1: All possible dynamic combinations for feedforward control and theoretical controller required for complete cancellation of disturbance for different combinations

Case	Lead time(τ_{ld})	Lag time(τ_{lg})
III c	$0.8\tau_m + 0.4(\tau_{dm} - \tau_{dq})$	$\tau_q - 0.2\tau_m - 0.6(\tau_{dm} - \tau_{dq})$
I c	τ_m	τ_q
II c	$\tau_m + \tau_{dm}$	$\tau_q + \tau_{dq}$
III b	$1.1(\tau_{dm} - \tau_{dq})$	$\tau_{ld}/10$
I b	τ_m	τ_q
II b	$-(\tau_{dq} - \tau_{dm})/2$	$(\tau_{dq} - \tau_{dm})/2$
III a	$\tau_m + \tau_{dm}$	$\tau_q + \tau_{dq}$
I a	τ_m	τ_q
II a	$\tau_m - 1.4(\tau_{dq} - \tau_{dm})$	$\tau_q - 0.4(\tau_{dq} - \tau_{dm})$

Table 1.2: Shinskey's tuning rules for lead-lag feedforward compensators

on the basis of a single frequency point is found to result in a crude controller. Such a controller might accurately satisfy the open-loop performance specifications like gain-margin or phase-margin but can result in poor closed-loop performance. Using multiple points on the frequency response for controller tuning purposes has been proposed by Goberdhansingh *et al.*[13], Barnes *et al.*[14]. Several ways to obtain multiple frequency response points have been explored in the literature. Wang *et al.*[15] proposed a method for obtaining multiple frequency response points on the basis of relay feedback method. Natarajan and Gilbert[16] developed a parallel band pass filter approach for obtaining multiple frequency response points, where the identification at each frequency is independent of the identification at other frequencies.

Alternatively, the frequency response of a process can be obtained from its respective discrete transfer function coefficients, which can be estimated using standard recursive least squares techniques. Such an approach has been successfully implemented for the design of model reference adaptive systems using frequency domain performance specifications by Patel[4]. This thesis extends these frequency domain principles to feedforward control. The discrete time parameters of the process and disturbance transfer functions are used in generating the frequency responses. The feedforward controllers are designed by minimizing the function $G_{ff} + (G_d/G_p)$ over the frequency range of interest. A gain and lead-lag compensator of the form shown in Equation 1.3 is designed using Nelder-Mead sequential simplex method based optimization[17].

$$G_{ff}(s) = K_{ff}\frac{(\tau_{ld}s + 1)}{(\tau_{lg}s + 1)} \tag{1.3}$$

Several different identification structures and their effectiveness in tuning feedforward controllers in frequency domain are studied in this work.

1.5 Overview of the thesis

Literature survey done in the field of RLS identification and frequency domain control strategies is presented in this chapter. Chapter 2 illustrates the simultaneous identification of G_p and G_d and subsequent frequency domain feedforward control. Chapter 3 compares the effectiveness of three different closed loop identification and tuning combinations for frequency domain feedforward control. Chapter 4 tests the adaptive strategy illustrated in Chapter 2 on the lower temperature loop of a methanol-water distillation column. Chapter 5 summarizes the results and conclusions of this thesis along with future work that can be undertaken in this area.

Chapter 2

Frequency domain feedforward control tuning based on simultaneous identification of process(G_p) and disturbance(G_d) transfer functions

2.1 Introduction

Continuous online identification of processes is a key step in adaptive control. Feedforward control design requires information of both process and disturbance dynamics. It is possible in practical situations for the dynamics in either path to change with time. In such cases, an adaptive strategy based on continuous estimation of both process and disturbance characteristics will be effective. In this chapter, an extended recursive least squares technique which simultaneously identifies both process and disturbance transfer functions is used. The regressor vector for recursive estimation consists of the process outputs(y), process inputs(u) and disturbance measurements(d) respectively. The process input u, is the sum of the control effort from the feedback and feedforward controllers. A familiar drawback of online identification techniques is the necessity for advance knowledge of model structure. In recursive least squares identification the model order should also be chosen appropriately. The choice of model order is usually a trade off between accuracy of estimation and speed of estimation. As explained in the previous chapter, in this work the need for accurate knowledge of order of the system is avoided by using the overparameterization approach to account for changes in system dynamics.

2.2 Continuous G_p and G_d identification and frequency domain feedforward control - Simulation results

In this section, the simulation results for joint identification of process and disturbance transfer functions and subsequent frequency domain adaptive feedforward controller design

based on this estimation is presented. The process and disturbance models, G_p and G_d that are used in the simulation are of the form shown below:

$$G_p = \frac{\mathrm{K_m}\, e^{-\tau_{dm}s}}{\tau_m s + 1} \qquad G_d = \frac{\mathrm{K_q}\, e^{-\tau_{dq}s}}{\tau_q s + 1}$$

where:

K_m and K_q are the process and disturbance gains
τ_{dm} and τ_{dq} are the process and disturbance dead times
τ_m and τ_q are the process and disturbance time constants

The process and disturbance transfer functions are simulated with a time step of 0.001 sec. The RLS identification and control is performed with a sampling period of 0.05 sec. The process simulation time is chosen 50 times slower than the identification rate in order to simulate the process as continuous. The process parameters taken in the simulation are $K_m = 2$, $\tau_m = 0.4$ sec and $\tau_{dm} = 0.6$ sec and these parameters are unchanged throughout the simulation. The disturbance gain is kept constant at $K_q = 2$. Dynamic parameters of the disturbance process τ_q and τ_{dq} are varied during the simulation as shown in Table 2.1 in order to simulate various dynamic combinations shown in Table 1.1.

Joint identification of process and disturbance transfer functions using extended least squares type of estimation necessitates a common denominator polynomial for both the transfer functions. As all the process and disturbance characteristics considered are of first order type, it is natural to choose either one or two coefficients in the denominator polynomial. However, in this set of simulations, the number of coefficients in the denominator polynomial is taken to be five. In the presence of measurement noise, the frequency response obtained from the recursive least squares coefficients is accurate with more coefficients in the denominator. As the process conditions are assumed to be constant, the number of coefficients for numerator of the process is taken to be three. Hence the discrete transfer function used for the estimation of the process dynamics is of the form given below in Equation 2.1:

$$G_p(z^{-1}) = \frac{y}{u} = \frac{z^{-12}(b_0 + b_1 z^{-1} + b_2 z^{-2})}{(1 + a_1 z^{-1} + a_2 z^{-2} + a_3 z^{-3} + a_4 z^{-4} + a_5 z^{-5})} \tag{2.1}$$

The z^{-12} factor corresponds to the continuous time process delay of 0.6 sec, sampled at 0.05 sec. On the other hand, the numerator polynomial of the disturbance transfer function G_d is significantly over-parameterized to account for changes in the time delay. In this run, the number of numerator coefficients for G_d is taken as fourteen. A few more coefficients than actually required are added to the numerator polynomial in order to obtain better estimate of frequency response of the disturbance transfer function. The discrete version of the disturbance transfer function G_d used in the estimation has the following structure:

$$G_d(z^{-1}) = \frac{y}{d} = \frac{z^{-8}(c_0 + c_1 z^{-1} + c_2 z^{-2} + ... + c_{13} z^{-13})}{(1 + a_1 z^{-1} + a_2 z^{-2} + a_3 z^{-3} + a_4 z^{-4} + a_5 z^{-5})} \tag{2.2}$$

In Equation 2.2, the z^{-8} factor corresponds to the lower limit of continuous time disturbance delay of 0.4 sec, sampled at 0.05 sec. The parameter vector of the extended recursive least squares is made up of the common denominator coefficients, process transfer function numerator coefficients and disturbance transfer function numerator coefficients

Simulation time (sec)	τ_{dq} (sec)	τ_q (sec)	Case
300	0.4	0.25	III c
500	0.6	0.25	I c
700	0.8	0.25	II c
900	0.4	0.4	III b
1100	0.6	0.4	I b
1300	0.8	0.4	II b
1500	0.4	0.5	III a
1700	0.6	0.5	I a
1900	0.8	0.5	II a

Table 2.1: Changes in disturbance dynamics introduced during the simulation with $\tau_m = 0.4$ sec, $\tau_{dm} = 0.6$ sec, $K_m = K_q = 2$

respectively. Hence the process output(y_k) at time instant k depends on the previous process outputs($y_{k-1}, y_{k-2}, ...$), previous process inputs($u_{k-dm}, u_{k-dm-1}, ...$) and disturbance measurements($d_{k-dq}, d_{k-dq-1}, ...$) as shown below:

$$y = G_p u + G_d d \tag{2.3}$$

$$y = \frac{z^{-12}(b_0 + b_1 z^{-1} + b_2 z^{-2})}{(1 + a_1 z^{-1} + a_2 z^{-2} + a_3 z^{-3} + a_4 z^{-4} + a_5 z^{-5})} u + \frac{z^{-8}(c_0 + c_1 z^{-1} + c_2 z^{-2} + ... + c_{13} z^{-13})}{(1 + a_1 z^{-1} + a_2 z^{-2} + a_3 z^{-3} + a_4 z^{-4} + a_5 z^{-5})} d \tag{2.4}$$

$$y_k = f(y_{k-1}, y_{k-2}, ..., u_{k-12}, u_{k-13}, ..., d_{k-8}, d_{k-9}, ..) \tag{2.5}$$

All estimated coefficients are initialized to zero at the beginning of the simulation. An exponential forgetting factor(λ) of 0.999 is used. The initial values of the diagonal elements of the covariance matrix are taken as 100. It is assumed that the process and measurement noise present in the system is Gaussian and the measured output used in the estimation procedure is taken to be the sum of the actual process output and the measurement noise. The noise used in the simulation has a standard deviation of 0.05. The setpoint excitation used is of square wave type with a period of 20 sec. This period is chosen so that the square wave cycle has enough harmonics in the frequency range over the process to be estimated. The nature of disturbance used in the simulations is also of square wave type with a period of 15 sec. On the basis of the range over which the disturbance dynamics are varied, a square wave with a period of 15 sec is needed to provide enough harmonics in the frequency range of interest. The very low frequency disturbances are attenuated through the integral action of the PI controller and the high frequency disturbances are attenuated by the disturbance process itself. Therefore the actual requirement for feedforward control arises only in a limited frequency range. The disturbance sensitivity function magnitude plot provides an

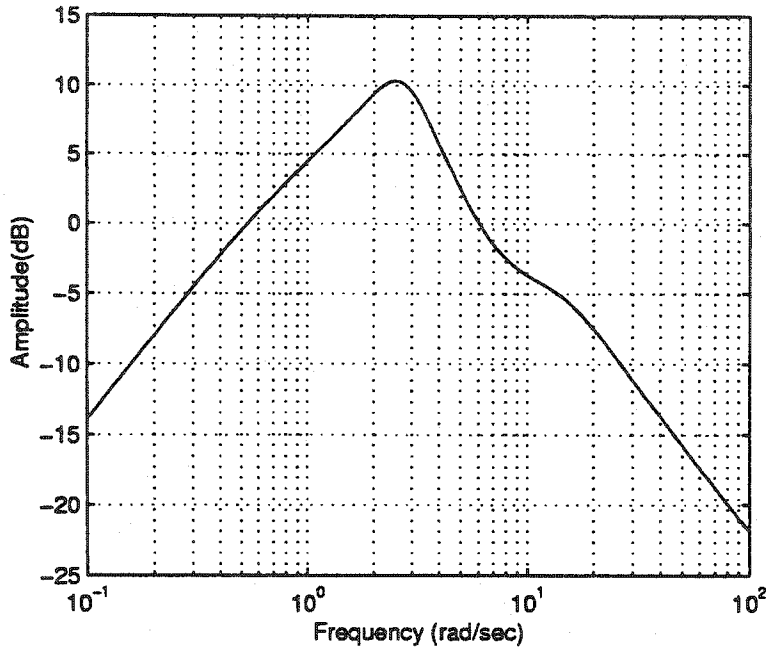

Figure 2.1: Magnitude plot of the actual disturbance sensitivity function corresponding to Case III c

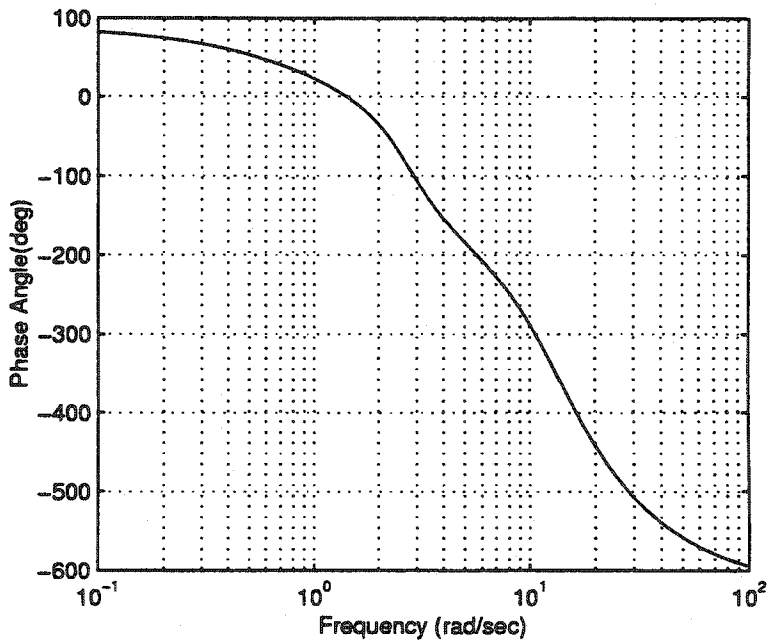

Figure 2.2: Phase plot of the actual disturbance sensitivity function corresponding to Case III c

indication of this frequency range. Hence the magnitude plot of the frequency response of disturbance sensitivity functions are observed over the range of disturbance dynamics used in this simulation in order to obtain the window of frequencies over which feedforward control is needed. The magnitude plot in Figure 2.1 illustrates the above discussion. An observation of such plots for all the cases as given in Table 2.1, showed a requirement for feedforward control in the frequency range of 0.5 - 6 rad/sec.

The feedback PI controller used in all the simulations in this chapter and in the next chapter is of constant gain type and it is tuned on the basis of Cianconne tuning rules[1]. The value of the controller proportional gain(K_P) calculated from the above mentioned process parameters is 0.325 and that of the integral gain(K_I) is 0.4924. The feedforward controller is designed at each control sampling instant by means of minimizing the magnitude of the function $G_{ff} + (G_d/G_p)$(where G_{ff} is the lead-lag with gain compensator shown in Equation 1.3) over the desired frequency range using sequential simplex optimization method. At each instant, the discrete frequency response of the process and disturbance transfer functions are obtained from the overparameterized recursive least squares coefficients. The discrete version of the feedforward controller is obtained from the continuous lead-lag with gain compensator shown in Equation 1.3 using the approximation $s = \frac{1-z^{-1}}{T}$ as shown in Equation 2.6.

$$G_{ff}(z^{-1}) = \frac{K_{ff}(\tau_{ld}(\frac{1-z^{-1}}{T}) + 1)}{(\tau_{lg}(\frac{1-z^{-1}}{T}) + 1)} = \frac{K_{ff}(\frac{\tau_{ld}}{T} + 1) - K_{ff}(\frac{\tau_{ld}}{T})z^{-1}}{(\frac{\tau_{lg}}{T} + 1) - (\frac{\tau_{lg}}{T})z^{-1}} \tag{2.6}$$

The value of the magnitude of the function $G_{ff} + (G_d/G_p)$ is evaluated at a set of normalized frequencies in the interval of interest and the sum of the value of the function at each frequency weighted by the normalized frequency(wT) is minimized using the sequential simplex optimization routine. The minimization involved is three dimensional and hence the shape of the simplex is a tetrahedron. Initial simplex is taken as a regular tetrahedron of size 0.5 with one of the vertices being (0.4, 0.4, -1.0). The optimization routine starts at the same initial point with the simplex of same dimension at every control instant in order to prevent the simplex from converging into a local minimum and not being able to adapt to the changing parameters. The maximum number of function evaluations for the optimization is chosen to be 200. The maximum function tolerance is taken to be 0.01. The optimization routine stops when it satisfies either of the above two conditions. The closed loop stability is guaranteed through out the set of simulations in this chapter and the next chapter, by imposing the condition that the lag time(τ_{lg}) is always greater than zero. This is implemented by imposing a huge penalty on the function value, every time the optimization routine returns a value for lag time less than zero.

The simulation run is started with equal process and disturbance parameters, $K_m = K_q = 2, \tau_m = \tau q = 0.4$ sec, $\tau_{dm} = \tau_{dq} = 0.6$ sec. The square wave setpoint changes with a period of 20 sec is carried out throughout the length of the simulation. The constant gain PI feedback controller is implemented with a sampling period of 0.05 sec, with P and I gains remaining the same. The square wave disturbance with a period of 15 sec is introduced at 60 sec and a constant parameter feedforward controller with parameters of $K_{ff} = -1.0, \tau_{ld} = 0.4$ sec and $\tau_{lg} = 0.5$ sec is switched on at the same time. After the RLS estimation sufficiently converges

initially, the frequency domain feedforward control is switched on and the effectiveness of the adaptive control strategy is tested by introducing changes in the disturbance dynamics as given in Table 2.1. The adaptive feedforward control is started at 120 sec. From this point, to the end of simulation the RLS estimation and subsequent frequency domain feedforward control takes place at every controller sampling period of 0.05 sec in conjunction with the constant gain PI controller.

The simulation results indicate that the overparameterized recursive least squares strategy employed accurately estimates both the disturbance and process dynamics in the presence of moderate levels of noise. Table 2.2 lists the error in the estimated process and disturbance frequency responses for all cases. The error($\tilde{G}$) is calculated by subtracting the magnitude/phase of the RLS estimated frequency response from that of the actual frequency response. Clearly, the estimated process and disturbance characteristics are accurate to 1 dB in magnitude and 15 deg in the phase in a majority of cases in the frequency range of 0.5 - 6 rad/sec where the feedforward control is implemented. The corresponding H_∞ and H_2 errors in the estimated process and disturbance frequency responses are given in Table 2.3. The H_∞ error is calculated as the maximum error in the frequency range, and H_2 error is calculated as the square root of sum of the square of the errors at three distinct points in the frequency range. In a majority of the cases these values are < 1 dB in magnitude and < 15 deg in phase angle. The feedforward controllers are designed in the frequency domain by minimizing the magnitude of the function $G_{ff} + (G_d/G_p)$ in the frequency interval of 0.5 - 6 rad/sec. The ratio (G_d/G_p) is therefore of equal importance to the accuracy of the individual factors, G_p and G_d in the design of feedforward controllers. The estimated magnitude and phase characteristics of (G_d/G_p) are given in Table 2.4. These estimation results are accurate to 1 dB in the magnitude plot and to 10 deg in the phase plot for almost all the cases in the frequency range of 0.5 - 6 rad/sec where the feedforward control is implemented.

The first change in the disturbance dynamics is introduced at 300 sec which corresponds to the dynamic combination Case III c. The magnitude plot and phase plot of the estimated process transfer function are shown in Figure 2.3 and Figure 2.4. The corresponding plots for the disturbance transfer function are shown in Figure 2.5 and Figure 2.6. These frequency response plots are obtained after 3000 samples by which time both the process and disturbance frequency responses converge. Bias changes in the process input that develop because of changes in the dynamics affect the convergence speed of the recursive least squares estimation. This is obvious in all the sets of simulations indicated in this chapter as well as in the next chapter. Hence all the frequency response plots that are included in this chapter are shown after 3000 samples(150 sec) following the change in dynamics. Figure 2.7 shows the magnitude plot and Figure 2.8 shows the phase plot of the feedforward controller obtained from the frequency domain design method, along with the theoretical controller required for perfect cancellation and the frequency response of the controller based on Shinskey's tuning rules. Figure 2.9 shows the magnitude plot of the distubance sensitivity function with and without feedforward control and Figure 2.10 shows the corresponding phase plot. Figure 2.11 shows the setpoint, process output and the disturbance introduced in the simulation. It is clear that feedforward control is not effective in completely eliminating the disturbance effect in this case because of the larger dead time in the manipulated variable path compared to that of the load path. The difference in magnitude and phase characteristics of actual

(G_d/G_p) ratio required for perfect cancellation and the feedforward controllers designed in frequency domain(based on the the (G_d/G_p) ratio obtained from individual RLS estimation of G_p, G_d coefficients) at three distinct frequencies in the interval of interest is given in Table 2.5. This difference is compared with the frequency response difference between the actual (G_d/G_p) ratio and a lead-lag with gain feedforward controller tuned using Shinskey's rules. These results for various dynamic combinations obtained by changing the disturbance dynamics as shown in Table 2.1 can be summarized as follows:

1. For Case III c, the frequency domain tuning method results in a better fit of the magnitude plot compared to Shinskey's tuning rules over all frequencies, where as the fit of the phase plot of Shinskey's tuning is better than that of the frequency domain method at low frequencies.

2. For Case I c, this method provides almost exact fit with both the theoretical magnitude and phase plots resulting in complete cancellation of the disturbance.

3. For Case II c, both the magnitude and phase plots resulted by the frequency domain method are close to the theoretical over all frequencies compared to Shinskey's tuning rules. A significant improvement in phase plot is observed particularly in the frequency domain approach.

4. For Case III b, the frequency domain method provides a significantly better magnitude fit to the theoretical than Shinskey's tuning rule based controller at high frequencies whereas both the methods result in almost identical phase plots.

5. For Case I b, the magnitude and phase plot of the feedforward controller designed are shown in Figure 2.13 and Figure 2.14. As it is seen the designed controller accurately matches the theoretical and hence complete compensation is obtained in this case. The corresponding time response is shown in Figure 2.12.

6. For Case II b, the frequency domain approach matches the theoretical over all the frequencies in both the magnitude and phase plots indicating complete cancellation of disturbance.

7. For Case III a, the frequency domain fit very closely approximates Shinskey's fit as indicated in Table 2.5 both giving a large phase error. This indicates the shortcoming of the nature of the lead-lag controller not being able to provide the required combination of lag plus prediction.

8. For Case I a, the frequency domain design method is found to provide a very close fit to the theoretical controller in both magnitude and phase plots indicating perfect cancellation.

9. For Case II a, the frequency response characteristics of the designed controller are shown in Figure 2.15 and Figure 2.16. Clearly the frequency domain design provides a better fit to the theoretical, in both the magnitude and phase plots compared to the controller based on Shinskey's rules.

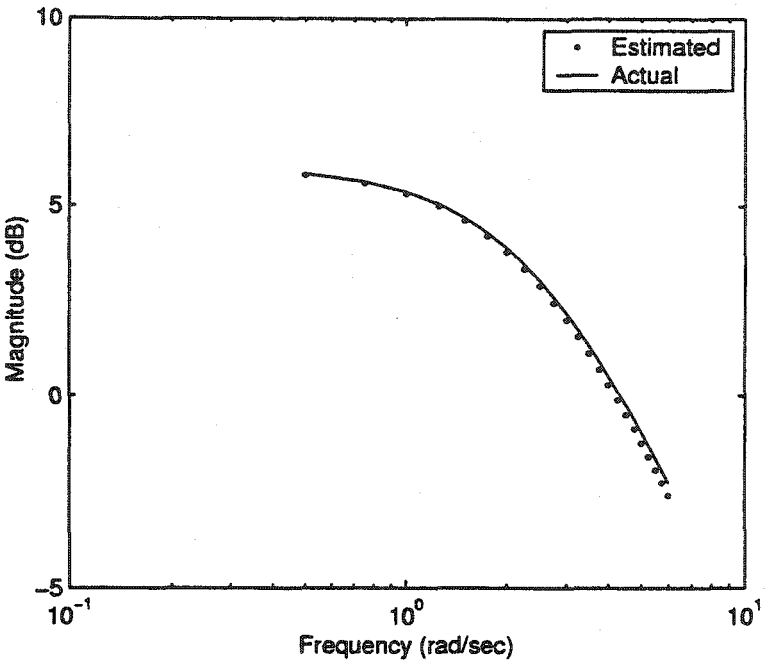

Figure 2.3: Magnitude plots of the estimated and actual process transfer function(G_p) corresponding to Case III c in the desired frequency range of 0.5 - 6 rad/sec

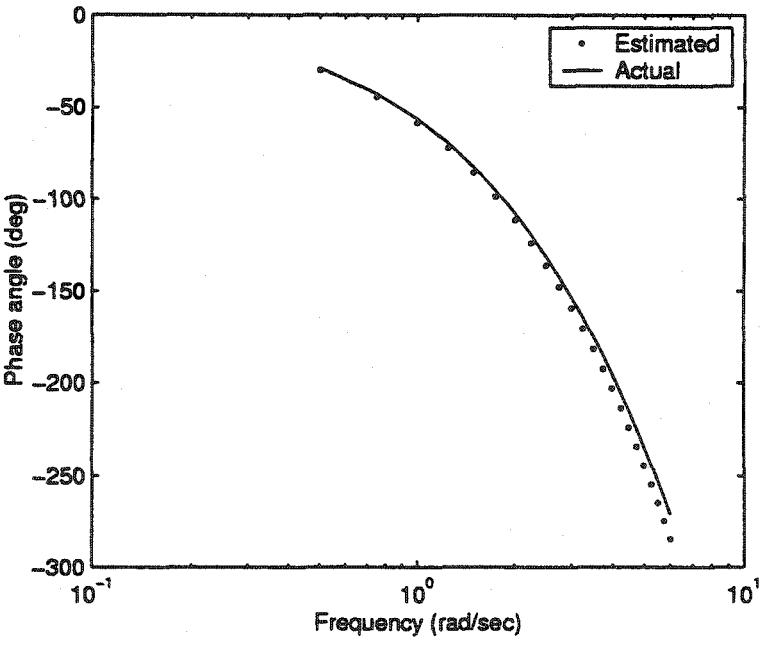

Figure 2.4: Phase plots of the estimated and actual process transfer function(G_p) corresponding to Case III c in the desired frequency range of 0.5 - 6 rad/sec

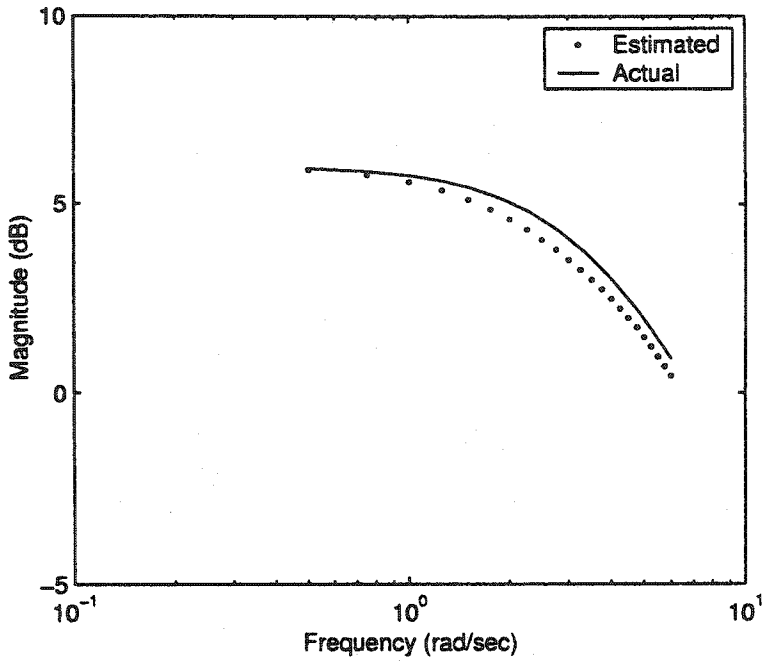

Figure 2.5: Magnitude plots of the estimated and actual disturbance transfer function(G_d) corresponding to Case III c in the desired frequency range of 0.5 - 6 rad/sec

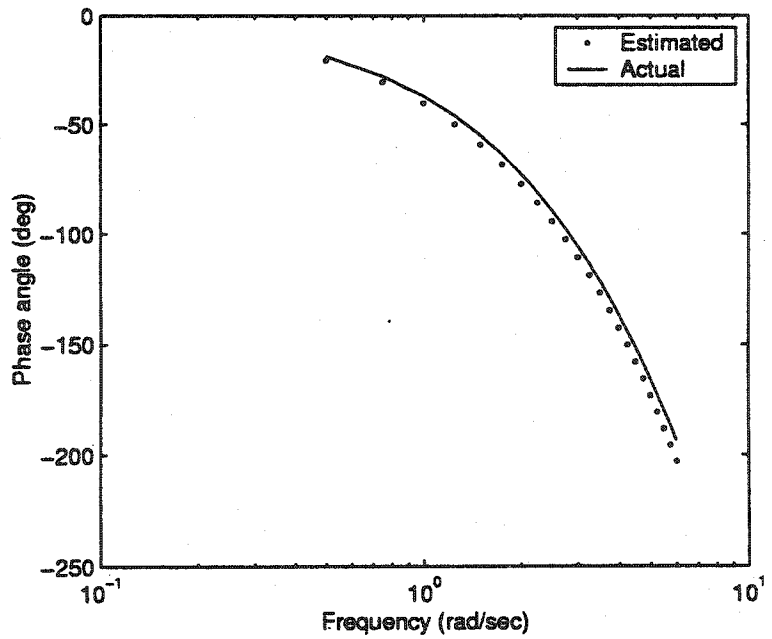

Figure 2.6: Phase plots of the estimated and actual disturbance transfer function(G_d) corresponding to Case III c in the desired frequency range of 0.5 - 6 rad/sec

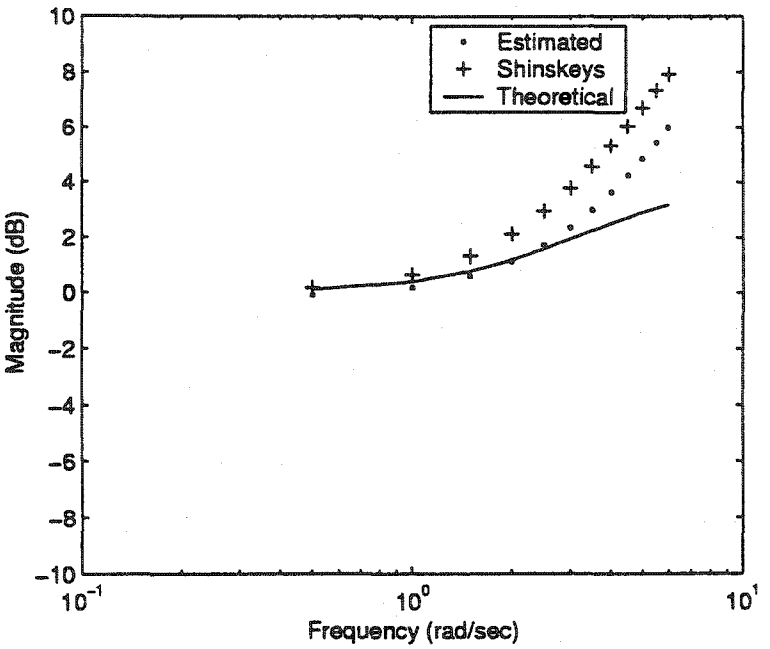

Figure 2.7: Magnitude plots of the frequency domain tuned(Simultaneous G_p, G_d identification), theoretical and Shinskey's tuning rule based feedforward controllers for Case III c

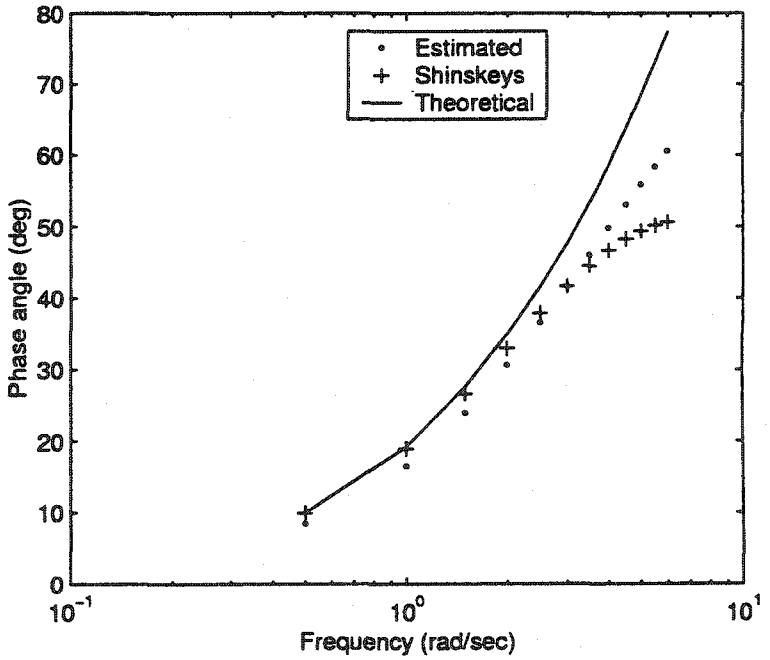

Figure 2.8: Phase plots of the frequency domain tuned(Simultaneous G_p, G_d identification), theoretical and Shinskey's tuning rule based feedforward controllers for Case III c

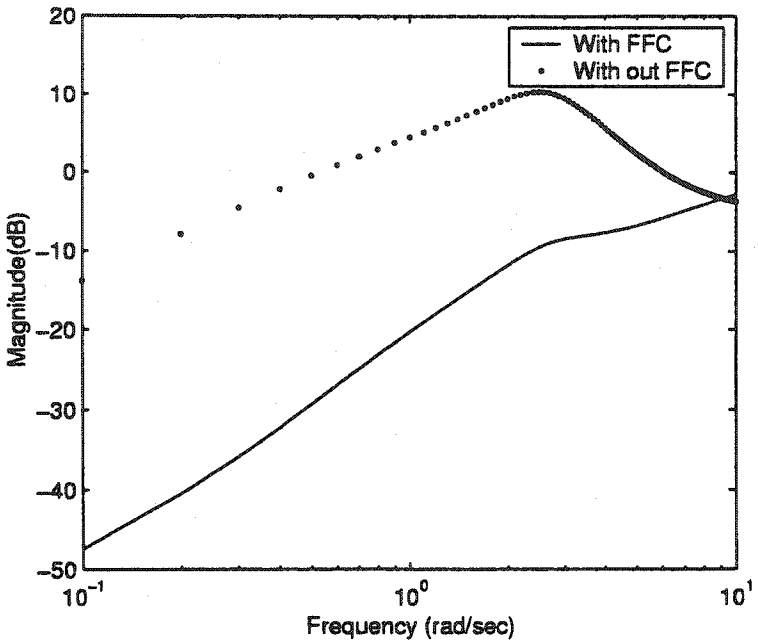

Figure 2.9: Magnitude plot of the disturbance sensitivity function with and without feedforward control for Case III c

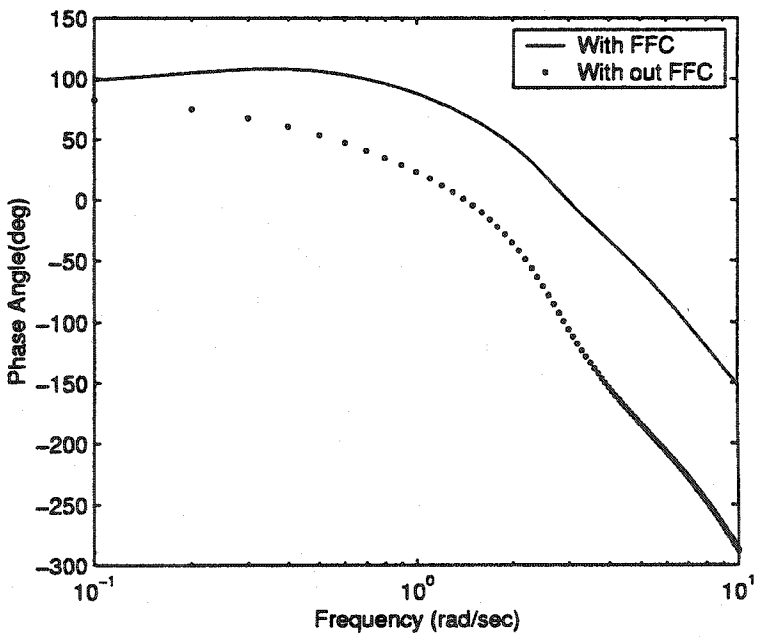

Figure 2.10: Phase plot of the disturbance sensitivity function with and without feedforward control for Case III c

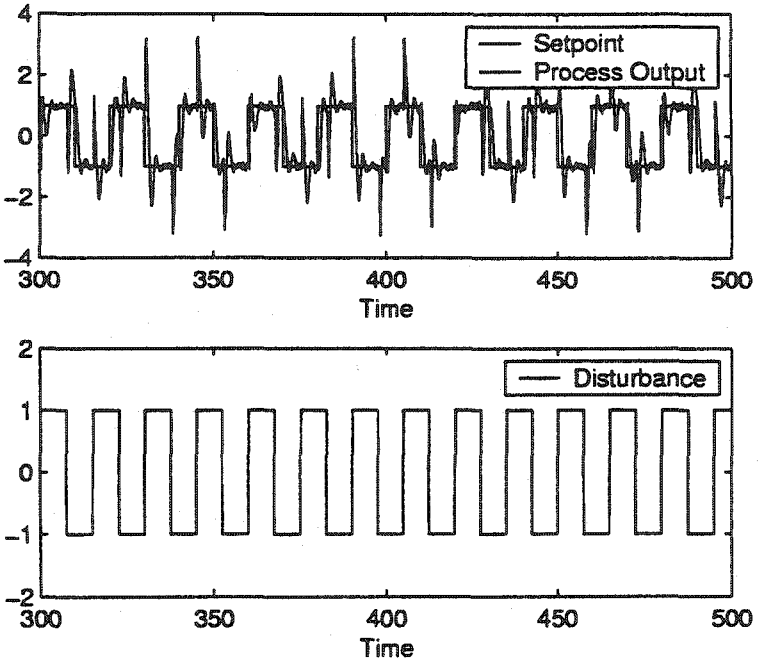

Figure 2.11: Time response for Case III c using frequency domain(Simultaneous G_p, G_d identification) approach

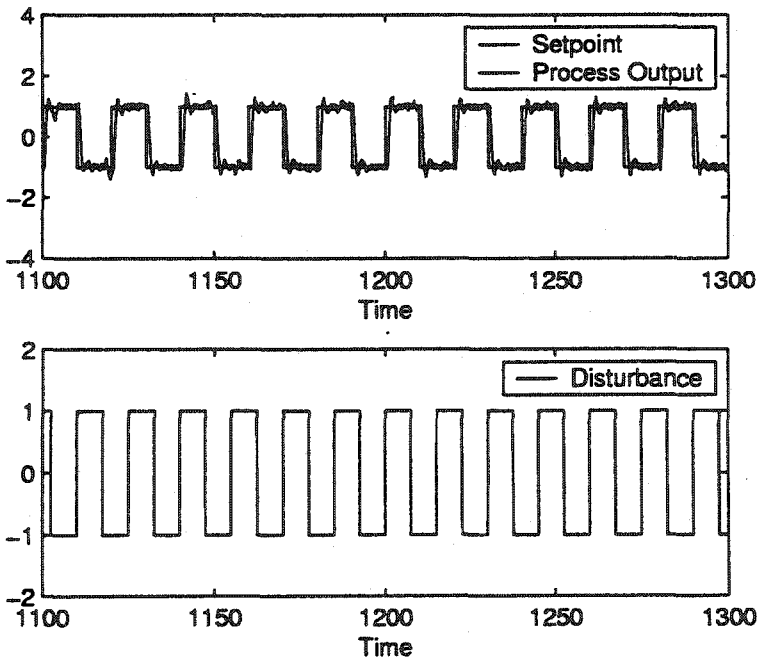

Figure 2.12: Time response for Case I b using frequency domain(Simultaneous G_p, G_d identification) approach

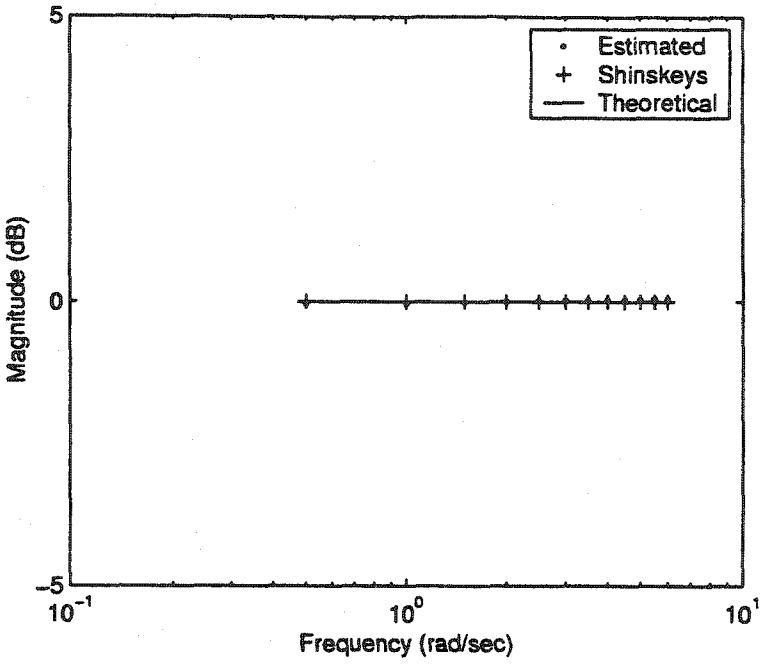

Figure 2.13: Magnitude plots of the frequency domain tuned(Simultaneous G_p, G_d identification), theoretical and Shinskey's tuning rule based feedforward controllers for Case I b

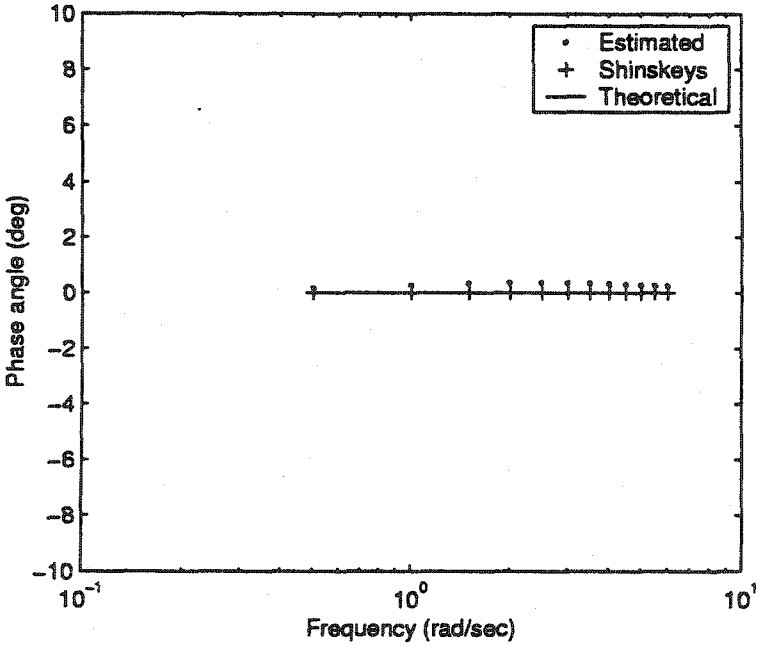

Figure 2.14: Phase plots of the frequency domain tuned(Simultaneous G_p, G_d identification), theoretical and Shinskey's tuning rule based feedforward controllers for Case I b

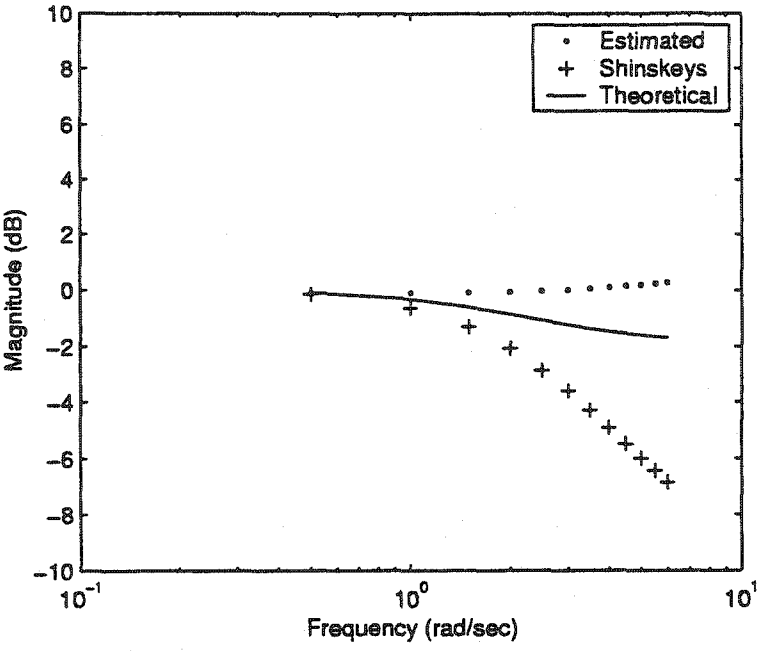

Figure 2.15: Magnitude plots of the frequency domain tuned(Simultaneous G_p, G_d identification), theoretical and Shinskey's tuning rule based feedforward controllers for Case II a

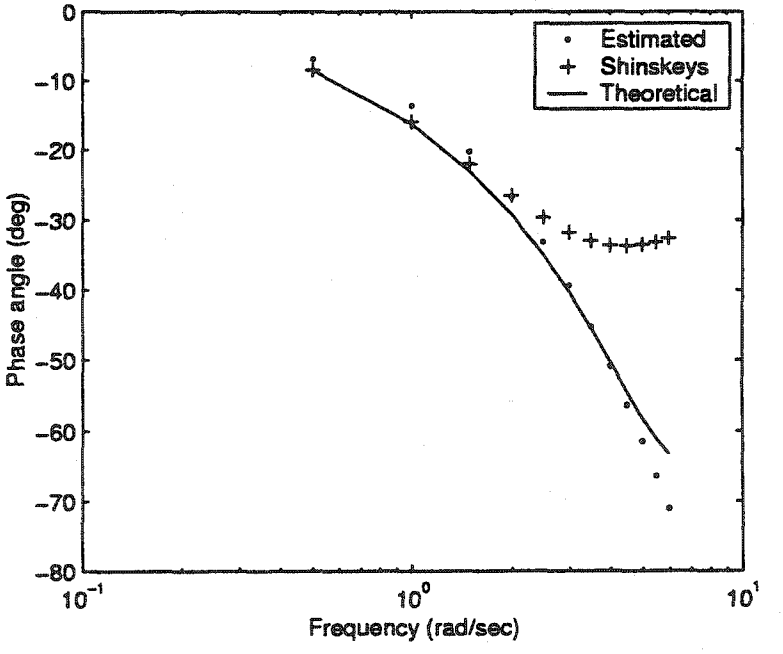

Figure 2.16: Phase plots of the frequency domain tuned(Simultaneous G_p, G_d identification), theoretical and Shinskey's tuning rule based feedforward controllers for Case II a

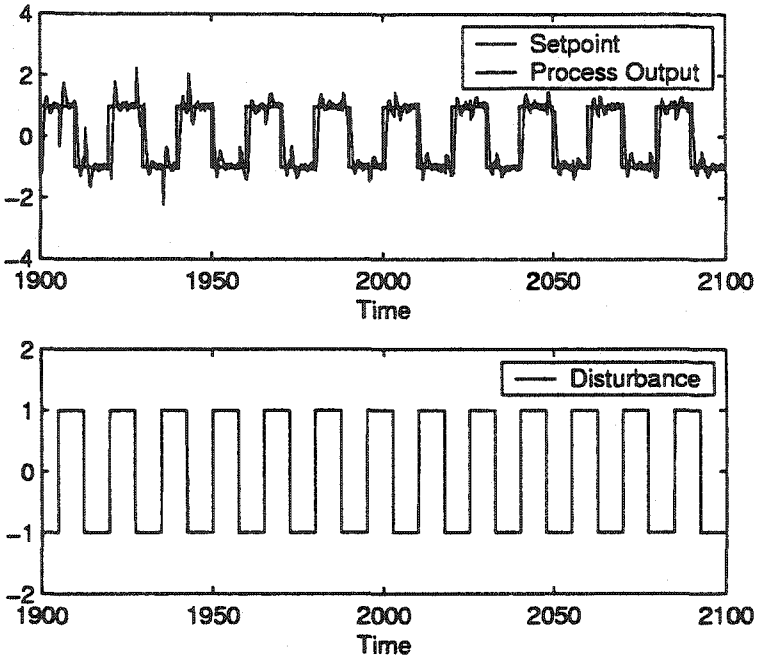

Figure 2.17: Time response for Case II a using frequency domain(Simultaneous G_p, G_d identification) approach

Case	w = 0.5 rad/sec				w = 2 rad/sec				w = 6 rad/sec			
	$\tilde{G}_p$ (dB)	$\tilde{G}_p$ (deg)	$\tilde{G}_d$ (dB)	$\tilde{G}_d$ (deg)	$\tilde{G}_p$ (dB)	$\tilde{G}_p$ (deg)	$\tilde{G}_d$ (dB)	$\tilde{G}_d$ (deg)	$\tilde{G}_p$ (dB)	$\tilde{G}_p$ (deg)	$\tilde{G}_d$ (dB)	$\tilde{G}_d$ (deg)
III c	0.05	2.0	0.05	2.0	0.1	4.0	0.46	5.0	0.30	13.5	0.43	9.0
I c	0.02	1.0	0.05	1.50	0.15	3.0	0.5	2.0	0.42	8.50	0.40	2.50
II c	0.05	0.50	0.0	0.50	0.40	2.0	0.20	2.0	0.07	17.0	0.30	17.0
III b	0.02	0.50	0.05	2.0	0.05	3.0	0.01	5.0	0.3	13.0	0.95	13.0
I b	0.01	0.50	0.02	1.0	0.13	2.0	0.2	1.0	0.15	7.0	0.50	3.50
II b	0.02	1.0	0.02	2.0	0.21	3.50	0.30	3.0	0.47	9.0	0.85	18.0
III a	0.02	2.0	0.02	1.0	0.01	4.5	0.20	8.0	0.32	16.0	2.60	11.0
I a	0.03	1.0	0.1	0.30	0.20	3.0	0.22	1.80	0.38	9.0	1.20	12.50
II a	0.05	3.0	0.10	1.0	0.75	6.50	0.13	4.0	1.35	9.0	0.95	24.0

Table 2.2: Difference in magnitude and phase plots between the actual and estimated, process($\tilde{G}_p$) and disturbance($\tilde{G}_d$) frequency responses for the 9 possible combinations

Case	H_∞ error				H_2 error			
	$\tilde{G}_p$ (dB)	$\tilde{G}_p$ (deg)	$\tilde{G}_d$ (dB)	$\tilde{G}_d$ (deg)	$\tilde{G}_p$ (dB)	$\tilde{G}_p$ (deg)	$\tilde{G}_d$ (dB)	$\tilde{G}_d$ (deg)
III c	0.3	13.5	0.55	9.0	0.32	14.22	0.63	10.49
I c	0.42	8.5	0.68	2.5	0.45	9.07	0.64	3.54
II c	0.55	17	0.35	17.0	0.41	17.10	0.36	17.10
III b	0.30	13.0	0.95	13.0	0.31	13.35	0.95	14.07
I b	0.20	7.0	0.50	3.50	0.20	7.30	0.54	3.78
II b	0.47	9.0	0.85	18.0	0.52	9.71	0.90	18.36
III a	0.32	16.0	2.60	16.0	0.32	16.74	2.61	13.64
I a	0.38	9.0	1.20	12.5	0.43	9.54	1.22	12.63
II a	1.35	9.0	0.95	24.0	1.55	11.5	0.96	24.36

Table 2.3: H_∞ and H_2 error in magnitude and phase plots between the actual and estimated, process($\tilde{G}_p$) and disturbance($\tilde{G}_d$) frequency responses for the 9 possible combinations

Case	w = 0.5 rad/sec		w = 2 rad/sec		w = 6 rad/sec		H_∞ error		H_2 error	
	$\frac{\tilde{G}_d}{G_p}$ (dB)	$\frac{\tilde{G}_d}{G_p}$ (deg)	$\frac{\tilde{G}_d}{G_p}$ (dB)	$\frac{\tilde{G}_d}{G_p}$ (deg)	$\frac{\tilde{G}_d}{G_p}$ (dB)	$\frac{\tilde{G}_d}{G_p}$ (deg)	$\frac{\tilde{G}_d}{G_p}$ (dB)	$\frac{\tilde{G}_d}{G_p}$ (deg)	$\frac{\tilde{G}_d}{G_p}$ (dB)	$\frac{\tilde{G}_d}{G_p}$ (deg)
III c	0.01	1.0	0.35	1.0	0.13	4.0	0.40	4.0	0.37	4.24
I c	0.01	0.50	0.38	1.0	0.01	5.9	0.45	6.1	0.38	6.0
II c	0.01	1.0	0.60	0.20	0.22	0.80	0.90	5.50	0.64	1.30
III b	0.0	0.50	0.10	2.0	0.65	0.0	0.65	3.5	0.66	2.06
I b	0.0	0.10	0.08	1.20	0.38	3.50	0.38	3.50	0.39	3.70
II b	0.0	0.10	0.05	0.80	0.40	9.0	0.40	9.0	0.40	9.04
III a	0.01	0.2	0.15	2.80	2.35	4.25	2.35	6.25	2.35	5.09
I a	0.04	1.50	0.42	1.30	0.82	3.50	0.82	3.75	0.92	4.02
II a	0.10	1.80	0.60	2.78	0.48	15.8	0.88	15.8	0.77	16.14

Table 2.4: Difference in magnitude and phase plots between the actual and estimated along with the corresponding H_∞ and H_2 error for (G_d/G_p) frequency responses for the 9 possible combinations

Case	w = 0.5 rad/sec				w = 2 rad/sec				w = 6 rad/sec			
	$\tilde{F}$ (dB)	$\tilde{F}$ (deg)	$\tilde{S}$ (dB)	$\tilde{S}$ (deg)	$\tilde{F}$ (dB)	$\tilde{F}$ (deg)	$\tilde{S}$ (dB)	$\tilde{S}$ (deg)	$\tilde{F}$ (dB)	$\tilde{F}$ (deg)	$\tilde{S}$ (dB)	$\tilde{S}$ (deg)
III c	0.10	2.0	0.05	0.0	0.01	5.0	0.4	2.0	2.80	17.0	4.75	29.0
I c	0.0	1.0	0.0	0.0	0.42	0.50	0.0	0.0	0.10	9.0	0.0	0.0
II c	0.10	1.0	0.25	0.50	1.10	1.0	1.50	10.0	2.10	20.0	3.60	58.0
III b	1.20	1.0	0.05	0.50	0.75	4.0	0.78	2.0	3.1	19.0	4.25	23.0
I b	0.03	0.20	0.0	0.0	0.0	0.60	0.0	0.0	0.10	0.20	0.0	0.0
II b	0.0	0.10	0.0	0.0	0.05	0.0	0.3	0.0	0.85	3.0	0.0	6.75
III a	0.20	1.0	0.25	2.0	1.10	11.0	1.60	13.0	2.80	59.0	2.60	64.0
I a	0.10	1.0	0.0	0.0	0.35	0.50	0.0	0.0	0.20	5.0	0.0	0.0
II a	0.10	1.50	0.10	0.0	0.80	2.50	1.23	3.0	2.0	8.50	5.20	41.0

Table 2.5: Difference in the magnitude and phase plots of theoretical and frequency domain(Simultaneous G_p, G_d identification) method($\tilde{F}$), theoretical and Shinskey's controllers($\tilde{S}$), for the 9 possible cases

Case	H_∞ error				H_2 error			
	$\tilde{F}$ (dB)	$\tilde{F}$ (deg)	$\tilde{S}$ (dB)	$\tilde{S}$ (deg)	$\tilde{F}$ (dB)	$\tilde{F}$ (deg)	$\tilde{S}$ (dB)	$\tilde{S}$ (deg)
III c	2.80	17.0	4.75	29.0	2.80	17.83	4.77	29.07
I c	0.50	9.0	0.0	0.0	0.43	9.07	0.0	0.0
II c	2.10	20.0	3.60	58.0	2.37	20.05	3.91	58.86
III b	3.10	19.0	4.25	23.0	3.41	19.44	4.32	23.09
I b	0.10	0.20	0.0	0.0	0.10	0.66	0.0	0.0
II b	0.85	3.0	0.0	6.75	0.85	3.0	0.0	6.76
III a	2.80	59.0	2.60	64.0	3.02	60.02	3.06	65.31
I a	0.60	5.0	0.0	0.0	0.42	5.12	0.0	0.0
II a	2.0	8.50	5.20	41.0	2.16	8.99	5.30	41.10

Table 2.6: H_∞ and H_2 error in the magnitude and phase plots of theoretical and frequency domain(Simultaneous G_p, G_d identification) method($\tilde{F}$), theoretical and Shinskey's controllers ($\tilde{S}$), for the 9 possible cases

Case	Shinskey's tuning			Frequency domain tuning		
	τ_{lead} (sec)	τ_{lag} (sec)	K_{ff} ($\frac{\%}{\%}$)	τ_{lead} (sec)	τ_{lag} (sec)	K_{ff} ($\frac{\%}{\%}$)
III c	0.40	0.05	-1.0	0.29	0.0003	-0.98
I c	0.40	0.25	-1.0	0.24	0.12	-1.00
II c	1.0	1.05	-1.0	-0.09	0.0002	-0.99
III b	0.22	0.022	-1.0	0.22	0.008	-0.86
I b	0.40	0.40	-1.0	0.43	0.42	-0.99
II b	-0.10	0.10	-1.0	-0.12	0.08	-1.00
III a	1.0	0.9	-1.0	0.53	0.40	-0.94
I a	0.40	0.50	-1.0	0.12	0.18	-0.98
II a	0.12	0.42	-1.0	-0.13	0.11	-0.99

Table 2.7: Tuning parameter values for the 9 cases used in the simulation based on Shinskey's tuning rules and frequency domain(Simultaneous G_p, G_d identification) method

Chapter 3

Frequency domain feedforward control tuning based on closed loop identification techniques

3.1 Introduction

Almost all processes in a plant operate in closed loop for various reasons of safety, performance etc. System identification in closed loop is explored by numerous authors in the literature and it is still an area of active research interest. In the previous chapter, the feedforward controllers were tuned by direct estimation of the process and disturbance transfer functions followed by frequency domain tuning based on the (G_d/G_p) ratio. Perfect feedforward control under any dynamic combination requires a controller which closely approximates this ratio. Hence the key step in designing feedforward controllers is the accurate estimation of this ratio. In this chapter various alternatives to obtain this ratio are tested and their effectiveness in designing feedforward controllers is studied.

The extended least squares type of estimation used in the previous chapter takes changes in both process and disturbance dynamics into account, in order to design feedforward controllers under various conditions. But in certain situations, the change in disturbance dynamics can be significant whereas the process dynamics can remain fairly constant. In such situations it will be more appropriate to estimate the disturbance dynamics alone continuously for the design of feedforward controllers.

In the closed loop system shown in Figure 1.1, two closed loop transfer functions are often of significant interest, disturbance sensitivity function(S_d) and complementary sensitivity function(T). The transfer function from the disturbance(d) to the process output(y) is known as the disturbance sensitivity function and before introducing feedforward control it has the transfer function of the form shown in Equation 3.1 below:

$$S_d = \frac{y}{d} = \frac{G_d}{(1 + G_p G_c)} \tag{3.1}$$

The complementary sensitivity function is the transfer function from the setpoint(r) to

the process output(y) and has the form shown in Equation 3.2:

$$T = \frac{y}{r} = \frac{G_p G_c}{(1 + G_p G_c)} \tag{3.2}$$

Three different methods for obtaining the ratio (G_d/G_p) through the estimation of these transfer functions are proposed in this chapter. In all the three methods it is assumed that the process dynamics are constant and the disturbance dynamics vary with time. In situations where process dynamics also change along with the disturbance dynamics, sequential probing and identification of process and disturbance dynamics can be carried out. In the first method the disturbance sensitivity function is estimated and the previously computed process data along with the knowledge of feedback controller are used to open this disturbance sensitivity function in order to obtain the disturbance transfer function, G_d. In the second method, an alternative to opening the closed loop disturbance sensitivity function is proposed by tuning the feedforward controller on the basis of the ratio ($S_d C/T$) where S_d is the disturbance sensitivity function shown in Equation 3.1, T is the complementary sensitivity function shown in Equation 3.2 and C is the PI feedback controller. In the third approach, the ratio of the transfer functions from the disturbance(d) to process input(u) and the transfer function from the setpoint(r) to process output(y), which is mathematically equivalent to the required ratio (G_d/G_p) is used for tuning.

3.2 Frequency domain tuning based on extraction of G_d from the disturbance sensitivity function - Simulation results

The effect of disturbance on any controlled variable can be characterized by the relevant disturbance sensitivity function. Frequency response of such a function is a convenient way of analyzing the effect of various frequency disturbances on the controlled variable. In this simulation, initially the square wave setpoint changes with a period of 20 sec is introduced. The process transfer function(G_p) estimation is carried out using the recursive least squares approach on the process input(u) and the process output(y). During this stage no disturbances are introduced in the loop and the output is only under the influence of the Gaussian measurement noise and the constant gain PI feedback controller. The process parameters, feedback controller gains, as well as RLS parameters and the various initial values are chosen the same as mentioned in Chapter 2. Unlike the case where G_p and G_d are estimated simultaneously, in this type of estimation the denominator coefficients of the two transfer functions can be chosen independently. As the process dynamics are not being varied, 3 coefficients in the numerator and 2 coefficients in the denominator are used in the discrete version of the estimated process transfer function as shown in Equation 3.3.

$$G_p(z^{-1}) = \frac{y(z^{-1})}{u(z^{-1})} = \frac{z^{-12}(b_0 + b_1 z^{-1} + b_2 z^{-2})}{(1 + a_1 z^{-1} + a_2 z^{-2})} \tag{3.3}$$

The z^{-12} term in the numerator corresponds to the continuous time process delay of 0.6 sec, discretized at a sampling period of 0.05 sec. After the process transfer function estimation has sufficiently converged indicated by the convergence of its frequency response, the estimation of G_p and changes in setpoint are stopped. Square wave disturbance with a period of 15 sec is introduced at 300 sec. From this point, the recursive least squares estimation is carried on the disturbance(d) and process output(y) so as to estimate the disturbance sensitivity function. The model of the discrete time disturbance sensitivity function used in the estimation is as shown in equation 3.4.

$$S_d(z^{-1}) = \frac{y(z^{-1})}{d(z^{-1})} = \frac{z^{-8}(c_0 + c_1 z^{-1} + c_2 z^{-2} + ... + c_{14} z^{-14})}{(1 + d_1 z^{-1} + d_2 z^{-2} + ... + d_{20} z^{-20})} \tag{3.4}$$

The choice of the z^{-8} factor in the numerator is based on the presence of the G_d term in the numerator of the disturbance sensitivity function(Equation 3.1), for which the lower limit of the continuous time delay is 0.4 sec sampled at 0.05 sec. The choice of 15 coefficients in the numerator is based upon the change in disturbance delay during the simulation. 20 coefficients are taken in the denominator to account for the presence of discrete process and controller transfer functions in Equation 3.1. A few more coefficients than actually needed are taken in both the numerator and denominator polynomials, as it is has been noticed to result in an accurate estimate of the frequency response in the presence of measurement noise. The recursive identification(of disturbance sensitivity function) is carried out only in the presence of the feedback controller. After the disturbance sensitivity function identification converges sufficiently in each case(as indicated by the convergence of the frequency response) the identification is stopped and the tuning is performed. The process frequency response is computed using the recursive least squares coefficients estimated during the process estimation stage. On the other hand, the disturbance frequency response is calculated in two stages. In the first stage the identified parameters of disturbance sensitivity function are used in calculating its frequency response. The knowledge of the PI gain values of the feedback controller is utilized in computing the controller frequency response. The second stage involves deriving the disturbance frequency response from the disturbance sensitivity function, process and controller frequency responses as shown below:

$$S_d(w) = \frac{G_d(w)}{1 + G_p(w)G_c(w)} \Rightarrow G_d(w) = S_d(w) \times [1 + G_p(w)G_c(w)] \tag{3.5}$$

The frequency response of the discrete lead-lag with gain feedforward controller is calculated using Equation 2.6. The value of the magnitude of the function $G_{ff} + (G_d/G_p)$ is computed at various frequencies in the normalized frequency(wT) range of 0.025 to 0.3 rads which corresponds to the unnormalized frequency of 0.5 to 6 rad/sec. The weighted sum of the magnitude of function at each frequency is minimized by using Nelder-Mead's simplex method. The weighting factor used is of the type $\frac{1}{wT}$, so that lower frequencies get more weighting compared to the higher frequencies. The various constraints imposed on the optimization routine are the same as mentioned in the previous chapter.

Initially the process transfer function G_p is estimated as before using the discrete time model shown in Equation 3.3. The magnitude plot of the estimated process is shown in Figure 3.1 and the phase plot of the process is shown in Figure 3.2. In all the sets of

simulations in this chapter, the disturbance dynamics are changed according to Table 2.1. The disturbance dynamics are changed every 200 sec in order to simulate the various cases. In each interval of 200 sec, the disturbance sensitivity function estimation is carried out for the first 150 sec, so that its frequency response converges sufficiently in all the cases and the frequency domain feedforward control tuning is applied during the next 50 sec. At 300 sec, the disturbance dynamics correspond to the dynamic combination Case III c. The RLS identification of the disturbance sensitivity function is performed until 450 sec, and at 450 sec the RLS identification is turned off and the frequency domain tuning as well as feedforward control on the basis of the tuning values returned by the optimization routine is applied. The magnitude and phase plots of the frequency response of the disturbance sensitivity function are shown in Figure 3.3 and Figure 3.4. The disturbance frequency response derived by opening the disturbance sensitivity function is shown in the magnitude plot, Figure 3.5 and phase plot, Figure 3.6.

The value of the disturbance sensitivity function magnitude is very small at very low frequencies because of the I gain of the PI feedback controller. On the other hand, the value of the disturbance sensitivity function magnitude also becomes very small value at higher frequencies because of the first order lag characteristic present in the disturbance process, G_d. Hence the magnitude of disturbance sensitivity function is above 0 dB only in a certain frequency range and this is the frequency range in which accurate estimation of disturbance sensitivity function is carried out for feedforward control. In all the cases that are considered in this simulation, this range of frequencies is observed to be 0.5 to 6 rad/sec. Hence all the frequency response plots that are shown in this chapter are plotted in this frequency range. The results of the estimation of the disturbance sensitivity function and the disturbance process frequency responses are tabulated in Table 3.1 and Table 3.2. It is clear that all the estimation of frequency responses are accurate to 1.5 dB in the magnitude plot and about 10 degrees in phase plot, for all the cases.

1. For Case III c, the feedforward controller magnitude plot is shown in Figure 3.7 and the phase plot is shown in Figure 3.8. It is clear that feedforward control is not effective in cancelling the disturbances at all frequencies because of the theoretical requirement of a lead plus prediction based controller. The frequency response of Shinskey's tuning based controller is close to the theoretical compared to the frequency domain method at low frequencies. Time response of the frequency domain tuned controller for this case is given in Figure 3.9 and the time response using Shinskey's tuning rules is given in Figure 3.10. As indicated in the fit of the frequency response, Shinskey's tuning provides better time response compared to the frequency domain method for this case.

2. For Case I c, both the approaches provide almost perfect cancellation of disturbance as observed through the fit of the frequency response of the controllers(Table 3.3 and Table 3.4).

3. For Case II c, the frequency domain approach provides a better fit of both the magnitude and the phase plots compared to Shinskey's tuning.

4. For Case III b, this method provides a better fit of the magnitude plot compared to Shinskey's fit at the expense of the phase plot.

5. For Case I b, both the magnitude and phase plots of the two methods match with the flat theoretical plots as can be seen in Figure 3.11 and Figure 3.12. The complete cancellation of disturbance is also obvious in the time response shown in Figure 3.13.

6. For Case II b, the magnitude and phase plots of both the frequency domain method and Shinskey's method very well match with the theoretical.

7. For Case III a, the theoretical controller calls for a combination of lag and prediction. With the nature of the controller used, both the Shinskey's and frequency domain tuning approach provide very close results indicating the conflicting requirement of lag along with lead for prediction.

8. For Case I a, both the methods provide accurate fit of magnitude and phase plots to the theoretical, providing complete cancellation of the disturbance.

9. For Case II a, the theoretical controller calls for a combination of lag plus dead time. The frequency domain method tuning used provides a better fit in the magnitude as well as the phase plots as shown in Figure 3.15 and Figure 3.16. The effectiveness of this method is also illustrated by comparing the time responses using this method in Figure 3.17 with that of Shinskey's tuning in Figure 3.18.

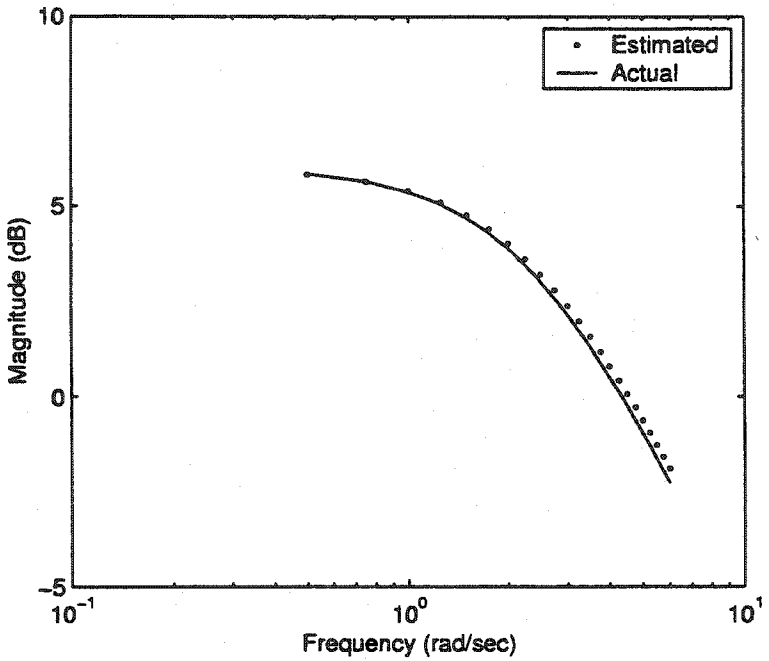

Figure 3.1: Magnitude plots of the estimated and actual process(G_p) in the desired frequency range of 0.5 to 6 rad/sec

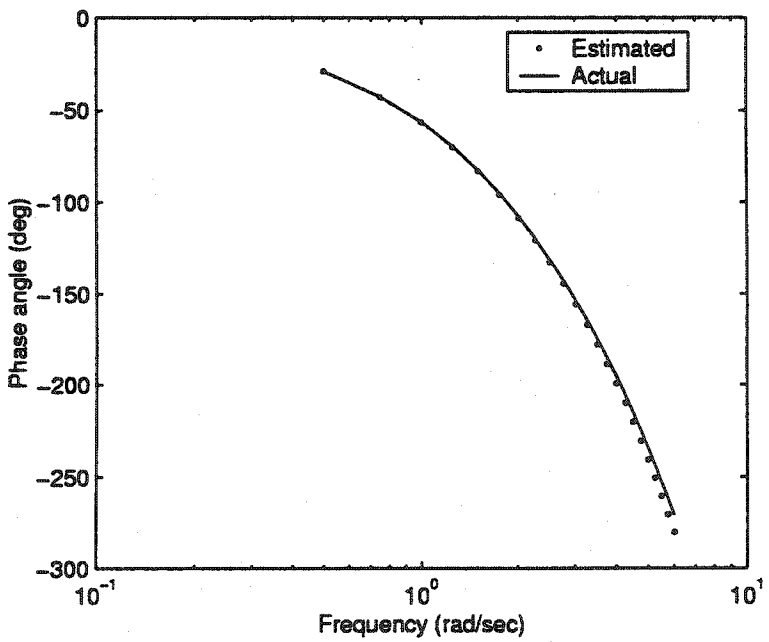

Figure 3.2: Phase plots of the estimated and actual process(G_p) in the desired frequency range of 0.5 to 6 rad/sec

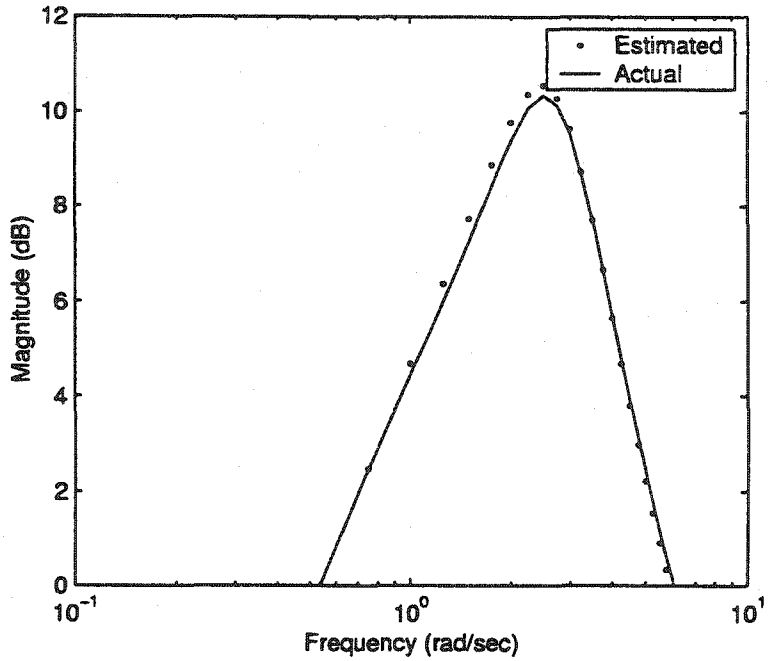

Figure 3.3: Magnitude plots of the estimated and actual disturbance sensitivity function(S_d) corresponding to Case III c in the desired frequency range of 0.5 to 6 rad/sec

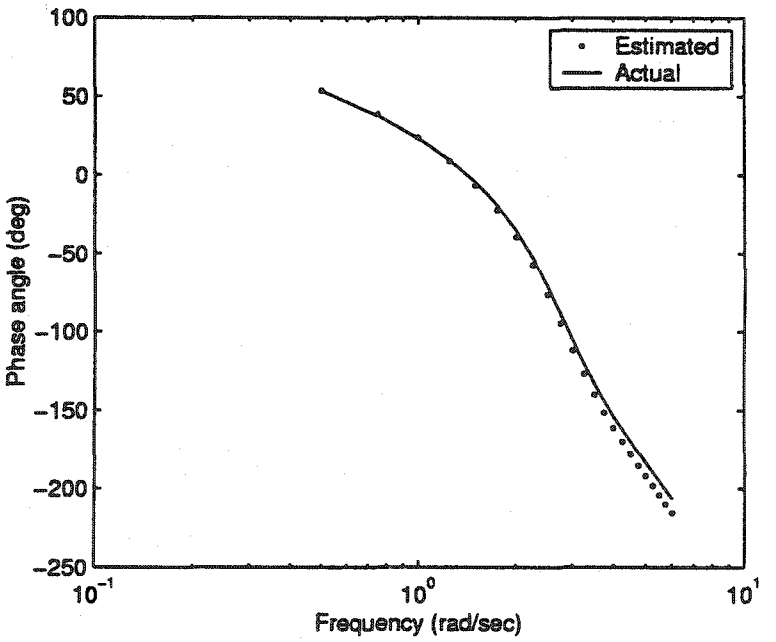

Figure 3.4: Phase plots of the estimated and actual disturbance sensitivity function(S_d) corresponding to Case III c in the desired frequency range of 0.5 to 6 rad/sec

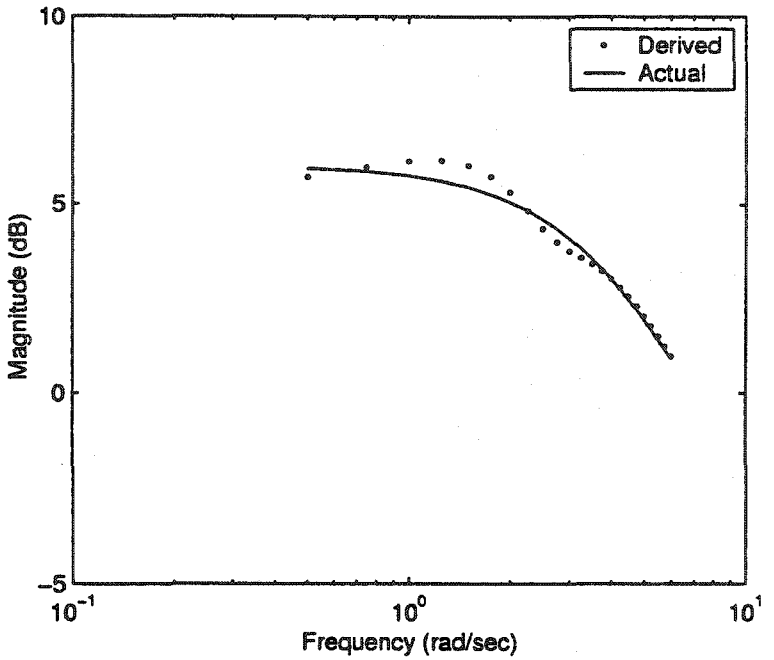

Figure 3.5: Magnitude plots of the derived(from S_d) and actual disturbance transfer function(G_d) corresponding to Case III c

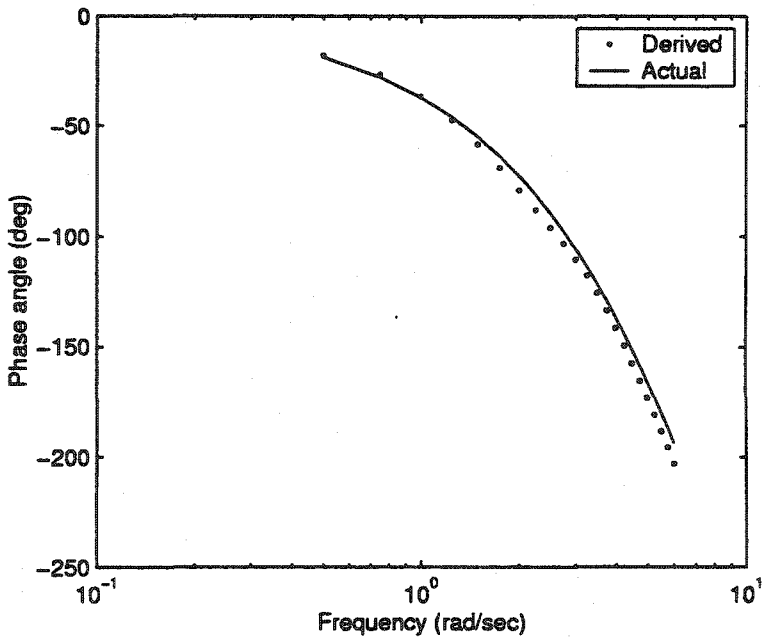

Figure 3.6: Phase plots of the derived(from S_d) and actual disturbance transfer function(G_d) corresponding to Case III c

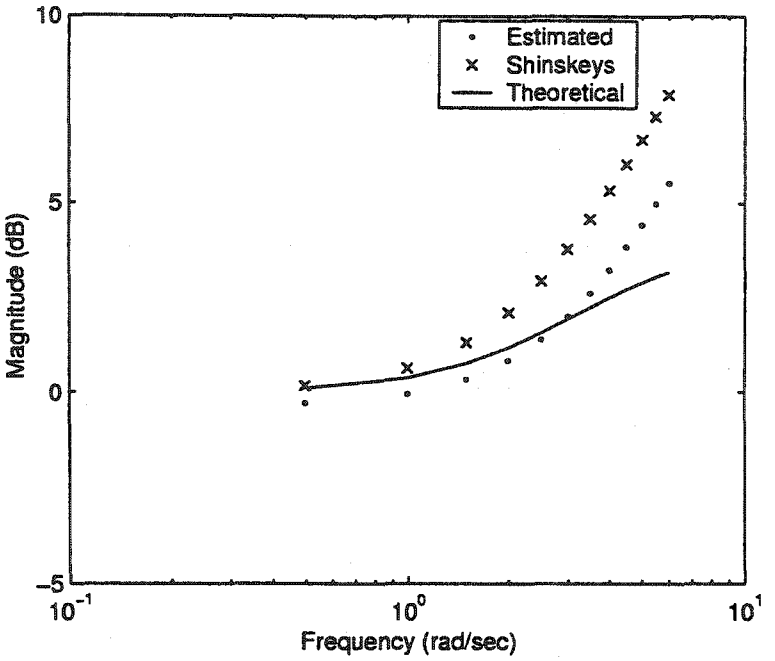

Figure 3.7: Magnitude plots of the frequency domain tuned(using G_d from S_d method), theoretical and Shinskey's tuning rule based feedforward controllers for Case III c

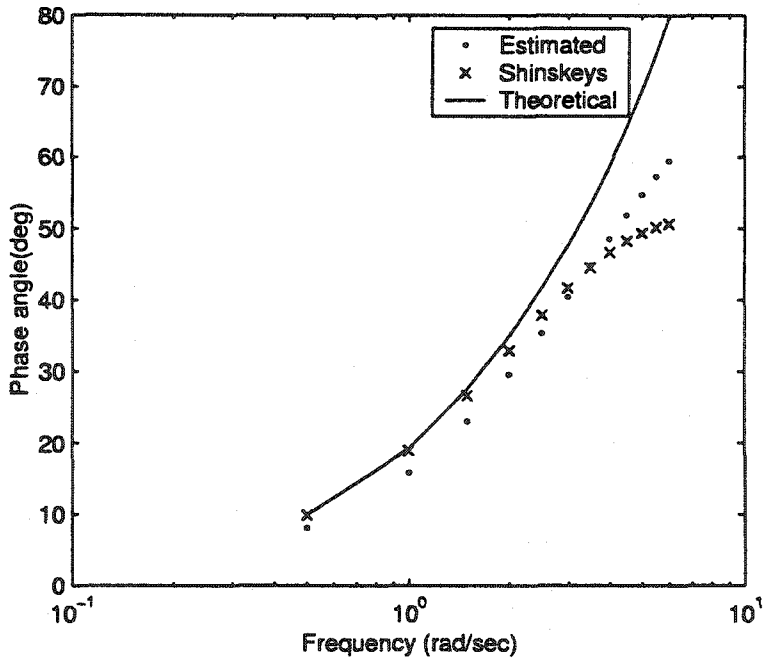

Figure 3.8: Phase plots of the frequency domain tuned(using G_d from S_d method), theoretical and Shinskey's tuning rule based feedforward controllers for Case III c

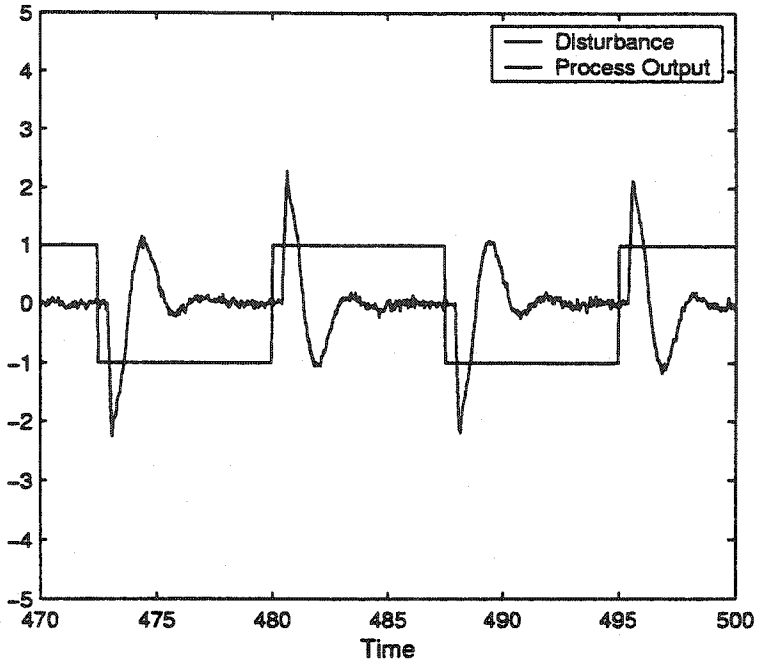

Figure 3.9: Time response for Case III c using frequency domain(G_d from S_d) approach

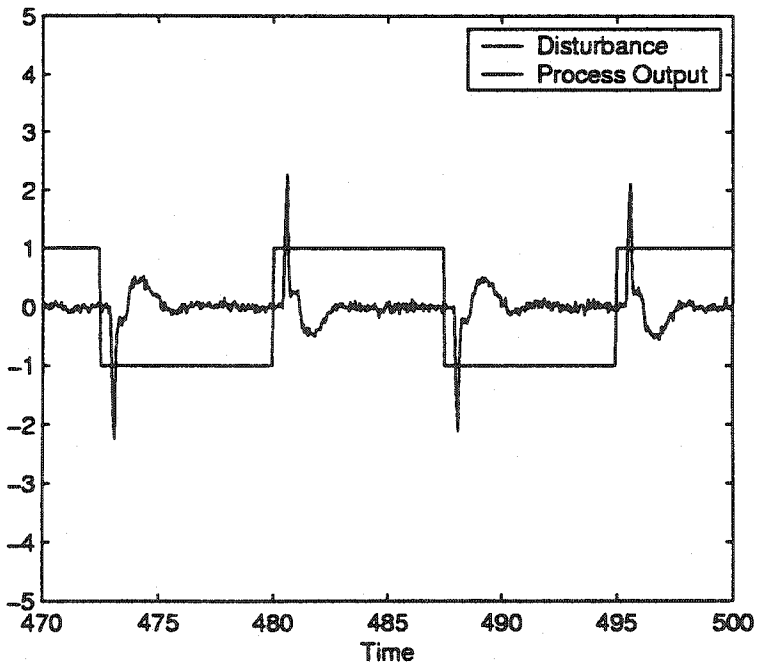

Figure 3.10: Time response for Case III c using Shinskey's tuning rules

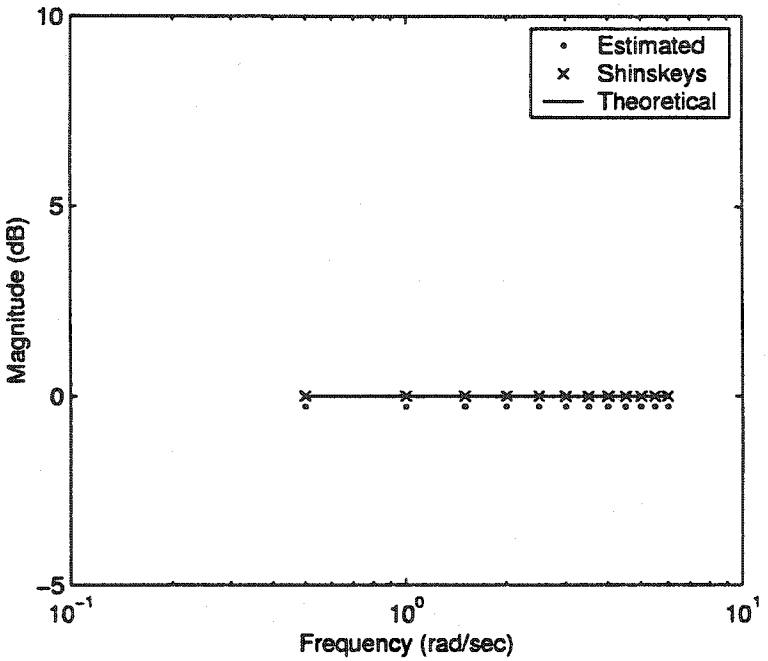

Figure 3.11: Magnitude plots of the frequency domain tuned(using G_d from S_d method), theoretical and Shinskey's tuning rule based feedforward controllers for Case I b

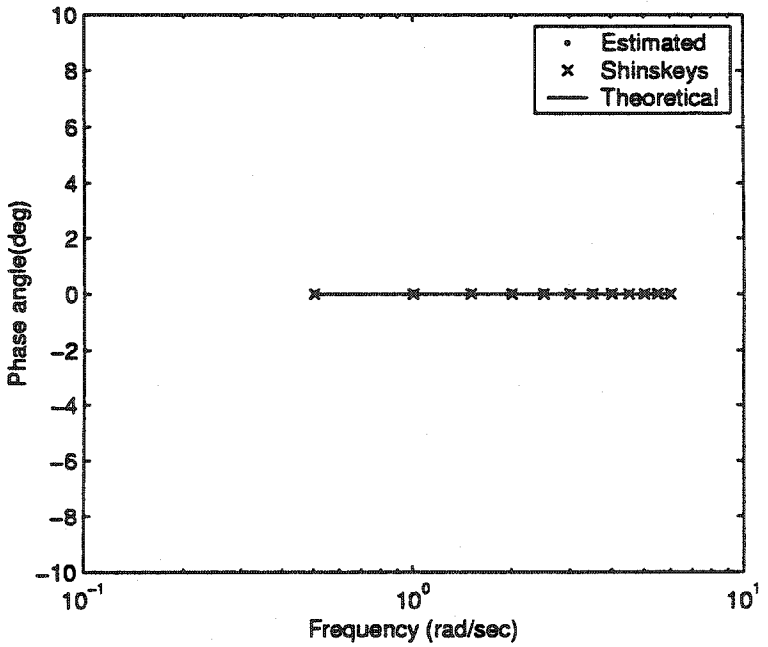

Figure 3.12: Phase plots of the frequency domain tuned(using G_d from S_d method), theoretical and Shinskey's tuning rule based feedforward controllers for Case I b

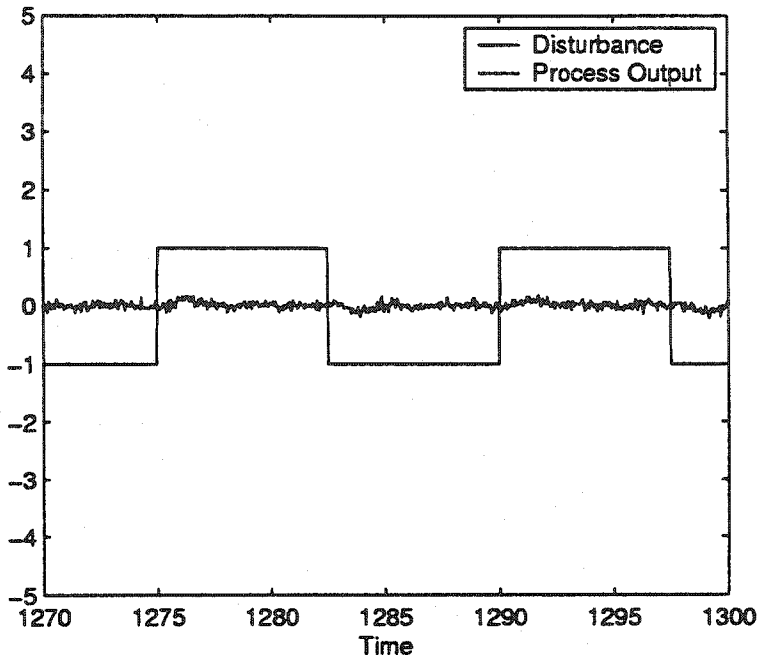

Figure 3.13: Time response for Case I b using frequency domain(G_d from S_d) approach

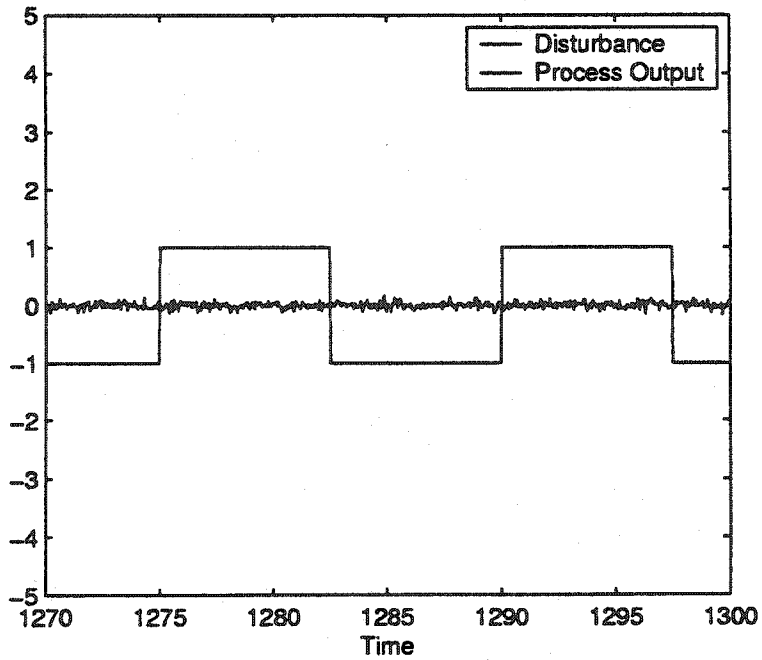

Figure 3.14: Time response for Case I b using Shinskey's tuning rules

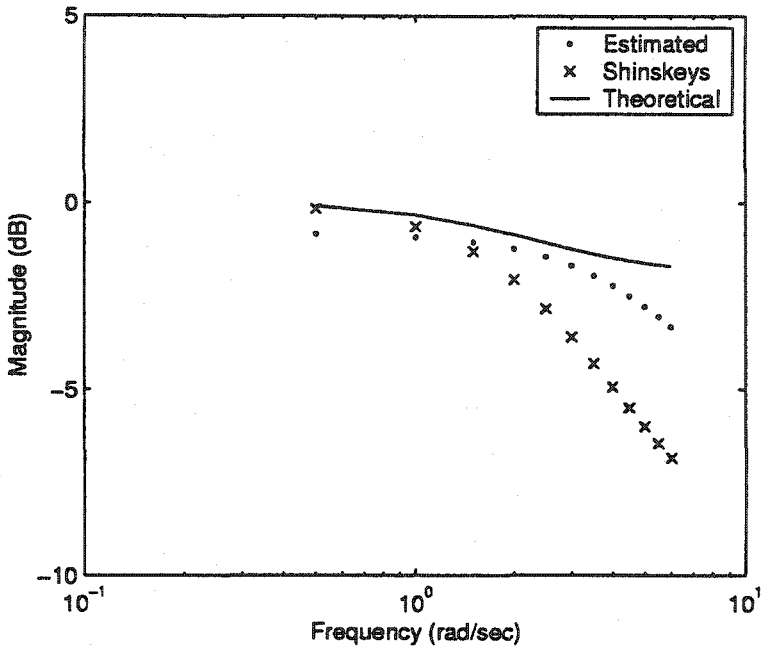

Figure 3.15: Magnitude plots of the frequency domain tuned(using G_d from S_d method), theoretical and Shinskey's tuning rule based feedforward controllers for Case II a

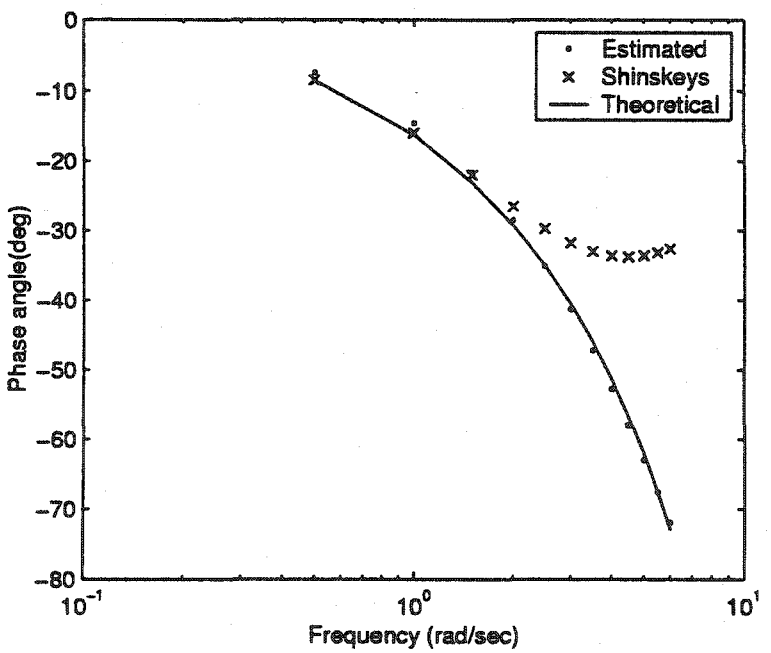

Figure 3.16: Phase plots of the frequency domain tuned(using G_d from S_d method), theoretical and Shinskey's tuning rule based feedforward controllers for Case II a

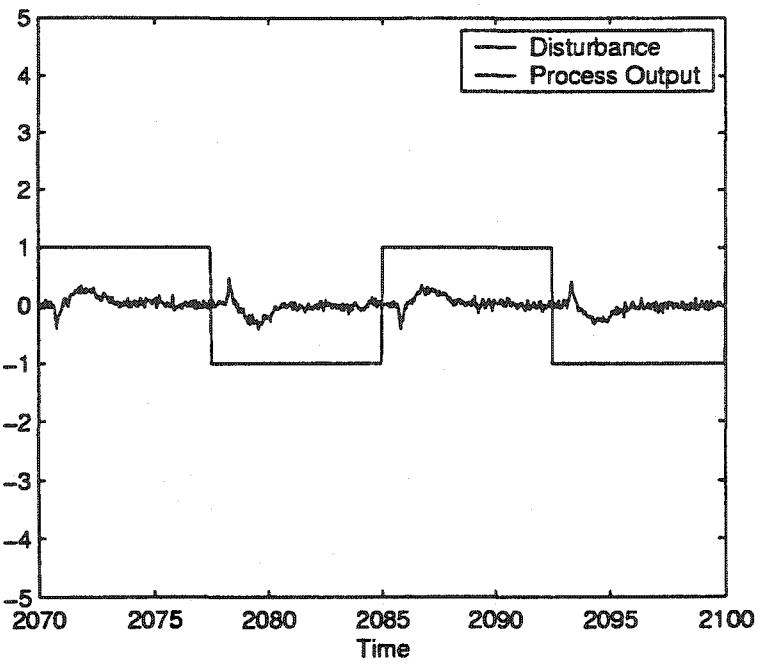

Figure 3.17: Time response for Case II a using frequency domain(G_d from S_d) approach

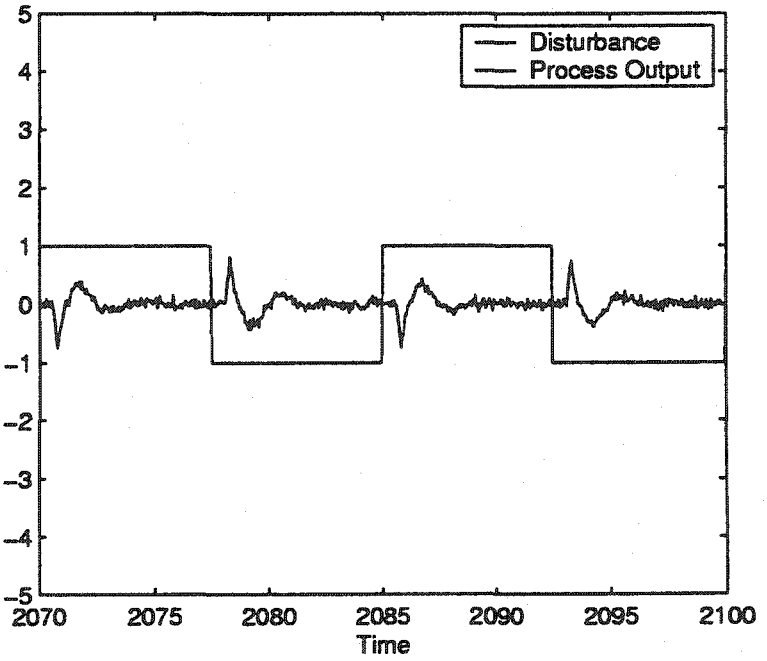

Figure 3.18: Time response for Case II a using Shinskey's tuning rules

Case	w = 0.5 rad/sec				w = 2 rad/sec				w = 6 rad/sec			
	$\tilde{S}$ (dB)	$\tilde{S}$ (deg)	$\tilde{G}_d$ (dB)	$\tilde{G}_d$ (deg)	$\tilde{S}$ (dB)	$\tilde{S}$ (deg)	$\tilde{G}_d$ (dB)	$\tilde{G}_d$ (deg)	$\tilde{S}$ (dB)	$\tilde{S}$ (deg)	$\tilde{G}_d$ (dB)	$\tilde{G}_d$ (deg)
III c	0.25	1.0	0.23	2.0	0.40	2.0	0.25	4.0	0.30	0.0	0.10	0.0
I c	0.50	1.0	0.50	2.0	0.25	1.0	0.0	3.0	0.55	0.0	0.25	0.0
II c	0.60	0.50	0.60	1.0	0.20	2.0	0.0	0.0	1.10	7.0	0.75	7.0
III b	0.60	0.0	0.50	1.0	0.20	2.25	0.0	4.50	0.75	6.50	0.40	7.0
I b	0.35	1.0	0.30	1.0	0.22	1.25	0.15	1.0	0.58	1.50	0.20	1.0
II b	0.75	2.80	0.70	1.0	0.10	3.75	0.15	1.75	0.90	4.25	0.60	4.50
III a	0.50	0.25	0.43	0.50	0.18	2.0	0.0	4.25	1.10	5.0	0.63	5.25
I a	0.40	0.25	0.35	0.50	0.25	1.50	0.18	1.0	0.50	1.0	0.18	1.0
II a	0.75	2.75	0.75	2.30	0.15	5.0	0.25	2.75	1.25	3.0	0.95	3.50

Table 3.1: Difference in magnitude and phase plots between the actual and estimated, disturbance sensitivity($\tilde{S}_d$) and disturbance($\tilde{G}_d$) frequency responses for the 9 possible combinations

Case	H_∞ error				H_2 error			
	$\tilde{S}$ (dB)	$\tilde{S}$ (deg)	$\tilde{G}_d$ (dB)	$\tilde{G}_d$ (deg)	$\tilde{S}$ (dB)	$\tilde{S}$ (deg)	$\tilde{G}_d$ (dB)	$\tilde{G}_d$ (deg)
III c	0.45	2.0	0.60	4.0	0.56	2.24	0.35	4.47
I c	0.55	3.0	0.60	5.0	0.78	1.41	0.56	3.61
II c	1.10	7.0	0.75	7.0	0.98	7.3	0.96	7.0
III b	0.75	6.50	0.60	7.0	0.98	6.88	0.64	8.38
I b	0.58	2.30	0.50	5.0	0.71	2.19	0.39	1.73
II b	1.10	4.25	0.90	4.50	1.18	6.32	0.93	4.93
III a	1.10	5.0	0.65	5.25	1.22	5.39	0.76	6.77
I a	0.50	3.0	0.60	5.0	0.69	1.82	0.43	1.50
II a	1.35	5.50	1.25	4.80	1.47	6.45	1.20	5.01

Table 3.2: H_∞ and H_2 error in magnitude and phase plots between the actual and estimated, disturbance sensitivity($\tilde{S}_d$) and disturbance($\tilde{G}_d$) frequency responses for the 9 possible combinations

Case	w = 0.5 rad/sec				w = 2 rad/sec				w = 6 rad/sec			
	$\tilde{F}$ (dB)	$\tilde{F}$ (deg)	$\tilde{S}$ (dB)	$\tilde{S}$ (deg)	$\tilde{F}$ (dB)	$\tilde{F}$ (deg)	$\tilde{S}$ (dB)	$\tilde{S}$ (deg)	$\tilde{F}$ (dB)	$\tilde{F}$ (deg)	$\tilde{S}$ (dB)	$\tilde{S}$ (deg)
III c	0.4	2.0	0.05	0.0	0.34	6.0	0.40	2.0	2.4	21.0	4.75	29.0
I c	0.4	1.0	0.0	0.0	0.15	1.0	0.0	0.0	0.60	4.0	0.0	0.0
II c	0.70	4.0	0.25	0.50	1.30	8.50	1.50	10.0	0.55	11.0	3.60	58.0
III b	0.70	2.0	0.05	0.50	0.50	14.0	0.78	2.0	1.5	63.0	4.25	23.0
I b	0.25	0.0	0.0	0.0	0.25	0.0	0.0	0.0	0.25	0.0	0.0	0.0
II b	0.60	0.10	0.0	0.0	0.50	0.30	0.0	0.30	0.10	5.75	0.0	6.75
III a	0.55	0.20	0.25	0.20	1.0	11.0	1.60	13.0	2.40	62.0	2.6	64.0
I a	0.05	2.75	0.0	0.0	0.75	6.25	0.0	0.0	1.70	4.25	0.0	0.0
II a	0.80	1.0	0.10	0.0	0.40	1.0	1.23	3.0	1.70	1.0	5.20	41.0

Table 3.3: Difference in the magnitude and phase plots of theoretical and frequency domain(G_d from S_d) method($\tilde{F}$), theoretical and Shinskey's controllers($\tilde{S}$), for the 9 possible cases

Case	H_∞ error				H_2 error			
	$\tilde{F}$ (dB)	$\tilde{F}$ (deg)	$\tilde{S}$ (dB)	$\tilde{S}$ (deg)	$\tilde{F}$ (dB)	$\tilde{F}$ (deg)	$\tilde{S}$ (dB)	$\tilde{S}$ (deg)
III c	2.40	21.0	4.75	29.0	2.46	21.93	4.77	29.07
I c	0.60	4.80	0.0	0.0	0.74	4.24	0.0	0.0
II c	1.50	11.0	3.60	58.0	1.58	14.46	3.91	58.86
III b	1.50	63.0	4.25	23.0	1.73	64.57	4.32	23.09
I b	0.25	0.0	0.0	0.0	0.43	0.0	0.0	0.0
II b	0.60	5.75	0.0	6.75	0.79	5.76	0.0	6.76
III a	2.40	62.0	2.60	64.0	2.66	62.97	3.06	65.31
I a	1.70	6.50	0.0	0.0	1.86	8.04	0.0	0.0
II a	1.70	2.0	5.2	41.0	1.92	1.73	5.30	41.1

Table 3.4: H_∞ and H_2 error in the magnitude and phase plots of theoretical and frequency domain(G_d from S_d) method($\tilde{F}$), theoretical and Shinskey's controllers ($\tilde{S}$), for the 9 possible cases

Case	Shinskey's tuning			Frequency domain tuning		
	τ_{lead} (sec)	τ_{lag} (sec)	K_{ff} ($\frac{\%}{\%}$)	τ_{lead} (sec)	τ_{lag} (sec)	K_{ff} ($\frac{\%}{\%}$)
III c	0.40	0.05	-1.0	0.29	0.0006	-0.96
I c	0.40	0.25	-1.0	0.55	0.37	-0.94
II c	1.0	1.05	-1.0	-0.18	0.0003	-0.93
III b	0.22	0.022	-1.0	0.573	0.42	-0.91
I b	0.40	0.40	-1.0	0.48	0.48	-0.97
II b	-0.10	0.10	-1.0	-0.12	0.09	-0.94
III a	1.0	0.9	-1.0	0.61	0.51	-0.92
I a	0.40	0.50	-1.0	0.43	0.55	-0.97
II a	0.12	0.42	-1.0	-0.075	0.18	-0.91

Table 3.5: Tuning parameter values for the 9 cases used in the simulation based on Shinskey's tuning rules and frequency domain(G_d from S_d) method

3.3 Frequency domain feedforward control tuning based on $\frac{S_dC}{T}$ ratio - Simulation results

The previous section illustrated the application of feedforward control through disturbance sensitivity function estimation. The tuning was based on deriving the disturbance transfer function(G_d) frequency response from that of the disturbance sensitivity function(S_d) and subsequent evaluation of the required ratio (G_d/G_p). Alternatively, this ratio of transfer functions can also be obtained with out the individual components, G_p and G_d through two closed loop procedures. One such procedure is to tune the feedforward controllers on the basis of the ratio (S_dC/T) where S_d is the disturbance sensitivity function from d to y given in Equation 3.1 and T is the complementary sensitivity function from r to y given in Equation 3.2, which is mathematically equivalent to (G_d/G_p) as shown below:

$$\frac{S_dC}{T} = \frac{(\frac{G_d}{(1+G_pG_c)})(G_c)}{(\frac{(G_pG_c)}{(1+G_pG_c)})} \Rightarrow \frac{G_d}{G_p} \tag{3.6}$$

In this section, the effectiveness of tuning the feedforward controllers in the frequency domain on the basis of this closed loop ratio is tested. Initially, the recursive least squares estimation of the complementary sensitivity function is carried out using the process output(y) and the setpoint(r). The model of the discrete time transfer function used during the estimation is as shown below:

$$T(z^{-1}) = \frac{z^{-12}(b_0 + b_1z^{-1} + b_2z^{-2})}{(1 + a_1z^{-1} + a_2z^{-2} + a_3z^{-3} + ... + a_{13}z^{-13})} \tag{3.7}$$

The selection of the z^{-12} term in the numerator is based on the continuous time process delay of 0.6 sec, sampled at 0.05 sec. Three coefficients are taken in the numerator and thirteen coefficients are taken in the denominator. The setpoint changes are introduced with a period of 20 sec and in this stage the process output is only under the influence of the measurement noise and the feedback PI controller. No disturbances are introduced at this stage. At 300 sec, the setpoint changes as well as the RLS estimation of the closed loop transfer function from r to y is stopped. At this point, the square wave disturbance with a period of 15 sec is introduced and the disturbance dynamics are changed as given in Table 2.1. As in the previous section, the estimation of the disturbance sensitivity function is carried for the first 150 seconds in each interval and the tuning is performed during the next 50 seconds. The model of the estimated discrete time disturbance sensitivity transfer function is taken as the same as in previous section, given in Equation 3.4. The frequency domain tuning used involves the evaluation of the frequency response of the ratio (S_dC/T) over the normalized frequency range of 0.025 to 3.0 rads with a step size of 0.05 rads, which is equivalent to unnormalized frequency of 0.5 to 6 rads/sec. The ($1/wT$) weighted sum of the magnitude of $G_{ff} + (S_dC/T)$ at these set of frequencies is minimized using the Nelder-Mead simplex method. All the parameters and constraints of the optimization are taken the same as mentioned in the Chapter 2.

The frequency response of the estimated and true complementary sensitivity function(T) are shown in Figure 3.19 and Figure 3.20. Since the process dynamics are unchanged, this

estimated frequency response of T is used for tuning purposes throughout the length of this simulation. Since the disturbance dynamics that are considered in this section are the same as in the previous section, the estimated disturbance sensitivity function magnitude and phase characteristics remain the same as given in Table 3.1 and Table 3.2 respectively. The feedforward controller magnitude and phase plot characteristics that are designed using this method are tabulated for the various combinations. Table 3.6 shows the difference between the theoretical and (S_dC/T) approach compared to the difference between the theoretical and Shinskey's tuning rules in the frequency domain at three distinct frequencies in the interval of interest, 0.5 - 6 rad/sec. Table 3.7 compares the equivalent difference using H_∞ and H_2 criteria. The simulation results for tuning feedforward controllers in this manner can be summarized as follows:

1. For Case III c, (S_dC/T) tuning method provides better fit to the theoretical in both the magnitude and phase plots compared to Shinskey's tuning rules. The magnitude and phase plots of the feedforward controller designed using (S_dC/T) tuning compared to the theoretical and Shinskey's tuning rules are shown in Figure 3.21 and Figure 3.22. The time response is shown in Figure 3.25.

2. For Case I c, both (S_dC/T) and Shinskey's tuning rules provide close magnitude and phase plots to the theoretical indicating complete cancellation of disturbances in this frequency range.

3. Case II c requires a combination of lead plus dead time for perfect cancellation. Both the (S_dC/T) approach and Shinskey's tuning rules fail to provide a good fit in both magnitude and phase plots for this case. Interestingly, both the methods show a similar trend of lag dominant controller. Whereas the frequency domain approach tends to fit both the magnitude and phase plots close to the theoretical, Shinskey's controller tend to favour the magnitude response at the expense of the phase plot.

4. For Case III b, both the tuning methods provide identical phase plot fit whereas the magnitude fit of the frequency domain tuning is better than that of Shinskey's tuning.

5. For Case I b, this method provides a perfect flat magnitude and phase characteristic, close to the theoretical and Shinskey's controller.

6. For Case II b, this method provides a reasonably accurate fit in the magnitude plot compared to the theoretical. Both the methods provide identical phase response fit.

7. For Case III a, this method provides a better fit in the magnitude plot compared to Shinskey's tuning at the expense of the phase plot.

8. For Case I a, both the methods provide good fit of the magnitude and phase plots close to the theoretical.

9. For Case II a, this method results in a better fit in both magnitude and phase plots to the theoretical compared to Shinskey's tuning method as shown in Figure 3.23 and Figure 3.24. The time response is shown in Figure 3.26.

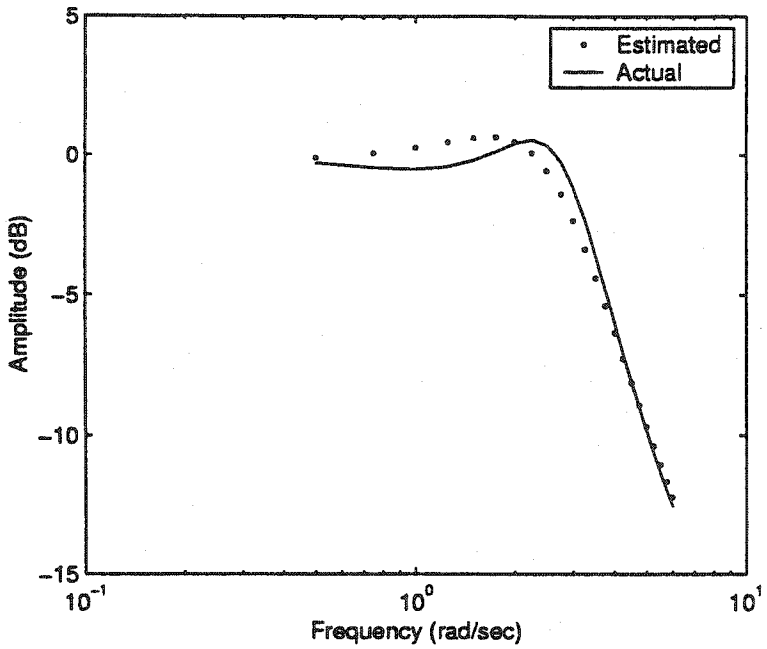

Figure 3.19: Magnitude plots of the estimated and actual closed loop complementary sensitivity function(T)

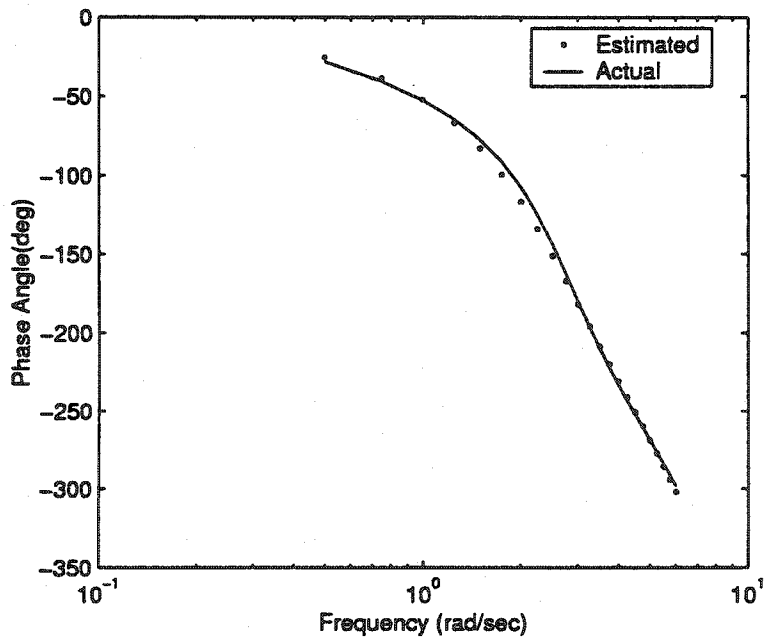

Figure 3.20: Phase plots of the estimated and actual closed loop complementary sensitivity function(T)

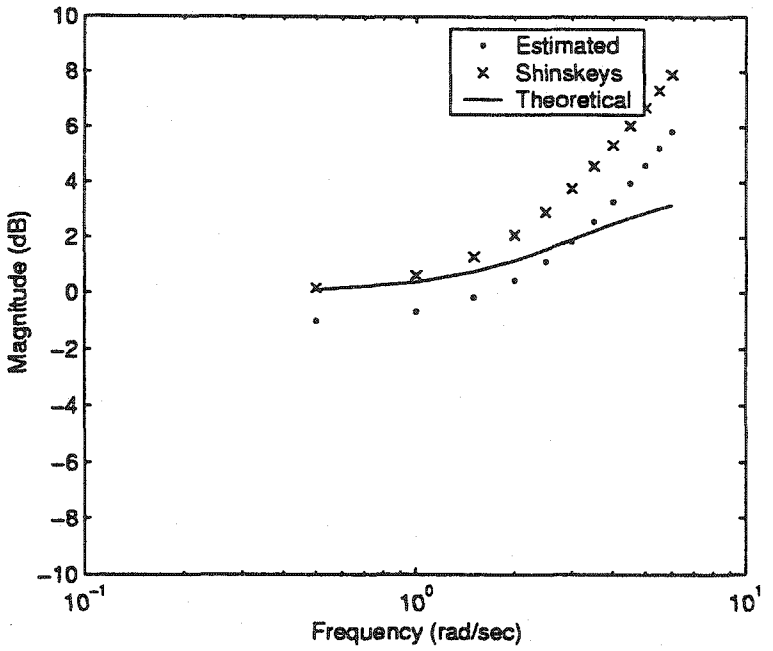

Figure 3.21: Magnitude plots of the frequency domain tuned(using (S_dC/T) method), theoretical and Shinskey's tuning rule based feedforward controllers for Case III c

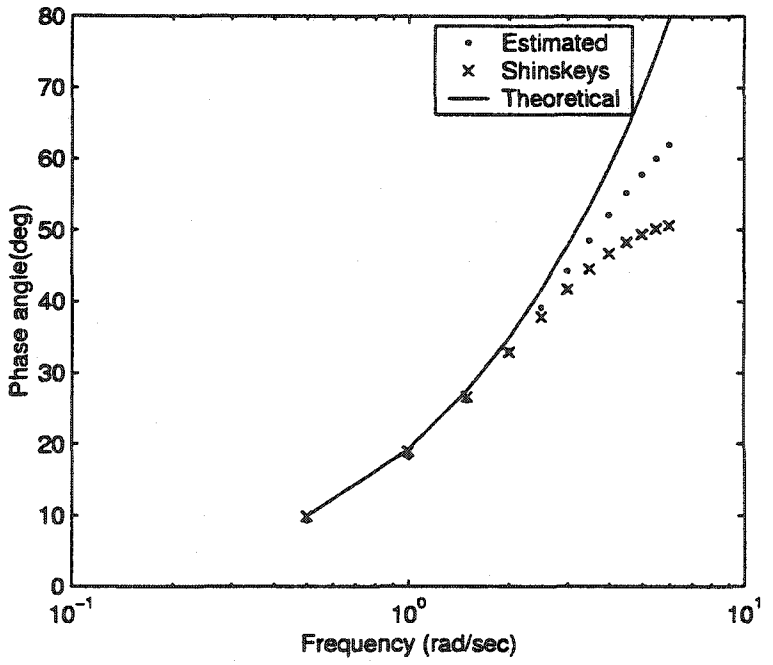

Figure 3.22: Phase plots of the frequency domain tuned(using (S_dC/T) method), theoretical and Shinskey's tuning rule based feedforward controllers for Case III c

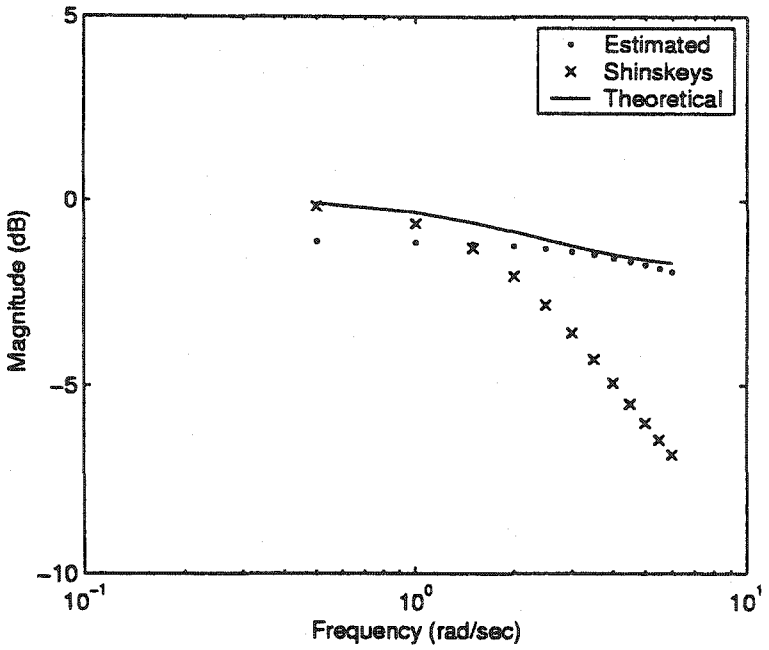

Figure 3.23: Magnitude plots of the frequency domain tuned(using (S_dC/T) method), theoretical and Shinskey's tuning rule based feedforward controllers for Case II a

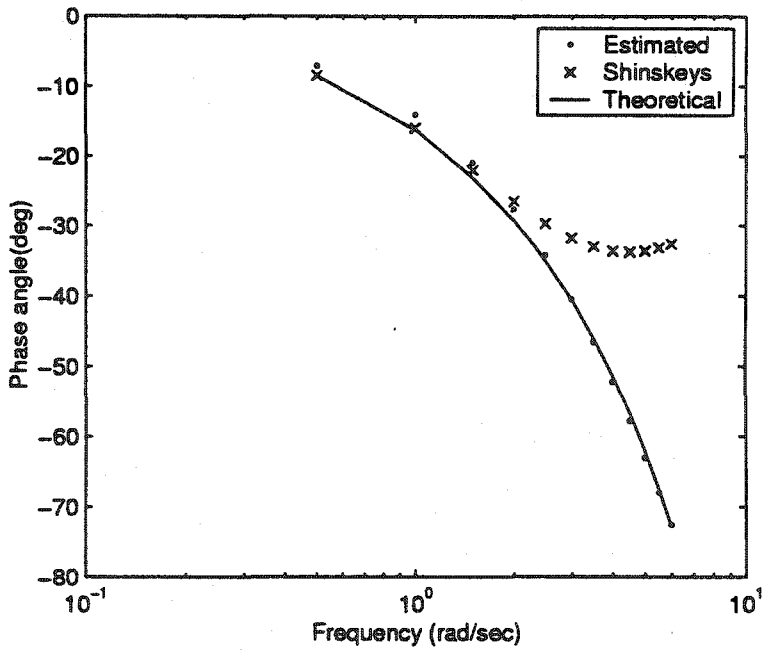

Figure 3.24: Phase plots of the frequency domain tuned(using (S_dC/T) method), theoretical and Shinskey's tuning rule based feedforward controllers for Case II a

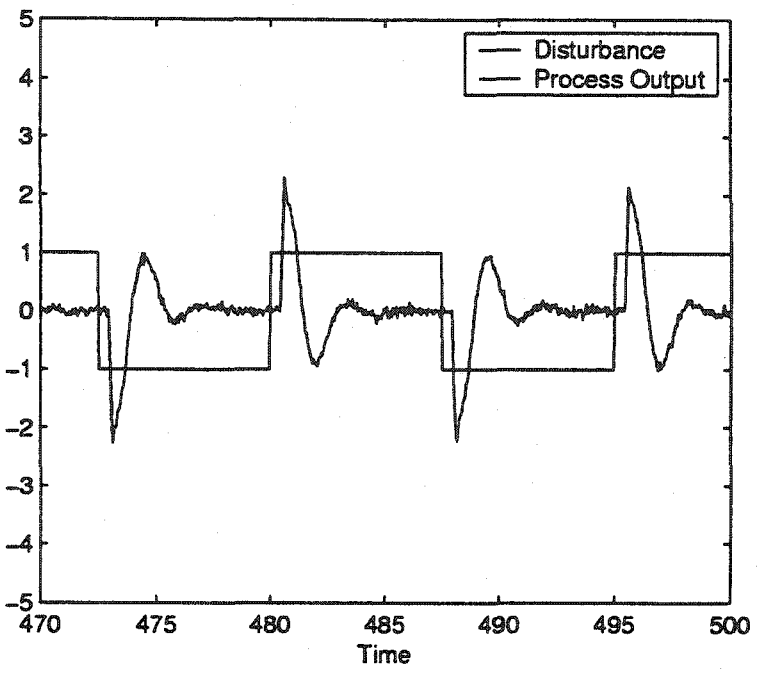

Figure 3.25: Time response for Case III c using frequency domain(S_dC/T) approach

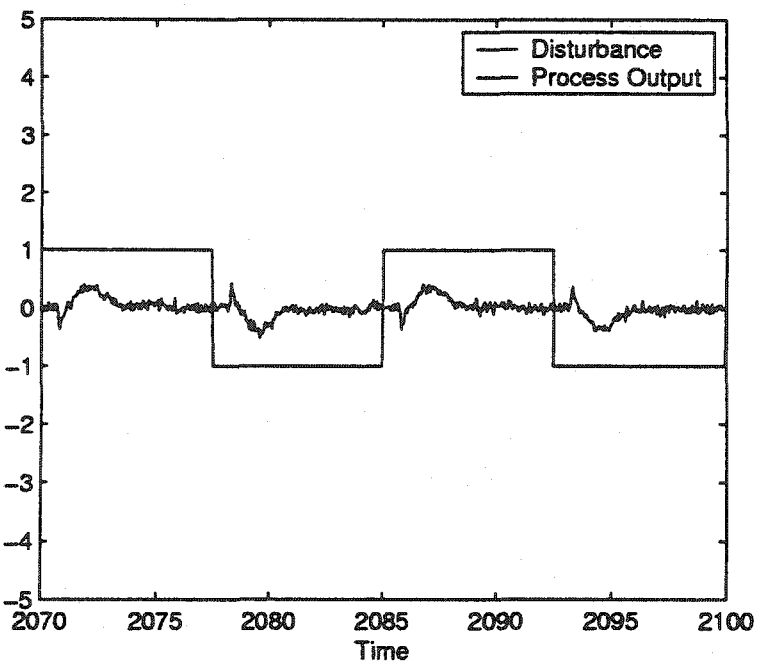

Figure 3.26: Time response for Case II a using frequency domain(S_dC/T) approach

Case	w = 0.5 rad/sec				w = 2 rad/sec				w = 6 rad/sec			
	$\tilde{F}$ (dB)	$\tilde{F}$ (deg)	$\tilde{S}$ (dB)	$\tilde{S}$ (deg)	$\tilde{F}$ (dB)	$\tilde{F}$ (deg)	$\tilde{S}$ (dB)	$\tilde{S}$ (deg)	$\tilde{F}$ (dB)	$\tilde{F}$ (deg)	$\tilde{S}$ (dB)	$\tilde{S}$ (deg)
III c	1.10	1.0	0.05	0.0	0.70	2.0	0.4	2.0	2.70	18.0	4.75	29.0
I c	0.55	1.90	0.0	0.0	0.10	1.30	0.0	0.0	0.15	2.20	0.0	0.0
II c	0.45	0.50	0.25	0.50	2.15	6.0	1.50	10.0	4.75	55.0	3.6	58.0
III b	0.78	1.0	0.05	0.50	0.30	3.40	0.78	2.0	2.53	22.50	4.25	23.0
I b	0.50	0.10	0.0	0.0	0.45	0.30	0.0	0.0	0.40	0.20	0.0	0.0
II b	1.10	0.75	0.0	0.0	0.90	2.40	0.0	0.30	0.35	2.0	0.0	6.75
III a	0.65	3.0	0.25	0.20	0.10	17.0	1.60	13.0	0.95	65.0	2.60	64.0
I a	0.10	2.80	0.0	0.0	0.85	6.30	0.0	0.0	1.65	4.20	0.0	0.0
II a	1.05	1.40	0.10	0.0	0.40	1.70	1.23	3.0	0.25	0.30	5.20	41.0

Table 3.6: Difference in the magnitude and phase plots of theoretical and frequency domain(S_dC/T) method($\tilde{F}$), theoretical and Shinskey's controllers($\tilde{S}$), for the 9 possible cases

Case	H_∞ error				H_2 error			
	$\tilde{F}$ (dB)	$\tilde{F}$ (deg)	$\tilde{S}$ (dB)	$\tilde{S}$ (deg)	$\tilde{F}$ (dB)	$\tilde{F}$ (deg)	$\tilde{S}$ (dB)	$\tilde{S}$ (deg)
III c	2.70	18.0	4.75	29.0	2.99	18.14	4.77	29.07
I c	0.55	2.20	0.0	0.0	0.58	3.18	0.0	0.0
II c	4.75	55.0	3.60	58.0	5.23	55.33	3.91	58.86
III b	2.53	22.5	4.25	23.0	2.66	22.78	4.32	23.09
I b	0.50	0.30	0.0	0.0	0.78	0.37	0.0	0.0
II b	1.10	3.0	0.0	6.75	1.46	3.21	0.0	6.76
III a	0.95	65.0	2.60	64.0	1.16	67.25	3.06	65.31
I a	1.65	4.4	0.0	0.0	1.86	8.07	0.0	0.0
II a	1.05	2.20	5.2	41.0	1.15	2.22	5.30	41.10

Table 3.7: H_∞ and H_2 error in the magnitude and phase plots of theoretical and frequency domain(S_dC/T) method($\tilde{F}$), theoretical and Shinskey's controllers ($\tilde{S}$), for the 9 possible cases

Case	Shinskey's tuning			Frequency domain tuning		
	τ_{lead} (sec)	τ_{lag} (sec)	K_{ff} ($\frac{\%}{\%}$)	τ_{lead} (sec)	τ_{lag} (sec)	K_{ff} ($\frac{\%}{\%}$)
III c	0.40	0.05	-1.0	0.33	0.004	-0.88
I c	0.40	0.25	-1.0	0.59	0.36	-0.93
II c	1.0	1.05	-1.0	0.43	0.51	-0.97
III b	0.22	0.022	-1.0	0.18	0.002	-0.91
I b	0.40	0.40	-1.0	0.46	0.45	-0.95
II b	-0.10	0.10	-1.0	-0.14	0.08	-0.88
III a	1.0	0.9	-1.0	0.56	0.56	-0.92
I a	0.40	0.50	-1.0	0.47	0.59	-0.96
II a	0.12	0.42	-1.0	-0.11	0.14	-0.88

Table 3.8: Tuning parameter values for the 9 cases used in the simulation based on Shinskey's tuning rules and frequency domain(S_dC/T) method

3.4 Frequency domain feedforward control tuning based on $\frac{u}{d}$ estimation - Simulation results

A different procedure to obtain the (G_d/G_p) ratio by closed loop identification is tested in this section. This method also utilizes the closed loop identification of the complementary sensitivity function(T) from r to y shown in Equation 3.2 as the initial step. Unlike the previous sections of this chapter where the disturbance sensitivity function from d to y is estimated, in this method the transfer function from the disturbance, d to process input, u is used as an alternative. In the absence of feedforward control, the closed loop transfer function from d to u with the process just under feedback control is as shown in Equation 3.8.

$$\frac{u}{d} = \frac{G_d G_c}{(1 + G_p G_c)} \tag{3.8}$$

This transfer function can be utilized in obtaining the required ratio for feedforward control tuning, (G_d/G_p), as shown in Equation 3.9

$$\frac{\frac{u}{d}}{\frac{y}{r}} = \frac{\frac{G_d G_c}{(1+G_p G_c)}}{\frac{G_p G_c}{(1+G_p G_c)}} = \frac{G_d}{G_p} \tag{3.9}$$

There are two reasons for using an estimation of this type.

1. The computed frequency response of the ratio (G_d/G_p) through this method is found to be more accurate compared to that of using the ratio $(S_d C/T)$. This is clearly noticeable by comparing the frequency response of the ratio computed by the two methods. The magnitude plots of the ratio for Case III c are shown in Figure 3.27 and Figure 3.28 and the phase plots are shown in Figure 3.29 and Figure 3.30. Similar trend has also been observed in all other cases.

2. Because of the presence of the feedback PI controller G_c in the numerator of the closed loop transfer function from d to u, the signal in the frequency range of interest using this ratio is stronger compared to that of d to y and hence the RLS convergence of (u/d) ratio is found to be faster than that of the disturbance sensitivity function.

Initially the complementary sensitivity function is estimated with a discrete transfer function model of the form shown in Equation 3.7. All the conditions during this estimation are taken the same as in the previous sections. At the time instant of 300 sec, square wave disturbance changes are introduced along with changes in disturbance dynamics at an interval of every 200 sec as shown in Table 2.1. During the first 150 seconds in each interval, the estimation from the disturbance(d) to process input(u) is carried out using a discrete transfer function of the type shown below in Equation 3.10.

$$\frac{u}{d} = \frac{z^{-8}(c_o + c_1 z^{-1} + c_2 z^{-2} + ... + c_9 z^{-9})}{(1 + d_1 z^{-1} + d_2 z^{-2} + d_3 z^{-3} + ... + d_{15} z^{-15})} \tag{3.10}$$

The z^{-8} factor in the numerator corresponds to the presence of the disturbance transfer function G_d in the numerator, with a lower limit of continuous time delay of 0.4 sec sampled at 0.05 sec. The variation of disturbance delay from 0.4 to 0.8 sec during the simulation

necessitates the presence of 10 coefficients in the numerator. 15 coefficients are used in the denominator polynomial to account for the $1 + G_pG_c$ term. In the next 50 second, the estimated coefficients are used in obtaining the frequency response of the transfer function (u/d) in the normalized frequency(wT) range of interest, 0.025-0.3 rads(0.5-6 rad/sec). The tuning is performed by minimizing the sum of the weighted magnitude function of $G_{ff} + ((u/d)/(y/r))$ in this frequency range using $(1/wT)$ frequency waiting.

The magnitude plot of the frequency response of the estimated transfer function from d to u for Case III c is shown in Figure 3.31 and the phase plot is shown in Figure 3.32 along with the true frequency response based on the actual process and controller parameters. The estimation details of the (u/d) frequency response for the other cases are summarized in Table 3.9 and Table 3.10. The details of the designed frequency domain feedforward controllers are tabulated in Table 3.11 and Table 3.12. The controllers designed in various cases show the same characteristics as mentioned in the earlier section. The difference is that the fit of the frequency response compared to the theoretical controller using this approach differs from that of the tuning using the ratio (S_dC/T) for various cases. This difference for various cases is summarized in the following discussion.

1. For Case III c, no improvement is observed in the fit of the magnitude plot of the controller whereas the fit of the phase plot is improved at low frequencies. The corresponding time response is shown in Figure 3.37.

2. For Case I c, improvement in the magnitude plot of the controller as well as the phase plot is observed at low frequencies.

3. For Case II c, improvement in magnitude and phase plots is observed over all frequencies.

4. For Case III b, minor improvement in magnitude plot is observed at low frequencies whereas the fit of phase plot is improved over all frequencies.

5. For Case I b, improvement in both magnitude and phase plots is produced over all frequencies.

6. For Case II b, both the magnitude and phase plot fits are improved at low frequencies at the expense of the fit at high frequencies.

7. For Case III a, improvement of magnitude plot fit is observed at low frequencies at the expense of high frequencies, whereas the fit of the phase plot is improved over all frequencies.

8. For Case I a, the magnitude plot is improved over all frequencies whereas the phase plot is improved at low frequencies at the expense of the high frequencies. This can be observed by comparing the corresponding magnitude plots for both cases in Figure 3.33 and Figure 3.34 and phase plots in Figure 3.35 and Figure 3.36.

9. For Case II a, both the magnitude and phase plot designs are improved at low frequencies at the expense of high frequencies. The corresponding time response is shown in Figure 3.38.

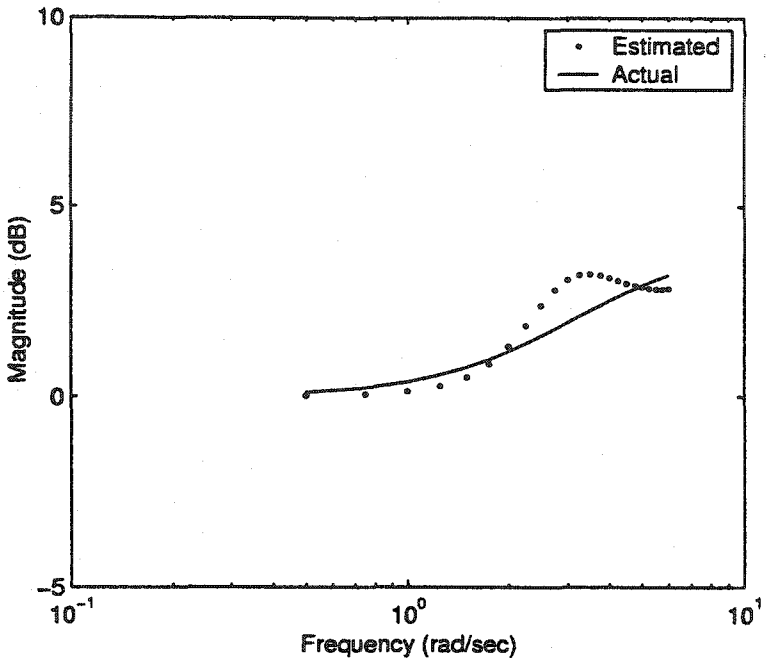

Figure 3.27: Magnitude plot of the estimated ratio $((u/d)/(y/r))$ equivalent to (G_d/G_p), corresponding to Case III c

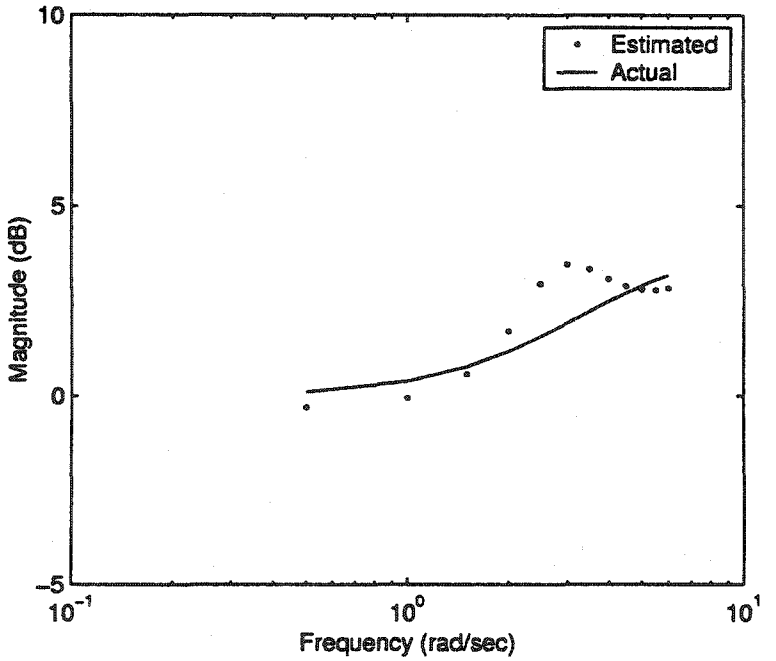

Figure 3.28: Magnitude plot of the estimated ratio (S_dC/T) equivalent to (G_d/G_p), corresponding to Case III c

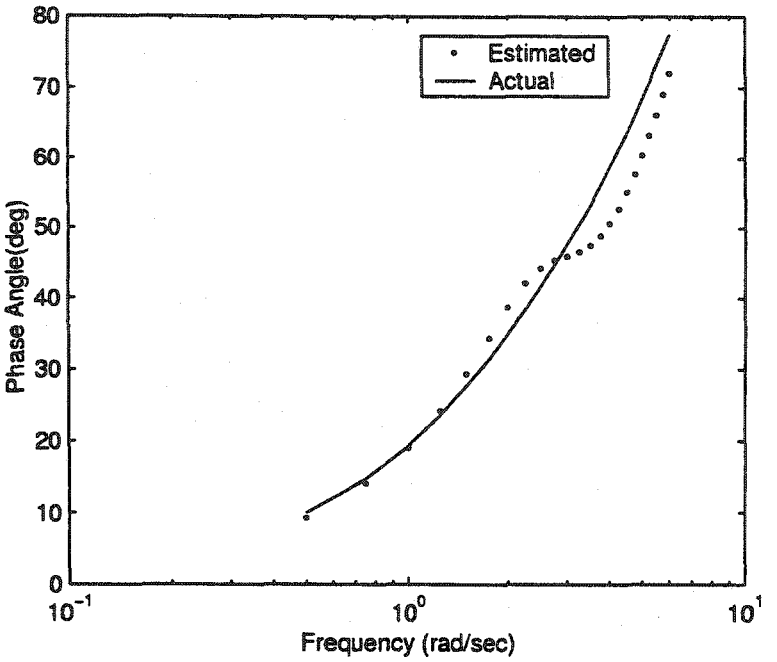

Figure 3.29: Phase plot of the estimated ratio $((u/d)/(y/r))$ equivalent to (G_d/G_p), corresponding to Case III c

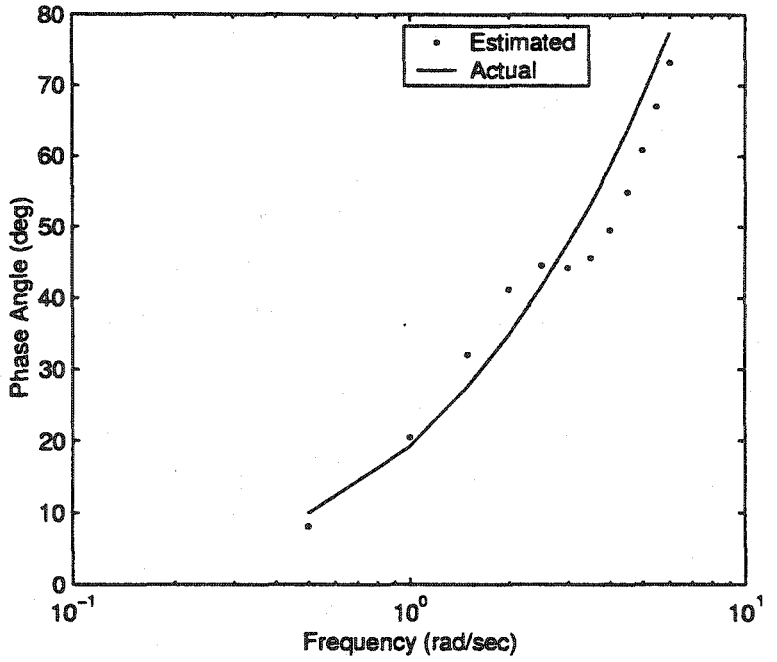

Figure 3.30: Phase plot of the estimated ratio (S_dC/T) equivalent to (G_d/G_p), corresponding to Case III c

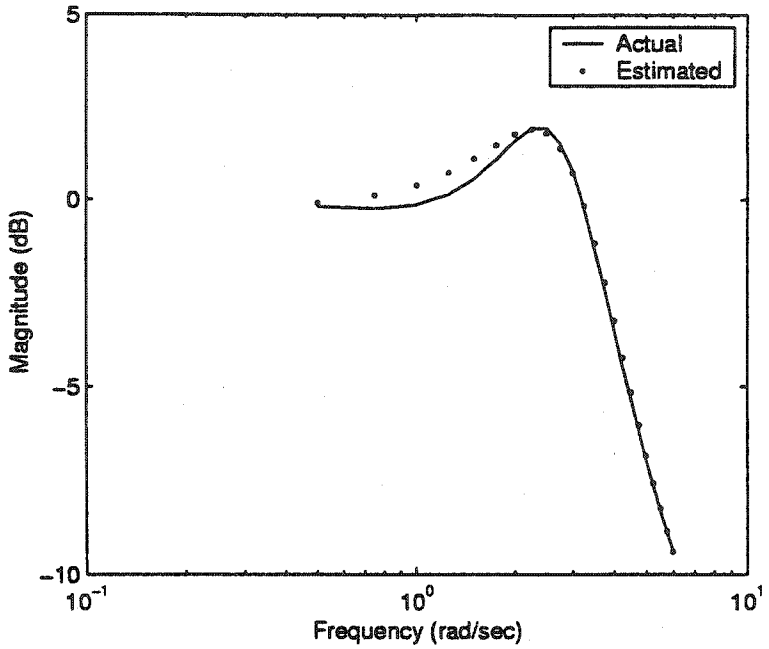

Figure 3.31: Magnitude plots of the estimated and actual (u/d) ratio corresponding to Case III c

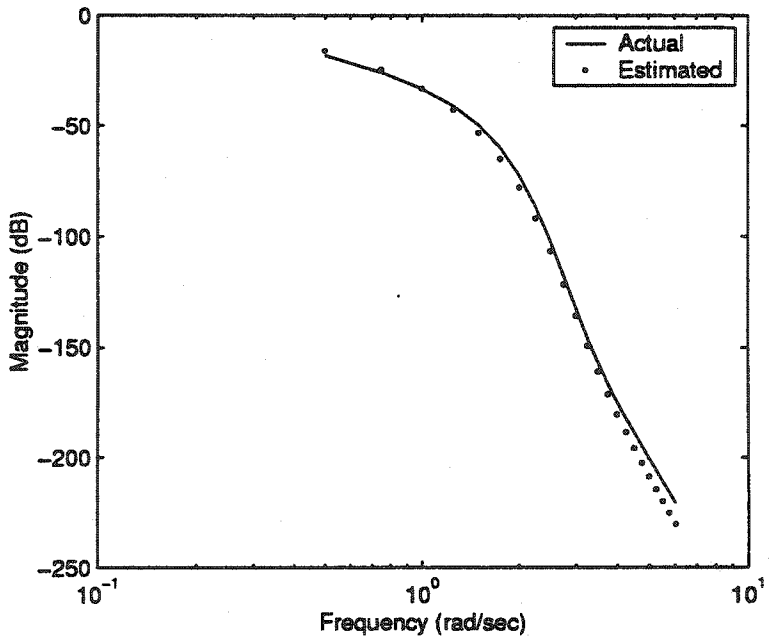

Figure 3.32: Phase plots of the estimated and actual (u/d) ratio corresponding to Case III c

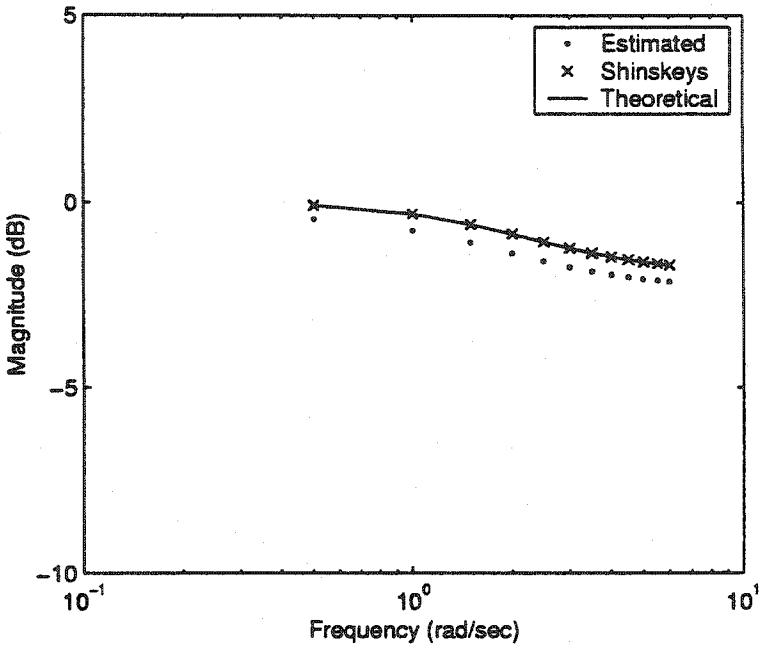

Figure 3.33: Magnitude plots of the frequency domain tuned(using (S_dC/T) method), theoretical and Shinskey's tuning rule based feedforward controllers for Case I a

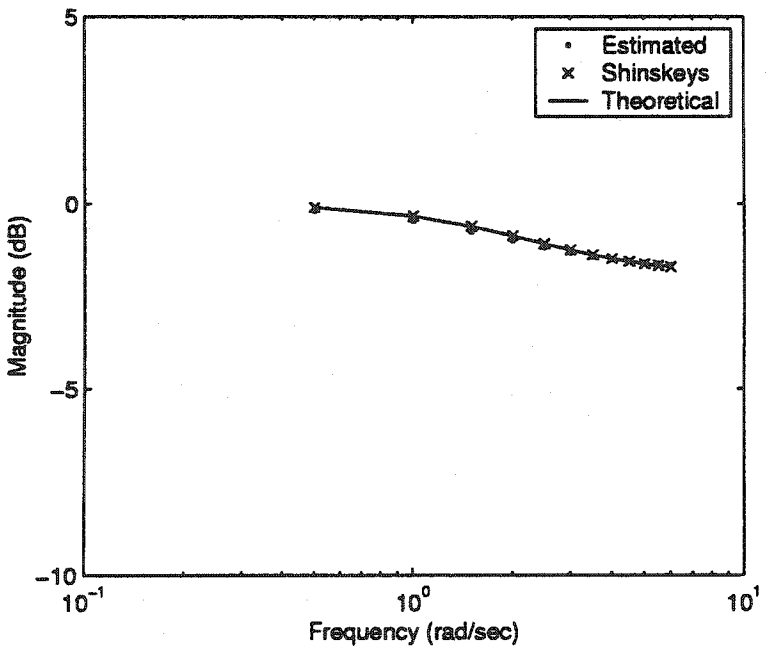

Figure 3.34: Magnitude plots of the frequency domain tuned(using (u/d) estimation), theoretical and Shinskey's tuning rule based feedforward controllers for Case I a

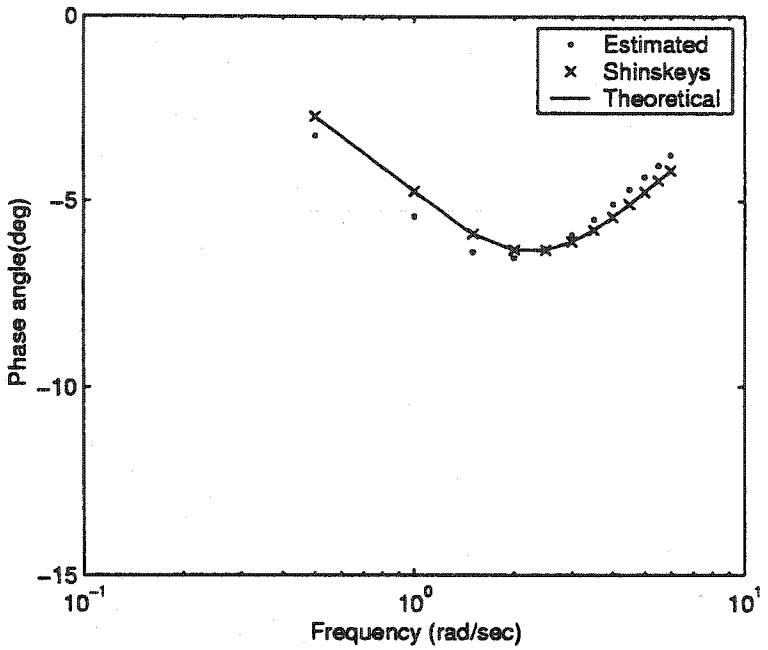

Figure 3.35: Phase plots of the frequency domain tuned(using (S_dC/T) method), theoretical and Shinskey's tuning rule based feedforward controllers for Case I a

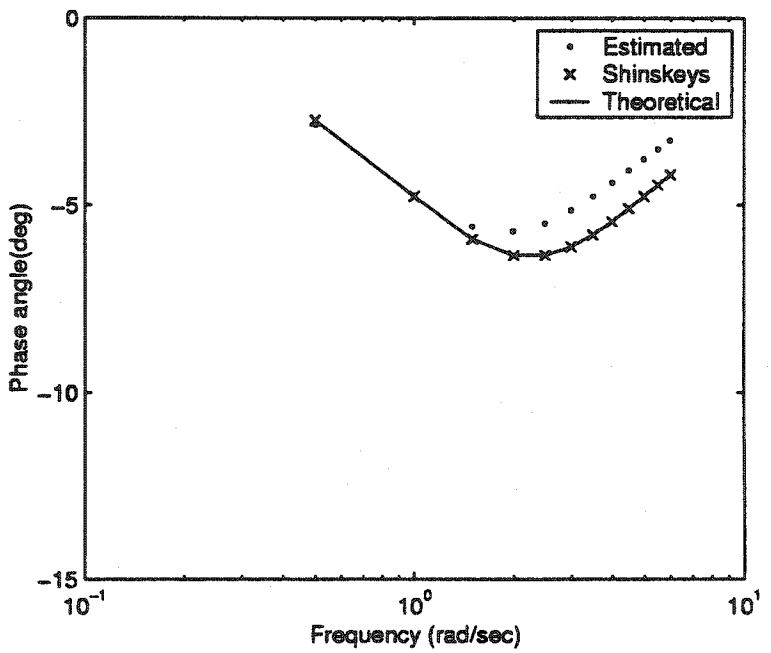

Figure 3.36: Phase plots of the frequency domain tuned(using (u/d) estimation), theoretical and Shinskey's tuning rule based feedforward controllers for Case I a

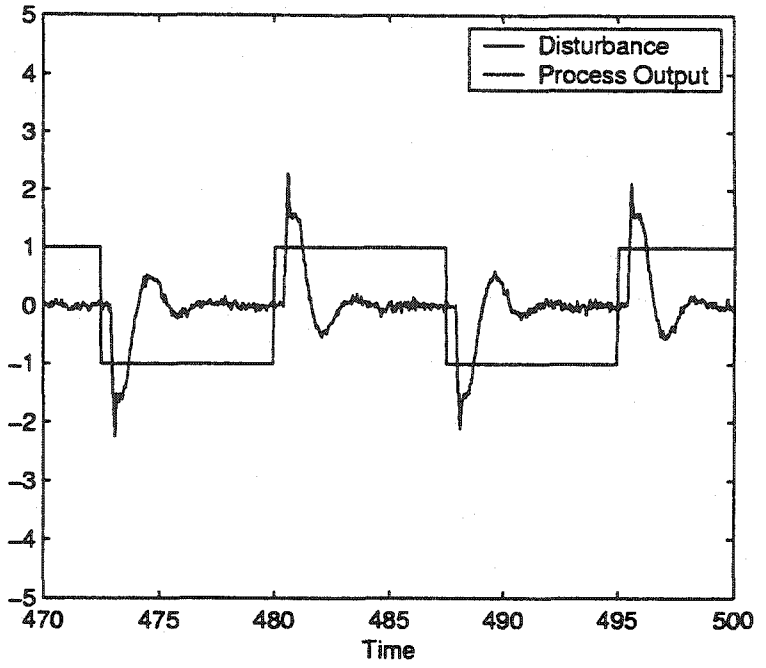

Figure 3.37: Time response for Case III c using frequency domain$((u/d)/(y/r))$ approach

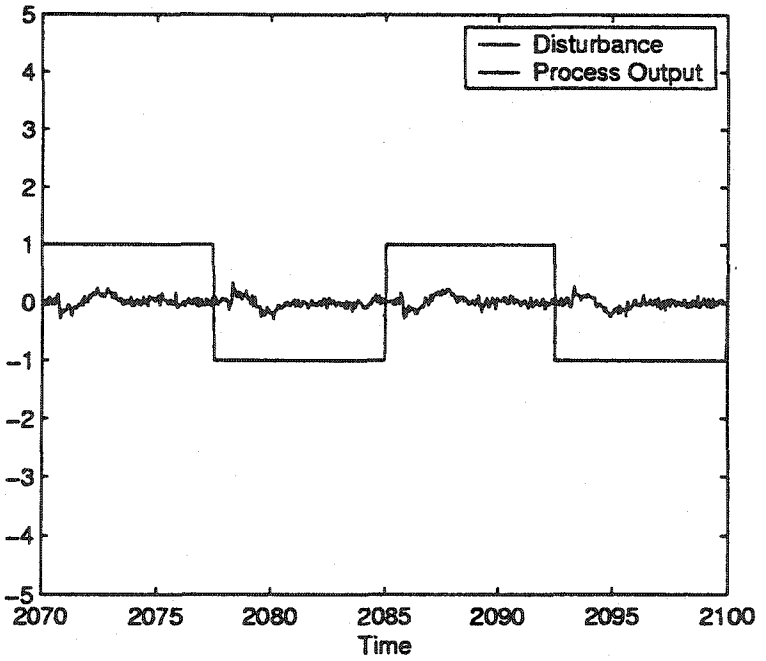

Figure 3.38: Time response for Case II a using frequency domain$((u/d)/(y/r))$ approach

Case	w = 0.5 rad/sec				w = 2 rad/sec				w = 6 rad/sec			
	$\frac{\tilde{u}}{d}$ (dB)	$\frac{\tilde{u}}{d}$ (deg)	$\frac{G_d}{G_p}$ (dB)	$\frac{G_d}{G_p}$ (deg)	$\frac{\tilde{u}}{d}$ (dB)	$\frac{\tilde{u}}{d}$ (deg)	$\frac{G_d}{G_p}$ (dB)	$\frac{G_d}{G_p}$ (deg)	$\frac{\tilde{u}}{d}$ (dB)	$\frac{\tilde{u}}{d}$ (deg)	$\frac{G_d}{G_p}$ (dB)	$\frac{G_d}{G_p}$ (deg)
III c	0.09	2.0	0.10	1.0	0.18	6.0	0.13	3.7	0.01	9.50	0.38	5.50
I c	0.07	2.25	0.12	0.20	0.14	5.10	0.10	4.30	0.05	10.25	0.40	6.0
II c	0.04	2.0	0.13	0.40	0.15	5.20	0.12	4.20	0.18	22.0	0.52	18.0
III b	0.08	1.80	0.10	1.0	0.02	8.20	0.05	1.40	0.80	15.5	1.15	11.0
I b	0.08	2.20	0.11	0.20	0.08	6.10	0.09	3.40	0.12	11.8	0.22	7.80
II b	0.05	2.30	0.13	0.25	0.0	7.0	0.02	3.0	0.38	22.0	0.01	17.5
III a	0.10	1.80	0.10	1.20	0.20	8.80	0.23	0.65	0.72	12.6	1.10	8.25
I a	0.08	2.25	0.11	0.20	0.18	7.0	0.19	2.25	0.38	13.2	0.01	9.0
II a	0.07	2.50	0.10	0.20	0.18	7.80	0.18	2.0	0.10	21.5	0.23	17.5

Table 3.9: Difference in magnitude and phase plots between the actual and estimated, (u/d) ratio and (G_d/G_p) ratio frequency responses for the 9 possible combinations

Case	H_∞ error				H_2 error			
	$\frac{\tilde{u}}{d}$ (dB)	$\frac{\tilde{u}}{d}$ (deg)	$\frac{G_d}{G_p}$ (dB)	$\frac{G_d}{G_p}$ (deg)	$\frac{\tilde{u}}{d}$ (dB)	$\frac{\tilde{u}}{d}$ (deg)	$\frac{G_d}{G_p}$ (dB)	$\frac{G_d}{G_p}$ (deg)
III c	0.60	9.50	1.10	8.60	0.20	11.41	0.41	6.70
I c	0.60	10.25	1.0	7.0	0.16	11.67	0.43	7.38
II c	0.6	22.0	1.10	18.0	0.24	22.69	0.55	18.50
III b	0.80	15.50	1.15	14.2	0.80	17.63	1.16	11.13
I b	0.62	11.8	0.79	7.80	0.17	13.46	0.26	8.50
II b	0.64	22.0	0.82	17.5	0.38	23.2	0.13	17.76
III a	0.75	12.6	1.10	11.20	0.75	15.47	1.13	8.36
I a	0.82	13.2	0.80	9.0	0.43	15.11	0.22	9.28
II a	0.84	21.50	0.75	17.5	0.22	23.0	0.31	17.61

Table 3.10: H_∞ and H_2 error in magnitude and phase plots between the actual and estimated, (u/d) ratio and (G_d/G_p) ratio frequency responses for the 9 possible combinations

Case	w = 0.5 rad/sec				w = 2 rad/sec				w = 6 rad/sec			
	$\tilde{F}$ (dB)	$\tilde{F}$ (deg)	$\tilde{S}$ (dB)	$\tilde{S}$ (deg)	$\tilde{F}$ (dB)	$\tilde{F}$ (deg)	$\tilde{S}$ (dB)	$\tilde{S}$ (deg)	$\tilde{F}$ (dB)	$\tilde{F}$ (deg)	$\tilde{S}$ (dB)	$\tilde{S}$ (deg)
III c	2.40	2.0	0.05	0.0	1.20	3.0	0.40	2.0	3.20	18.0	4.75	29.0
I c	0.15	1.0	0.0	0.0	0.18	0.10	0.0	0.0	0.20	2.50	0.0	0.0
II c	0.13	0.50	0.25	0.50	1.75	6.25	1.50	10.0	4.30	55.0	3.60	58.0
III b	0.72	0.50	0.05	0.50	0.15	2.60	0.78	2.0	2.85	21.0	4.25	23.0
I b	0.10	0.02	0.0	0.0	0.10	0.02	0.0	0.0	0.10	0.02	0.0	0.0
II b	0.10	0.40	0.0	0.0	0.16	0.78	0.0	0.30	1.83	6.50	0.0	6.75
III a	0.05	1.50	0.25	0.2	1.13	13.0	1.60	13.0	2.50	62.0	2.60	64.0
I a	0.10	2.80	0.0	0.0	0.85	6.30	0.0	0.0	1.70	4.20	0.0	0.0
II a	0.15	0.10	0.10	0.0	0.60	1.25	1.23	3.0	1.20	5.80	5.20	41.0

Table 3.11: Difference in the magnitude and phase plots of theoretical and frequency domain(from (u/d) estimation) method($\tilde{F}$), theoretical and Shinskey's controllers($\tilde{S}$), for the 9 possible cases

Case	H_∞ error				H_2 error			
	$\tilde{F}$ (dB)	$\tilde{F}$ (deg)	$\tilde{S}$ (dB)	$\tilde{S}$ (deg)	$\tilde{F}$ (dB)	$\tilde{F}$ (deg)	$\tilde{S}$ (dB)	$\tilde{S}$ (deg)
III c	3.20	18.0	4.75	29.0	4.17	18.36	4.77	29.07
I c	0.25	2.50	0.0	0.0	0.31	2.69	0.0	0.0
II c	4.30	55.0	3.60	58.0	4.64	55.30	3.91	58.86
III b	2.85	21.0	4.25	23.0	2.94	21.17	4.32	23.09
I b	0.10	0.02	0.0	0.0	0.17	0.03	0.0	0.0
II b	1.83	6.50	0.0	6.75	1.84	6.56	0.0	6.76
III a	2.50	62.0	2.60	64.0	2.74	63.37	3.06	65.31
I a	1.70	4.20	0.0	0.0	1.90	8.07	0.0	0.0
II a	1.2	7.0	5.20	41.0	1.35	5.93	5.30	41.10

Table 3.12: H_∞ and H_2 error in the magnitude and phase plots of theoretical and frequency domain(from (u/d) estimation) method($\tilde{F}$), theoretical and Shinskey's controllers($\tilde{S}$), for the 9 possible cases

Case	Shinskey's tuning			Frequency domain tuning		
	τ_{lead} (sec)	τ_{lag} (sec)	K_{ff} ($\frac{\%}{\%}$)	τ_{lead} (sec)	τ_{lag} (sec)	K_{ff} ($\frac{\%}{\%}$)
III c	0.40	0.05	-1.0	0.44	0.02	-0.75
I c	0.40	0.25	-1.0	0.53	0.34	-0.98
II c	1.0	1.05	-1.0	0.43	0.51	-1.00
III b	0.22	0.022	-1.0	0.19	0.002	-0.92
I b	0.40	0.40	-1.0	0.49	0.49	-0.99
II b	-0.10	0.10	-1.0	-0.15	0.06	-0.98
III a	1.0	0.9	-1.0	0.47	0.41	-0.98
I a	0.40	0.50	-1.0	0.48	0.59	-0.99
II a	0.12	0.42	-1.0	-0.14	0.14	-0.97

Table 3.13: Tuning parameter values for the 9 cases used in the simulation based on Shinskey's tuning rules and frequency domain($(u/d)/(y/r)$) method

Chapter 4

Frequency domain feedforward control tuning based on simultaneous process and disturbance transfer function identification - Experimental results

In chapters 2 and 3, the frequency domain tuning method has been tested in simulations. In this chapter the simultaneous identification and adaptive tuning strategy of chapter 2 is tested on an experimental distillation column. The tuning strategy is implemented on the lower temperature control loop of the column.

4.1 Experimental setup

The experimental work is performed on a methanol - water distillation column. The column is a Q.V.F.^{TM} pyrex column supplied by Pegasus Ltd., Agincourt, Ontario. It is 10 cm in diameter and consists of 11 trays. The bottom composition is controlled through temperature on the 2nd tray(from the bottom) which is cascaded to the steam flow controller of the reboiler. The top tray(tray 11 from the bottom) temperature is controlled by adjusting the reflux rate. The feed flow rate is controlled by adjusting the feed valve. The level of the reboiler is controlled by adjusting the flow of the bottom product. The distillation column control structure is shown in Appendix A. The data acquisition from the column, RLS Identification, tuning strategy and subsequent control implementation is done using a Bailey NETWORK 90^{TM} Distributed Control System(DCS). The RLS identification and frequency domain tuning is performed through real time C code on the Multi Function Controller(MFC) of the DCS. The management of C program on the MFC is done using Bailey C Utility Program(CUP) on a laptop computer(Commodore^{TM} C386SX-LT) communicating with the MFC through a serial port. The control strategy is implemented on Module 10 of the DCS. The configuration of various loops on different modules of the DCS are attached in Appendix A and a flow sheet describing the algorithm of the C program running in the MFC is shown in Appendix B.

4.2 RLS identification and feedforward controller tuning

The lower temperature loop is the feedback loop under control. Changes in the feed flow rate is a common disturbance to the lower temperature loop and is easily measurable. Hence feedforward control is implemented by measuring the feed flow rate and compensating for these changes through a combination of gain and lead-lag compensator. Square wave set point changes are induced by varying the setpoint of the lower temperature loop from 97°C to 98°C. Disturbance changes are induced by changing the setpoint of the feed flow controller from 0.40 L/min to 0.45 L/min. The feed flow output is measured as the disturbance. The upper temperature loop is kept on manual in order to eliminate the effect of changes in the upper temperature control output on the lower temperature.

Initially, the upper temperature is set at 65°C by adjusting the reflux rate. The lower temperature is brought to a setpoint of 97°C with appropriate tuning for the feedback controller. The process is run at a feed flow rate of 0.4 L/min. The feedback control used is of the standard PI type as shown in Equation 4.1.

$$C(s) = K_P + \frac{K_I}{s} \tag{4.1}$$

where K_P is the proportional gain and K_I is the integral gain. The feedback controller tuning parameters used in this experimental run are K_P=25 and K_I=9.0 respectively.

The experimental data is sampled at 15 seconds. After 60 seconds, i.e. after 4 samples, square wave setpoint changes from 97°C to 98°C are introduced with a period of 1200 sec. At the end of the first cycle, i.e. at 84 samples, square wave disturbance changes in the feed flow rate from 0.4 L/min to 0.45 L/min with a period of 1200 sec is introduced. During the second setpoint cycle, i.e. from 84-164 samples, the process is under the influence of the square wave disturbance with only the constant gain feedback controller. At sample 164, constant gain feedforward control is introduced to compensate for the measurable disturbance. The feedforward tuning parameters(chosen by the experience of the operator with the process) used during the 3^{rd} cycle are:

$$K_{ff} = 1.20 \ , \ \tau_{lead} = 80 \text{ sec}, \ \tau_{lag} = 110 \text{ sec}$$

Simultaneous identification of process and disturbance discrete time transfer functions is also started along with the implementation of feedforward controller during the 3^{rd} cycle. The structures of the process and disturbance transfer functions used in the identification are as shown in Equation 4.2 and Equation 4.3 respectively.

$$G_p(z^{-1}) = \frac{y}{u} = \frac{z^{-1}(b_0 + b_1 z^{-1} + b_2 z^{-2})}{1 + a_1 z^{-1} + a_2 z^{-2}} \tag{4.2}$$

$$G_d(z^{-1}) = \frac{y}{d} = \frac{z^{-1}(c_0 + c_1 z^{-1} + c_2 z^{-2})}{1 + a_1 z^{-1} + a_2 z^{-2}} \tag{4.3}$$

The bias in the process input and the measured disturbance is calculated by using a first order filter of the form shown below:

$$B_k = \alpha M_k + (1 - \alpha) B_{k-1} \tag{4.4}$$

Where B_k is the bias at time instant k, B_{k-1} is the bias at time instant k-1 and the M_k is the measured process variable at k. The filter factor, α is chosen to be 0.95. For the process output, the last step is considered as the mean or reference, i.e. when the setpoint is 97°C the reference is taken to be 98°C and vice versa. The bias removed process input, process output and the disturbance variables are used in the RLS estimation of the transfer functions G_p and G_d. Initially all the RLS coefficients are initialized to zero. A forgetting factor of 0.999 is used. All the diagonal elements of the initial covariance matrix are initialized to 100. In the presence of feedforward and feedback control, the process output, process input and the disturbance are related as shown in Equation 2.3.

At the end of the 3^{rd} period, i.e. at sample number 244, frequency domain tuning is started. The optimization is performed by minimizing the sum of the magnitude of the function $G_{ff} + (G_d/G_p)$ over the normalized frequency(wT) range of 0.015 to 1.5 rads(i.e. 0.001 to 0.1 rad/sec) at 13 frequency points using Nelder-Mead sequential simplex method. A weighting factor of $(1/wT)$ is used so that the lower frequency estimates get higher weighting compared to the noise affected high frequency estimates. The optimization routine is initialized to the tuning parameters (80,110,1.2) as one vertex after each time it converges, in order to prevent the optimization from falling into a false minimum. The initial simplex is of size 0.5 units with one of the vertices chosen to be (0.4,0.4,1.0). As explained in Chapter 2, the optimization is three dimensional and the shape of simplex is a tetrahedron. Since the process and disturbance dynamics and there by the feedforward control parameters vary based on the operating conditions, the optimization routine is generalized by using appropriate scaling factors. In the beginning, the initial tuning parameters are scaled down to the general starting simplex by using a scaling factor and the optimization is carried out. After the optimization converges, the converged simplex vertices are scaled up based on the scaling factor, to obtain the corresponding tuning constants as shown below:

Scaling factor = (Initial tuning parameter) / (Initial coordinate of the simplex vertex)

Final tuning parameter = (Final coordinate of simplex vertex) X (Scaling factor)

The optimization procedure is terminated when the number of iterations exceed 30 or when a function tolerance of 0.001 is reached. Because of the processing speed of the MFC(Motorola^{TM} 68000 processor) the optimization took about 6-8 samples to converge. Hence the tuning parameters are adapted approximately every 6-8 samples. At the end of the 4^{th} cycle, i.e. at sample 324, the frequency domain tuning is replaced by constant gain Shinskey's tuning parameters.

Shinskey's tuning rules are based on the parameters of the FOPDT models of process and disturbance transfer functions. The frequency response of the process and disturbance

transfer functions(obtained from the RLS estimation) at sampling instant 295 (Sample arbitrarily chosen after both the frequency responses converged) is used offline in obtaining the FOPDT parameters. The low frequency point in the magnitude plot is used in computing the gain. The frequency at which the magnitude plot falls by 3 dB is equivalent to the reciprocal of the time constant from which the time constant is calculated. The time delay is calculated from the RLS estimated phase plot using the previously estimated time constant.

The FOPDT transfer functions that are fitted to the RLS estimate based frequency response are as shown below:

$$G_p = 0.052\frac{e^{-15s}}{63s+1} \tag{4.5}$$

$$G_d = -0.063\frac{e^{-15s}}{67s+1} \tag{4.6}$$

From these estimates the process and disturbance dynamic combination corresponds to Case I a(Table 1.1). The corresponding Shinskey's tuning parameters(shown below) calculated from tuning rules given in Table 1.2 are used for tuning the feedforward controller during the 5^{th} cycle, i.e. from samples 324-403.

$$K_{ff} = 1.21,\ \tau_{lead} = 63 \text{ sec},\ \tau_{lag} = 67 \text{ sec}$$

4.3 Results and Discussion

The magnitude and phase plots of the process frequency response derived from the estimated RLS coefficients are shown in Figure 4.1 and Figure 4.2 respectively. The corresponding magnitude and phase plots of disturbance frequency response are shown in Figure 4.3 and Figure 4.4. The magnitude and phase plots of the feedforward controllers designed using frequency domain tuning along with the Shinskey's tuning rule based feedforward controller are shown in Figure 4.5 and Figure 4.6.

The time response of the lower temperature of the distillation column in the presence of square wave setpoint and disturbance changes is shown in Figure 4.7. The first cycle indicates the response to the setpoint changes from 97°C to 98°C in the presence of constant gain PI feedback control(with no changes in feed flow rate). The second cycle(84-163 samples) shows the effect of the square wave setpoint and feed flow rate disturbance on the lower temperature, in the presence of constant gain feedback control alone. The third cycle(164-243 samples) shows the lower temperature response to setpoint and disturbance square wave changes, in the presence of constant gain tuned feedforward and feedback controllers. The fourth cycle(244-323 samples) shows the lower temperature response in the presence of constant gain feedback and frequency domain tuned feedforward controllers. The fifth cycle(324-403 samples) shows the response in the presence of constant gain feedback and Shinskey's rule based feedforward controllers.

The process and disturbance dynamics of the distillation column correspond to Case I a($\tau_m < \tau_q, \tau_{dm} = \tau_{dq}$). The tuning parameters returned by the frequency domain tuning

method are $K_{ff} = 1.17$, $\tau_{lead} = 124.44$ sec, $\tau_{lag} = 124.88$ sec. The frequency domain tuning method returned a lead-lag compensator with almost equal lead and lag times indicating the cancellation of the disturbance being dominated by the gain rather than through the lead-lag combination. Cancellation of the disturbance is seen in the time response shown in Figure 4.7 during the fourth cycle in the presence of frequency domain feedforward control.

The Shinskey's tuning values of lead time and lag time are also almost equal(differing by 5 seconds). As observed in the time response(during cycles 4 and 5), both the Shinskey's tuning as well as the frequency domain tuning method provide almost identical setpoint response. This result is in agreement with the simulation results for Case I processes given in Chapter 2. The presence of feedforward control provides significant improvement in the lower temperature response as observed in the time response from 3 to 5 cycles, compared to the lower temperature response with out feedforward controller during the 2^{nd} cycle.

In order to test the effectiveness of the optimization based tuning strategy, another experimental run is performed with different starting tuning parameters from the previous run. The corresponding time response is shown in Figure 4.9. The first cycle shows the lower temperature response with a constant gain PI feedback controller($K_p = 18$, $K_I = 9$). The 2^{nd} and 3^{rd} cycles shows the response in the presence of square wave disturbance and setpoint changes, with constant gain PI and constant gain feedforward controller($K_{ff} = 2.5$, $\tau_{lead} =$ 50 sec, $\tau_{lag} = 100$ sec). The frequency domain tuning strategy with initial tuning parameters of (30,30,2.5) is introduced during the fourth cycle. The final tuning parameters returned by the optimization routine are $\tau_{lead} = 29$ sec, $\tau_{lag} = 36$ sec, $K_{ff} = 1.34$. As observed from the time response during the fourth cycle, the frequency domain tuning is able to cancel the disturbance, irrespective of the point where the optimization routine is started.

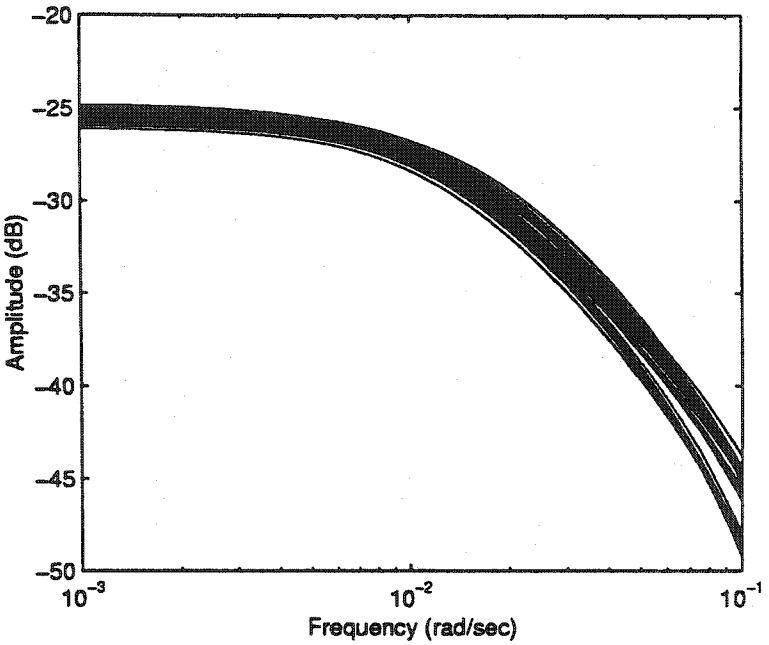

Figure 4.1: Magnitude plot of the RLS estimated process transfer function from 240-320 samples

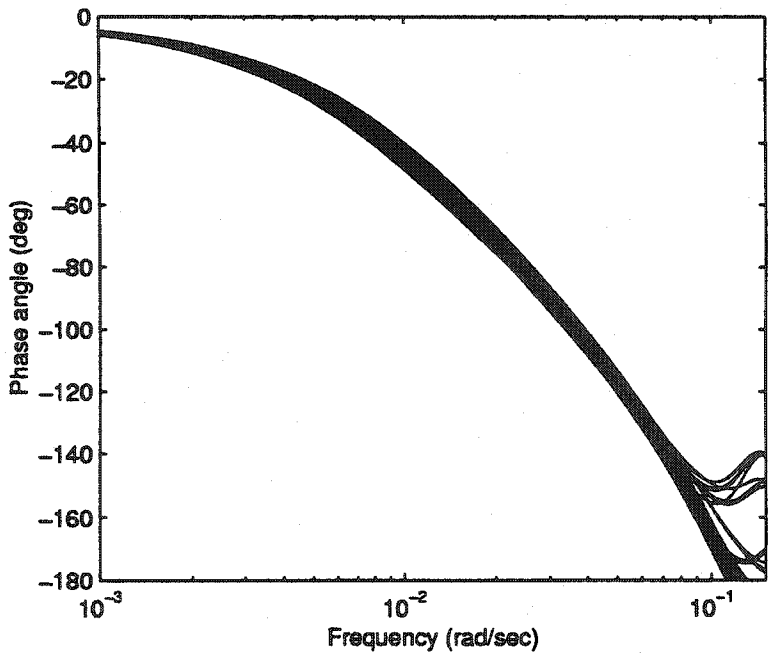

Figure 4.2: Phase plot of the RLS estimated process transfer function from 240-320 samples

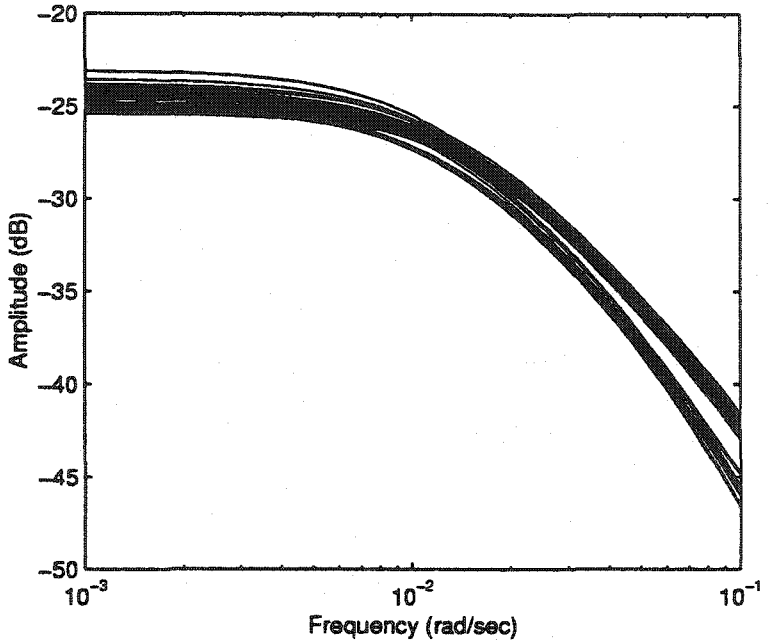

Figure 4.3: Magnitude plot of the RLS estimated disturbance transfer function from 240-320 samples

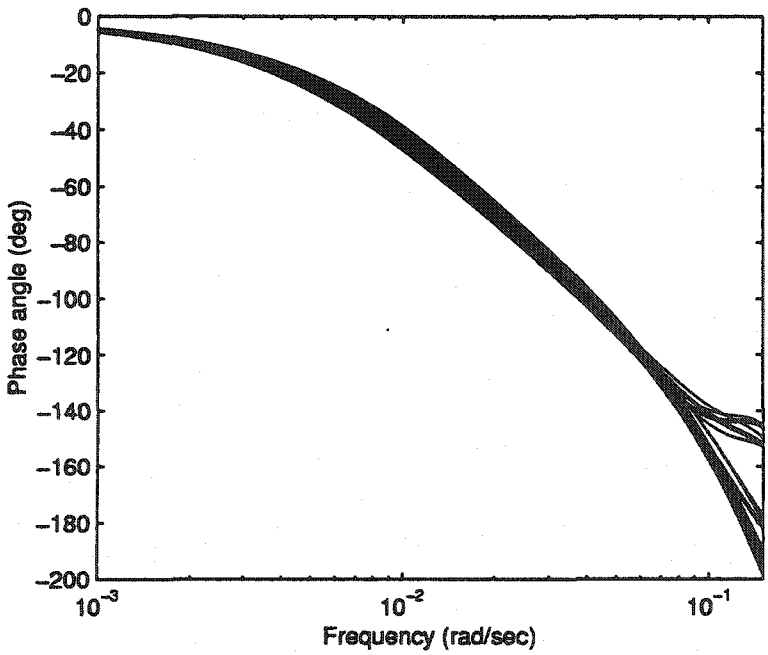

Figure 4.4: Phase plot of the RLS estimated disturbance transfer function from 240-320 samples

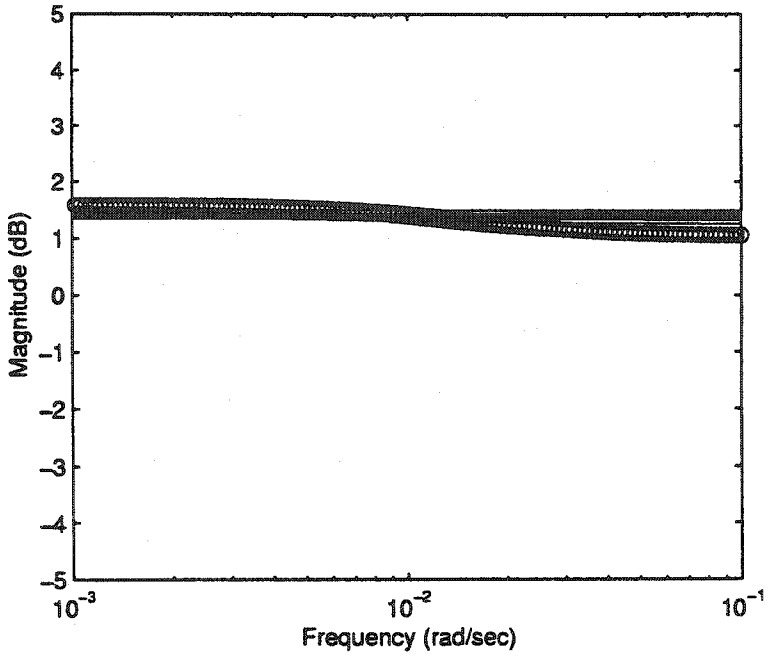

Figure 4.5: Magnitude plot of the frequency domain tuned(-) and Shinskey's tuning based(o) controllers

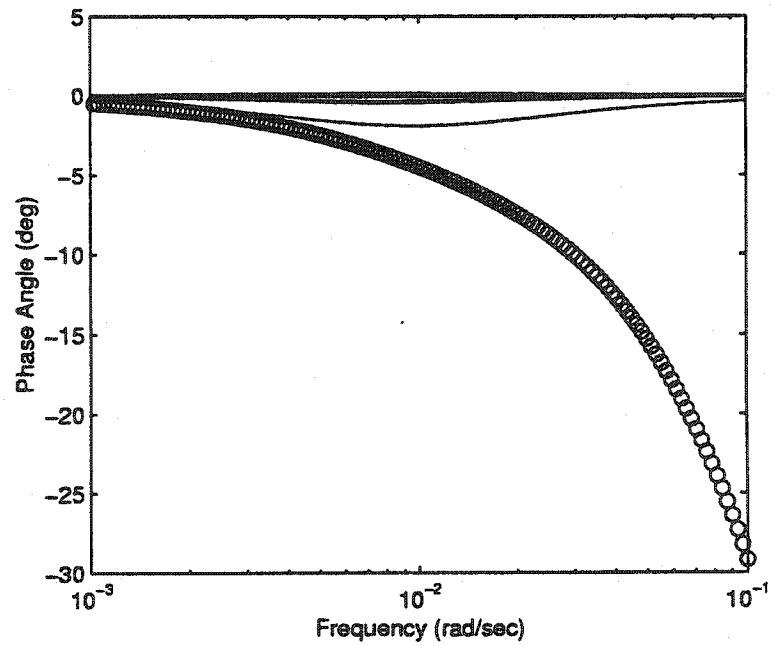

Figure 4.6: Phase plot of the frequency domain tuned(-) and Shinskey's tuning based(o) controllers

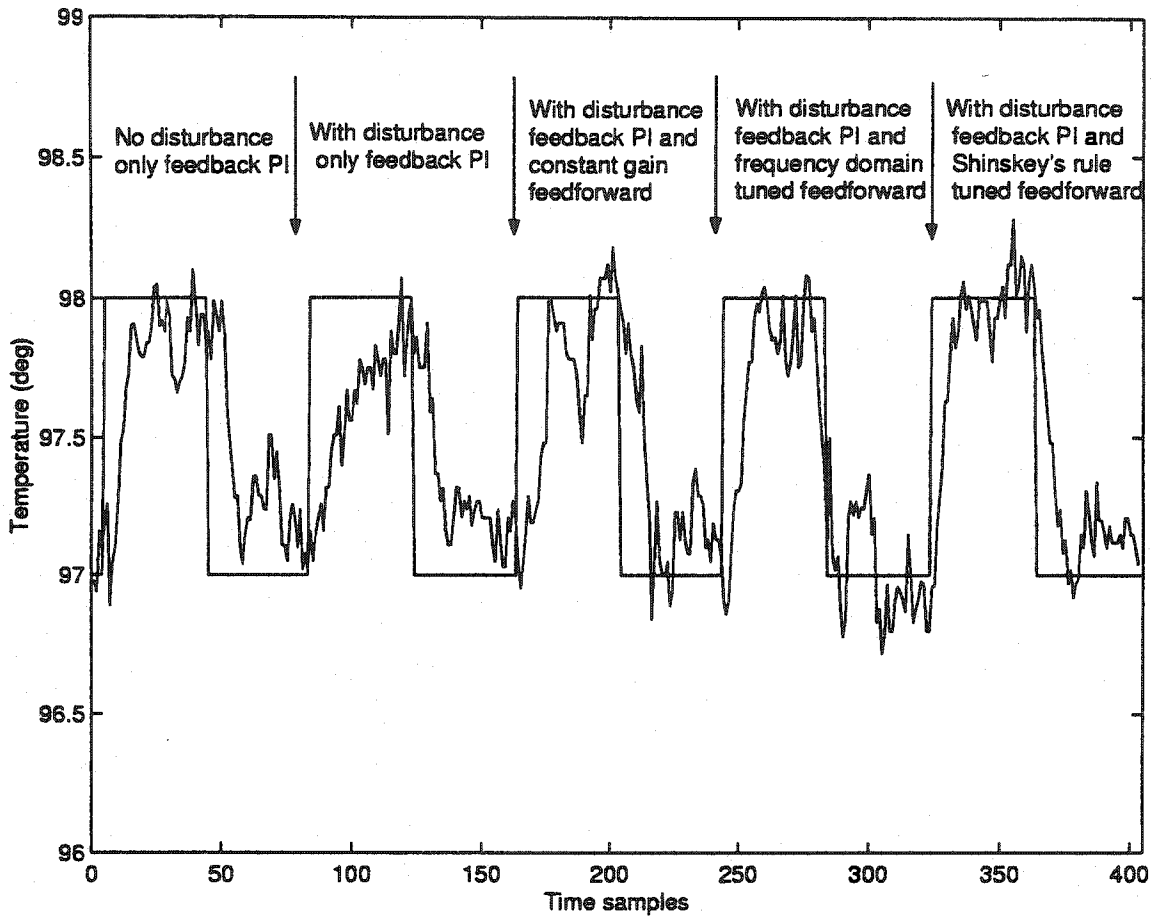

Figure 4.7: Lower temperature response in the presence of square wave setpoint and feed flow disturbance changes. 4-84 samples: Setpoint changes with constant gain PI, 84-164 samples: Setpoint and disturbance changes with constant gain PI, 164-244 samples: Setpoint and disturbance changes with constant gain PI and constant gain(untuned) feedforward controllers, 244-324 samples: Setpoint and disturbance changes with constant gain PI and frequency domain tuned feedforward controllers, 324-403 samples: Setpoint and disturbance changes with constant gain PI and Shinskey's rule tuned feedforward controllers

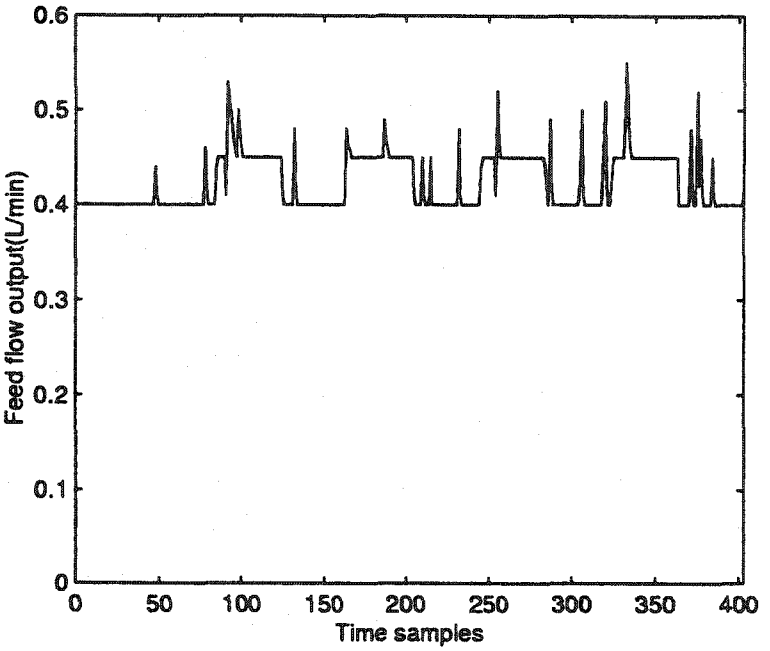

Figure 4.8: Measured disturbance, i.e. the feed flow output for square wave setpoint changes to the feed flow controller

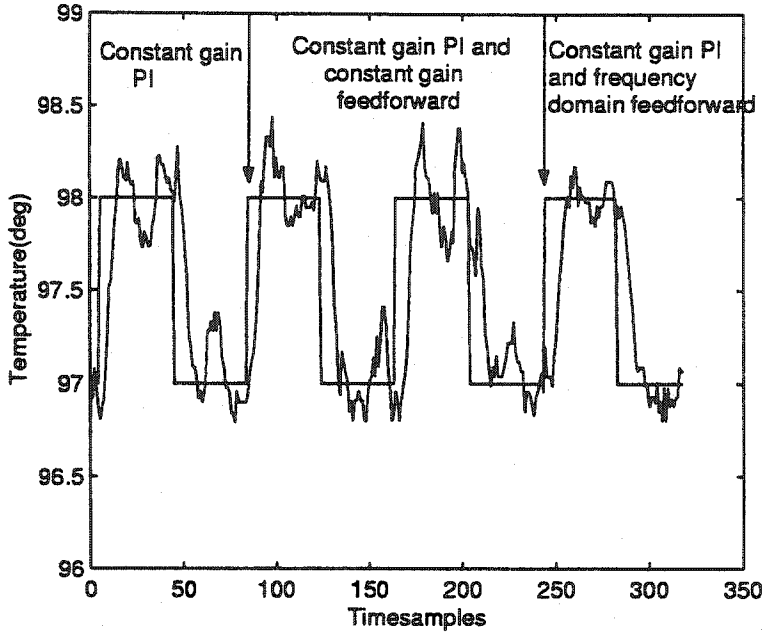

Figure 4.9: Lower temperature response in the presence of square wave setpoint and feed flow disturbance changes. 4-84 samples: Setpoint changes with constant gain PI, 84-244 samples: Setpoint and disturbance changes with constant gain PI and constant gain(untuned) feedforward controllers, 244-324 samples: Setpoint and disturbance changes with constant gain PI and frequency domain tuned feedforward controllers

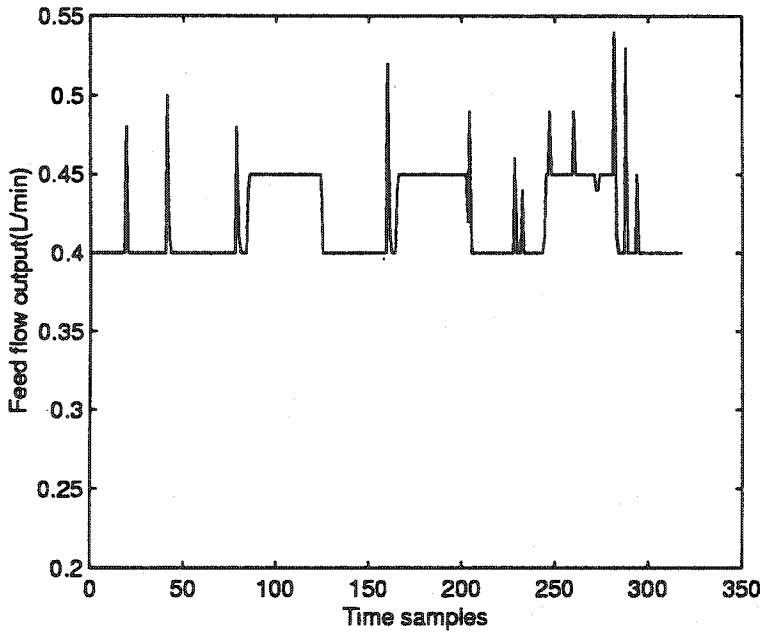

Figure 4.10: Measured disturbance during the second experimental run

Chapter 5

Conclusions and Future work

In this chapter, a brief summary of the work done in the previous chapters and future work that can be undertaken in this area is presented. Section 5.1 illustrates the conclusions of the simulations in Chapters 2 and 3, along with the experimental work done in Chapter 4. Section 5.2 indicates some suggestions for future work.

5.1 Summary and conclusions of the thesis

An introduction to feedforward control and its tuning methods is presented in Chapter 1. Literature survey is performed in the areas of RLS based identification schemes and tuning strategies in time and frequency domain pertaining to feedforward control.

In Chapter 2, the combined identification approach of process and disturbance transfer function identification for adaptive feedforward control is presented. The efficiency of frequency domain tuning approach is demonstrated by means of simulations. In almost all cases, it can be infered that the frequency domain based tuning strategy gives accurate fit of the controller phase plot when compared to Shinskey's tuning. The magnitude fit of the frequency domain based method is definitely as good or better than Shinskey's controller fit for Case III and Case I processes. Considerable improvement is obvious in Case II processes, where the frequency domain tuning method provides a better fit than the corresponding Shinskey's controllers.

Different approaches for tuning feedforward controllers through closed loop identification are presented in Chapter 3. The approach based on obtaining the disturbance frequency response through the disturbance sensitivity function in Section 3.2 seems to be accurate of all the methods. But this method could suffer in the presence of high noise levels as the derivation of frequency response makes the disturbance frequency response(G_d) at each frequency dependent on all the frequencies of the disturbance sensitivity function from which it is derived. The approach $(u/d)/(y/r)$ in Section 3.4 seems to be the best in the presence of high levels of noise. The effectiveness of the three methods(Based on the closeness of fit of the controller frequency response to the theoretical (G_d/G_p) ratio) for all possible dynamic combinations under the conditions used for simulation in this work are ranked in Table 5.1.

Case	G_d from S_d method	(S_dC/T) method	$((u/d)/(y/r))$ method
III c	1	2	3
I c	1	3	2
II c	1	3	2
III b	1	3	2
I b	1	3	2
II b	1	3	2
III a	1	3	2
I a	1	3	2
II a	1	2	3

Table 5.1: Effectiveness of the three closed loop methods for different dynamic combinations

In Chapter 4 the simulation results in Chapter 2 are tested experimentally on a distillation column. With the delay in the process and disturbance paths of the column being equal, the frequency domain strategy based on combined identification of G_p and G_d using recursive least squares technique, is able to provide similar cancellation of the disturbance as with the tuning based on Shinskey's tuning rules. This is in agreement with the simulation results presented in Chapter 2 for Case I a processes. The experimental results while confirming validity for Case I a, yields validity to the simulations for the other cases which could not be experimentally tried.

5.2 Future work

The adaptive frequency domain tuning method based on open loop identification of process and disturbance transfer functions has been tested through experiments on the distillation column for a single dynamic combination. Because of the nature of the apparatus available for this work, experimental work is performed only for Case I a type combination. The method needs to be tested experimentally for other and more complex dynamic combinations(Case II and III processes). The frequency domain tuning simulation results based on closed loop identification techniques needs to be verified experimentally. The closed loop identification is not truly adaptive in the sense that the tuning and identification are done sequentially, instead of simultaneously. A continuous identification and tuning approach based on closed loop identification needs to be developed.

For Case III processes, which need prediction for complete cancellation of the disturbance, using a group of lead-lag compensators for feedforward control may give better fit in the frequency response of the controllers instead of just one used in this work. FIR filters and/or polynomial predictive filters can also be tested for performance improvement of Case II and Case III processes.

BIBLIOGRAPHY

[1] Marlin, T.J., "*PROCESS CONTROL Designing Processes and Control Systems for Dynamic Performance*", First edition, McGraw-Hill, Inc., 1995. ISBN 0-07-040491-7.

[2] Astrom, K.J. and Wittenmark, B. "*Adaptive Control*", Second edition, Addison Wesley Publishing, 1995. ISBN 0-201-55866-1.

[3] Shinskey, F.G., "*Process Control Systems Application, Design and Tuning*", McGraw-Hill Inc. Fourth Edition, 1996. ISBN-0-07-057101-5.

[4] Patel, B., "Model Reference Adaptive Control System using Frequency Domain Performance Specifications", Master's Thesis 1999, Lakehead University.

[5] Astrom, K.J. and Wittenmark, B., "On Self Tuning Regulators", Automatica, Vol. 9, pp. 185-199, 1973.

[6] Schumann, R. and Christ, H., "Adaptive Feedforward Controllers for Measurable Disturbances", Joint Automatic Control Conference, pp. 500-506, 1979.

[7] Fortescue, T.R., Kershenbaum, L.S. and Ydstie, B.E., "Implementation of Self-tuning Regulators with Variable Forgetting Factors", Automatica, Vol. 17, No. 6, pp. 831-835, 1981.

[8] Lee, T.H. and Hang, C.C., "A Performance Study of Parameter Estimation Schemes for Systems with Unknown Dead Time", Proc. of the 1985 American Control Conference, pp. 512-576, 1985.

[9] Marques Da Costa, P., Poinot, T., Trigeassou, J.C., "Identification of Linear Systems Using Overparameterized Models", Proc. of the 1995 American Control Conference: June 21-23, 1995, part 4 of 6, pp. 2913-2917.

[10] Hagglund, T. and Astrom, K.J., "Industrial Adaptive Controllers Based on Frequency Response Techniques", Automatica, Vol. 27, No. 4, pp. 599-609, 1991.

[11] Shah, S.L. and Fisher, D.G., "Multi-variable Frequency Domain Design Method for

Disturbance Minimization", International Journal of Control, Vol. 45, no. 1, pp. 107-115, 1987.

[12] Isermann, R., "*Digital Control Systems, Volume 2: Stochastic Control, Multivariable Control, Adaptive Control, Applications*", Second revised edition, Springer-Verlag, 1991. ISBN 3-540-50997-6.

[13] Goberdhansingh, E., Wang, L. and Cluett, W.R., "Robust Frequency Domain Identification", Chemical Engineering Science, Vol. 47, pp. 1989-1999, 1992.

[14] Barnes, T.J.D., Wang, L. and Cluett, W.R., "A Frequency Domain Design Method for PID Controllers", Proc. of the American Control Conference, San Francisco, CA, pp. 890-894, June 1993.

[15] Wang, Q.G., Hang, C.C. and Bi, Q., "A Frequency Domain Controller Design method", Transactions of Inst. of Chemical Engineers, Vol.75, Part A, January 1997.

[16] Natarajan, K. and Gilbert, A.F., "System Identification and PID Controller Tuning Using Band Pass Filters.", The Canadian Jou. of Chem. Engg., Vol. 75, pp. 765-777, August 1997.

[17] Nelder, J.A. and Mead, R., "A Simplex Method for Function Minimization", Computer Jou., Vol. 7, pp. 308-313, 1965.

[18] Ljung, L. and Soderstorm, T., "*Theory and Practice of Recursive Identification*", MIT Press, 1983. ISBN 0-262-12095-X.

[19] "Bailey NETWORK 90^{TM}, C Language Implementation Guide For The Multi-Function Controller(NMFC03)", Bailey Controls Company, 1997. I-E-96-703A

[20] "Bailey NETWORK 90^{TM}, Function Code Application Manual", Bailey Controls Company, 1997. I-E96-200

APPENDIX A

Distillation column control structure

and

Various module configuration diagrams

Distillation column control structure

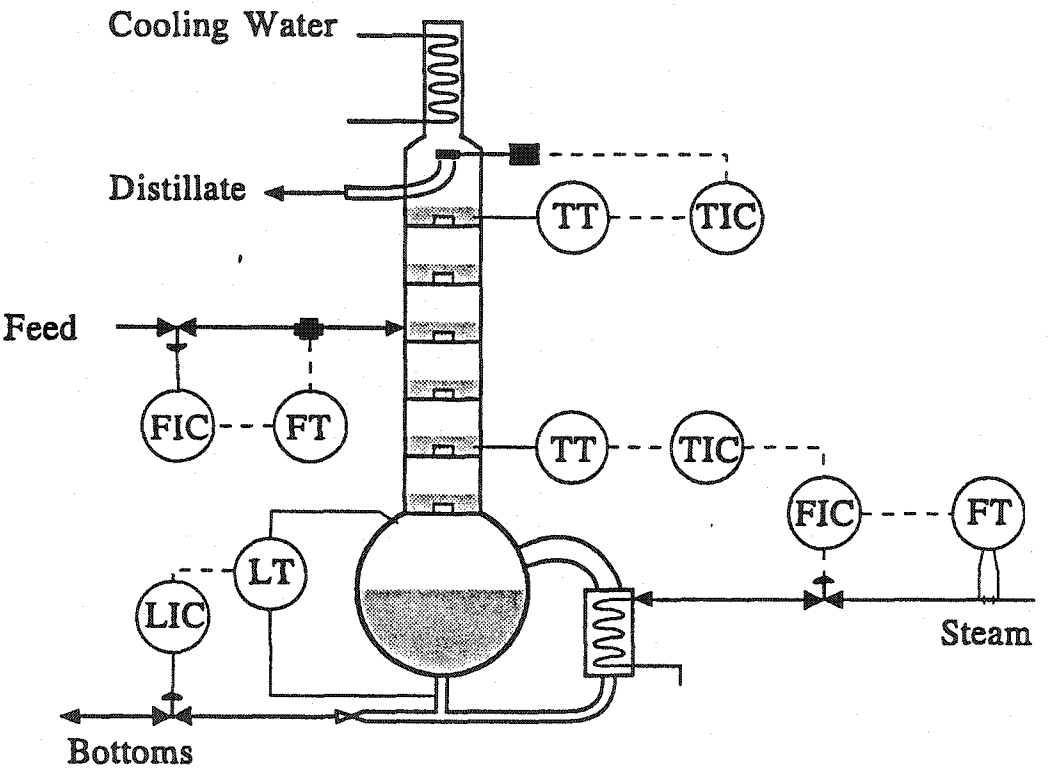

Distillation Column Feed Flow (Module 4)

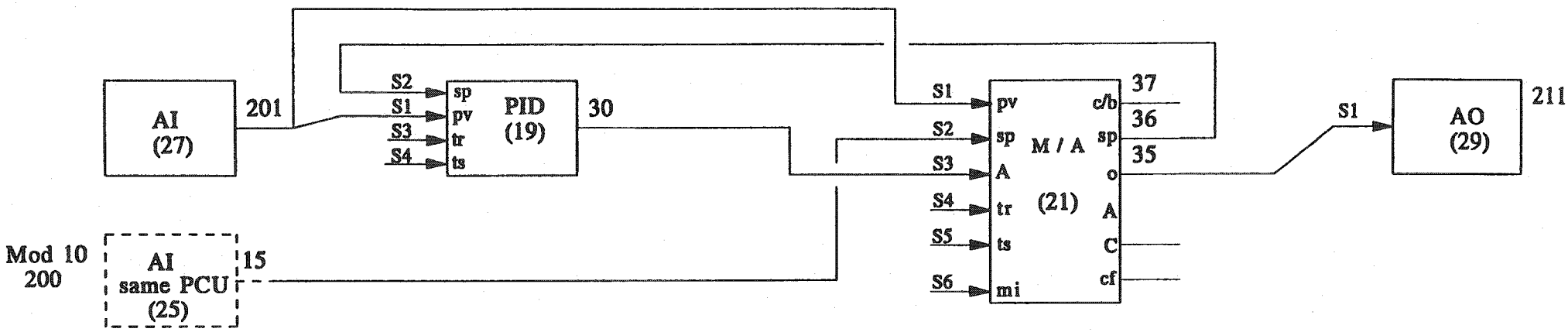

Distillation Column Lower Temperature (Module 6)

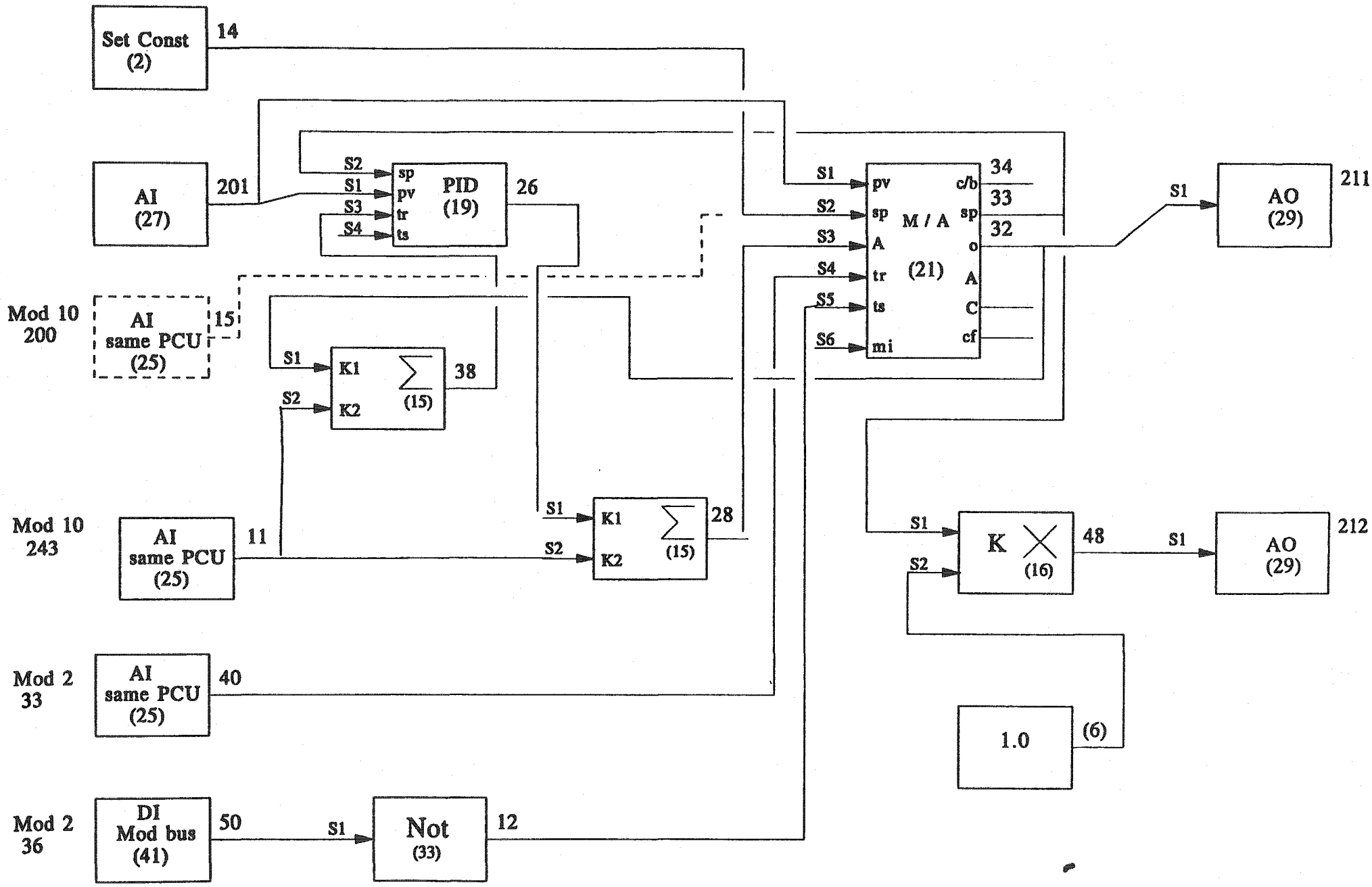

Distillation Column Upper Temperature (Module 8)

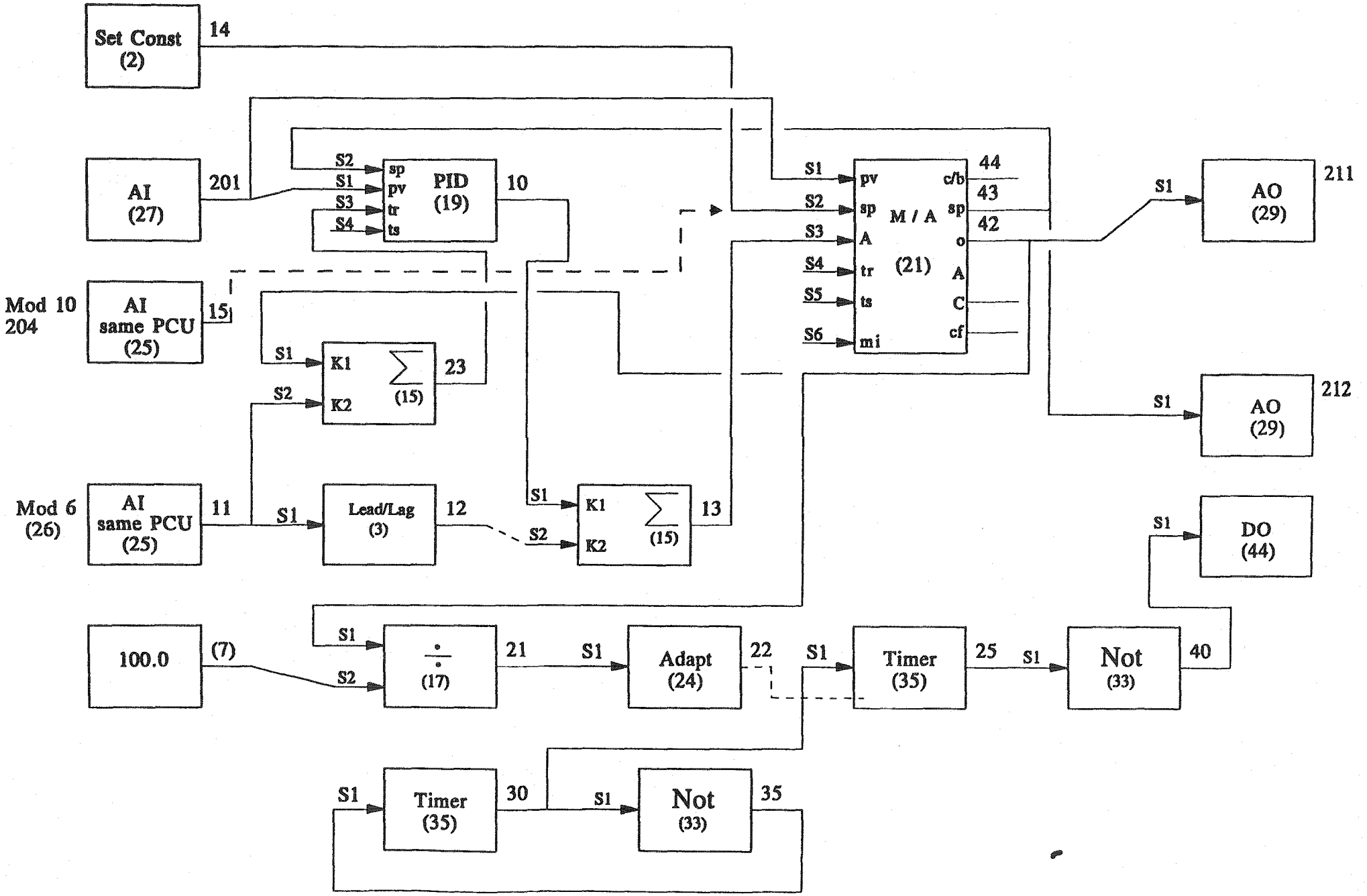

Distillation Column Multifunction Controller (Module 10)

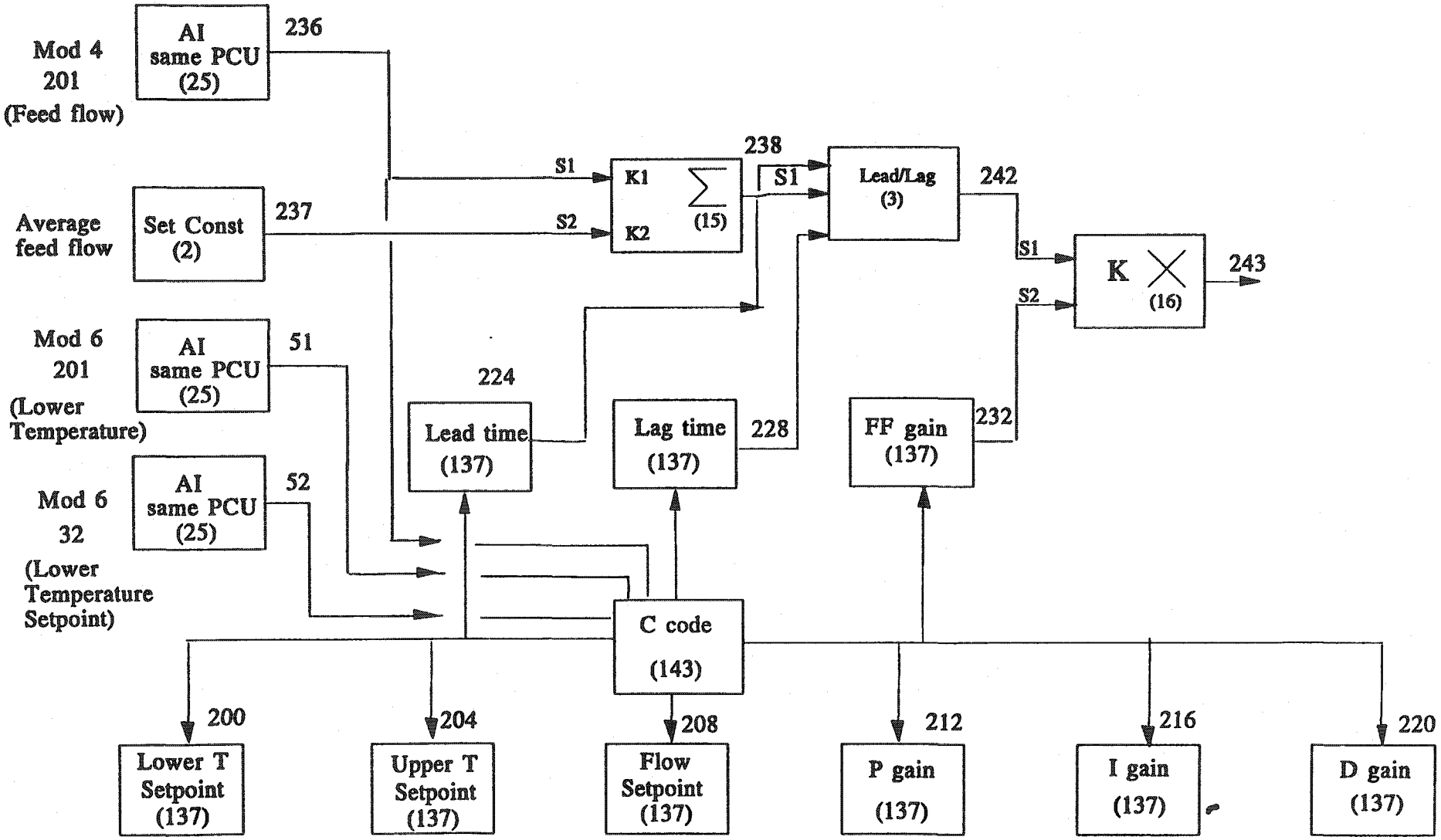

APPENDIX B

A schematic of the DCS - Computer

interface and

A flow sheet of the algorithm implemented